Plant monounsaturated fatty acids: diversity, biosynthesis, functions and uses

Sami Kazaz, Romane Miray, Loïc Lepiniec, Sébastien Baud

REVIEW

Plant monounsaturated fatty acids: diversity, biosynthesis, functions and uses

Sami Kazaz[1], Romane Miray[1], Loïc Lepiniec, Sébastien Baud*

Institut Jean-Pierre Bourgin, INRAE, CNRS, AgroParisTech, Université Paris-Saclay, 78000 Versailles, France

[1]Contributed equally to this work.

***Corresponding author**
E-mail address: sebastien.baud@inrae.fr (S. Baud)

Abstract
Monounsaturated fatty acids are straight-chain aliphatic monocarboxylic acids comprising a unique carbon-carbon double bond, also termed unsaturation. More than 50 distinct molecular structures have been described in the plant kingdom, and more remain to be discovered. The evolution of land plants has apparently resulted in the convergent evolution of non-homologous enzymes catalyzing the dehydrogenation of saturated acyl chain substrates in a chemo-, regio- and stereoselective manner. Contrasted enzymatic characteristics and different subcellular localizations of these desaturases account for the diversity of existing fatty acid structures. Interestingly, the location and geometrical configuration of the unsaturation confer specific characteristics to these molecules found in a variety of membrane, storage, and surface lipids. An ongoing research effort aimed at exploring the links existing between fatty acid structures and their biological functions has already unraveled the importance of several monounsaturated fatty acids in various physiological and developmental contexts. What is more, the monounsaturated acyl chains found in the oils of seeds and fruits are widely and increasingly used in the food and chemical industries due to the physicochemical properties inherent in their structures. Breeders and plant biotechnologists therefore develop new crops with high monounsaturated contents for various agro-industrial purposes.

Keywords
Monounsaturated, fatty acid, desaturase, lipid, triacylglycerol, membrane

Abbreviations
ACP, acyl carrier protein; ADS, acyl-CoA desaturase-like; Cb_5, cytochrome b_5; CER, ECERIFERUM; DGDG, digalactosyldiacylglycerol; DMDS, dimethyl disulfide; ELO, elongase; ER, endoplasmic reticulum; FAD, fatty acid desaturase; FAE, fatty acid elongase; GIPC, glycosyl inositol

phosphoceramide; FAT, acyl-acyl carrier protein thioesterase; HEAR, high erucic acid rapeseed; KAS, 3-ketoacyl-acyl carrier protein synthase; KCS, 3-ketoacyl-coenzyme A synthase; LCB, long-chain base; LEAR, low erucic acid rapeseed; MGDG, monogalactosyldiacylglycerol; PAD, palmitoyl-acyl carrier protein desaturase; PC, phosphatidylcholine; PDCT, phosphatidylcholine:diacylglycerol choline phosphotransferase; PE, phosphatidylethanolamine; PG, phosphatidylglycerol; SAD, stearoyl-acyl carrier protein desaturase; SLD, sphingolipid long-chain base Δ8 desaturase; SQDG, sulfoquinovosyldiacylglycerol; VLCFA, very long-chain fatty acid (>18C).

Content

1. Introduction
2. Diversity of plant monounsaturated fatty acids
    2.1. Potential number of monounsaturated fatty acids
    2.2. Structural analysis of monounsaturated acyl chains
    2.3. Natural structural diversity
3. Biosynthesis of monounsaturated acyl chains
    3.1. Plant desaturases: one reaction mechanism, different actors
    3.2. Soluble acyl-ACP desaturases
    3.3. Membrane-bound desaturases
        3.3.1. Acyl-CoA desaturase-like (ADS) enzymes
        3.3.2. FATTY ACID DESATURASE4 (FAD4)
        3.3.3. Cytochrome b_5 (Cb_5)-containing desaturases
        3.3.4. Sphingolipid Δ4-desaturases
4. Elongation of preexisting monounsaturated acyl chains
    4.1. The fatty acid elongase complex
    4.2. The fatty acid synthase complex
5. Known biological functions of plant monounsaturated fatty acids
    5.1. Monounsaturated acyl chains as intermediates in lipid metabolism
    5.2. Oleic acid - $18{:}1^{\Delta 9c}$
    5.3. *3E*-Hexadecenoic acid - $16{:}1^{\Delta 3t}$
    5.4. Monounsaturated acyl chains and membrane fluidity
    5.5. Monounsaturated acyl chains in surface lipids
6. Monounsaturated fatty acids in storage lipids
    6.1. Omega-9 monounsaturated fatty acids
        6.1.1. Oleic acid - $18{:}1^{\Delta 9c}$
        6.1.2. Erucic acid - $22{:}1^{\Delta 13c}$
        6.1.3. Nervonic acid - $24{:}1^{\Delta 15c}$
    6.2. Omega-7 monounsaturated fatty acids
    6.3. Delta-5 monounsaturated fatty acids
    6.4. Delta-6 monounsaturated fatty acids
7. Conclusion and perspectives

1. Introduction

Land plants collectively produce a tremendous diversity of fatty acids that differ in chain length, number and position of C-C double bonds (also referred to as unsaturations), or addition of unusual functional groups (*e.g.* hydroxyl, epoxyl, ketone, acetylenic). While introduction of a first unsaturation represents a widespread modification of saturated acyl chains, it nevertheless constitutes one of the most fascinating and critical reaction of plant lipid metabolism. From an enzymatic point of view, the unique ability of desaturases to oxidize unactivated hydrocarbon chains in a chemo-, regio- and stereoselective manner has been described as “approaching the limits of the discriminatory power of enzymes” [1-3]. Particularly intriguing is the precision with which these enzymes operate on substrates composed of essentially equivalent methylene chains that lack distinguishing features close to the site of dehydrogenation [4,5]. Yet, the evolution of land plants has resulted in the emergence of a variety of desaturase enzymes, with their diversification favoring the production of an increasing array of monounsaturated acyl chains. Importantly, location and geometrical configuration of the unsaturation, altogether with chain length, confer specific characteristics to monounsaturated fatty acids and deeply impact their metabolic use, leading to the biosynthesis of complex lipids with specific biological functions. When accumulated in the oils of seeds and fruits, these monounsaturated acyl chains have a considerable potential in the food and chemical industries due to the physicochemical properties inherent to their structures. This has led breeders and plant biotechnologists to develop new crops that can serve as renewable sources of carbon chains for agro-industrial purposes.

2. Diversity of plant monounsaturated fatty acids

2.1. Potential number of monounsaturated fatty acids

Monounsaturated fatty acids can be defined as straight-chain (unbranched) aliphatic monocarboxylic acids containing a unique double bond (Figure 1A). They can be noted n:$1^{\Delta z c/t}$, with n designating the number of carbon atoms in the acyl chain, z specifying the position of the carbon engaged in the double bond and closest to the carboxyl end (∆ nomenclature), while *c* (*cis*, *Z*) and *t* (*trans*, *E*) labels provide information regarding the geometrical configuration of the unsaturation. Carbon numbering from the methyl end of the fatty acid (ω nomenclature) also exists and will be adopted to discuss certain categories of unusual fatty acids.

The potential number of monounsaturated fatty acid structures increases with the length of the acyl chain (Figure 2A). In a first approach, we do not count *cis*- and *trans*-isomers of unsaturated fatty acids separately and let x_n denote the number of theoretically possible monounsaturated fatty acids involving n carbons. For n = 1, the carboxyl group is linked to one hydrogen, giving rise to formic acid. For n = 2, the carboxyl group is linked to one methyl group, making up acetic acid. None of these chemical structures can host a C-C double bond. Thus $x_1 = 0$, $x_2 = 0$. For n = 3, the saturated fatty acid is propionic acid, and there is the possibility to insert a double bond at position ∆2, yielding acrylic acid. Thus $x_3 = 1$. More generally, the number of monounsaturated fatty acids as a function of chain

length n for n > 1 can be calculated as follows: $x_n = n - 2$, as the carbon atom of the carboxyl group cannot engage in a C-C double bond, and the remaining n – 1 carbons are connected by n – 2 bonds [6]. Importantly, when the fatty acids involve non-terminal double bonds, *cis*- and *trans*-isomers can be distinguished. When such isomers are considered separately, the number of monounsaturated fatty acids as a function of chain length n for n > 2 becomes $x_n = 2 (n - 2) - 1 = 2n - 5$.

2.2. Structural analysis of monounsaturated acyl chains

Fatty acids are usually analyzed by gas chromatography-mass spectrometry as methyl ester derivatives (Figure 1B). While appropriate protocols and settings combined with the use of standards are routinely used for efficient separation and identification of common monounsaturated acyl chains, the structural characterization of unknown monounsaturated fatty acids (*e.g.* determination of the position of the double bond in the alkyl chain) cannot be obtained by mass spectrometry alone. Double bonds actually tend to migrate along the aliphatic chain under electron impact, making it impossible to directly locate the unsaturation by mass spectrometry without some chemical modifications of the molecule [7]. A first solution to this problem consists in the derivatization of the terminal carboxyl group with a reagent containing a nitrogen atom (remote functional group modification). When the molecule is ionized in the mass spectrometer, the nitrogen atom carries the charge, so that double-bond ionization and migration are minimized. Radical-induced cleavage occurs evenly along the chain, producing a series of relatively abundant ions of high mass from the cleavage of each C-C bond. When the double bond is reached, diagnostic ions tend to occur [8]. After using *N*-acyl pyrrolidines (Figure 1C), most analysts now prefer either picolinyl (3-hydroxymethylpyridinyl) esters (Figure 1D) or 4,4-dimethyloxazoline (DMOX) derivatives (Figure 1E), which both have their merits in terms of mass spectrometry [7-10]. Preparation of DMOX derivatives is more straightforward, but the interpretation of spectra obtained under electron-impact ionization tends to be more challenging when the double bond is located near either end of the molecule, requiring reference mass spectra [11].

Another way to locate double bonds relies on the ‘fixation’ of the double bond before gas chromatography–mass spectrometry analysis. Ozonolysis or oxidation/epoxidation can be used [7,12-13]. But dimethyl disulfide (DMDS) adducts (Figure 1F), which have excellent mass spectrometric properties and are prepared in a simple one-pot reaction, are more widely employed today by plant biochemists [14]. Electron impact ionization of these adducts gives an abundant molecular ion, and the cleavage between the methylthio-substituted carbons produces a set of key fragments that allows locating the position of the original double-bond [15].

Over the last decade, advances in mass spectrometry have significantly accelerated the lipidomic field, allowing to map the complete molecular composition of a lipidome and opening new exciting research perspectives. In recent years, increasing attention has been paid to the biology of lipid structural isomers, such as C-C double-bond location isomers, despite the difficulty in profiling the whole lipidome with such location information in a high-throughput and sensitive fashion [16-18]. To reveal the detailed structure of acyl chains comprising complex lipids, alternative tandem mass spectrometric (MS/MS) methods have been developed, including ultraviolet photodissociation [19], electron impact excitation of ions from organics [20], or ozonolysis [21]. Double-bond chemical

derivatization strategies have also been paired with MS/MS, including the Paternò-Büchi reaction [22] and epoxidation [23]. What is more, imaging of lipid isomers on tissue sections has been made possible by matrix-assisted laser desorption ionization (MALDI)-MS/MS imaging paired with ozonolysis [24] or Paternò-Büchi reaction [25], as well as desorption electrospray ionization (DESI)-MS/MS imaging paired with ultraviolet photodissociation [26]. These analytical techniques have not been used so far to characterize unsaturated fatty acid isomers in plants but could provide useful information regarding their precise location in a near future.

As for the analysis of geometrical isomers, the state-of-the-art of *cis* and *trans* fatty acid resolution still involves intense research into finding efficient analytical methods suitable for complex biological samples [27]. Gas chromatography remains the benchmark method allowing for a preliminary separation of geometrical isomers of fatty acids prior to mass spectrometry analysis, the approach requiring comparison to appropriate standards (which are not always easily available). Formation of DMDS adducts being entirely stereospecific, with threo- and erythro-derivatives formed from *cis*- and *trans*-isomers, respectively, it is possible to separate geometrical isomers while investigating the location of double bonds [15]. In a few cases, mass spectrometry of monounsaturated fatty acid methyl esters can provide some structural information regarding the geometry of the double bond [28,29]. However, the characterization of geometrical isomers has historically relied on a number of spectroscopy techniques including NMR, IR, UV and Raman spectroscopies [16]. In the case of Raman spectroscopy for example, the stretching vibration of the C-C double bond for a *cis*-isomer is near 1,655 cm^{-1} and that of the *trans*-isomer is near 1,670 cm^{-1} [27].

2.3. Natural structural diversity

Over 450 distinct fatty acids synthesized by land plants have been described so far and many new structures remain to be discovered in the plant kingdom [30]. In contrast with the conservative fatty acid composition of plant membrane lipids, tremendous fatty acid diversity exists in storage lipids, so that triacyglycerols are often regarded as the primary source for the huge diversity in unusual fatty acids [31]. The specific physical and chemical properties of many unusual fatty acids might explain why they are excluded from membrane lipids, where they would perturb the integrity of the membrane bilayer and have deleterious effects on cell biology [32]. Meticulous accumulation of datasets from several decades of research has allowed the development of the Seed Oil Fatty Acid (SOFA) database [33,34] and the plantFAdb.org resource, an internet-based database displaying fatty acid composition for over 9,000 plants [30]. Examination of these databases reveals more than 50 structurally distinct monounsaturated fatty acids (Figure 2). Comparing the diversity of naturally occurring monounsaturated fatty acid species characterized so far with potential diversity, there appears to be an over-representation of structures with chain lengths ranging from 16 to 20 carbons combined with a significant under-representation of odd-chain fatty acids. These biases faithfully reflect the general diversity of plant fatty acids, since most of these exhibit even-numbered chain-lengths up to 22 carbon atoms [6]. The prevalence of fatty acids having chain length of 16-20 carbons most certainly derives from the characteristics acquired during the evolution by the enzymes involved in their synthesis, these enzymatic characteristics possibly stemming from biological constraints like

the thickness of the biomembrane bilayers that often host these fatty acids in the form of glycerolipids at some point of their biosynthesis even when their final destination consists in non-membrane lipid pools. What is more, an additional physico-chemical constraint stems from the fact that melting point temperatures of fatty acids increase with chain length [35], so that the biosynthesis of rigid very long-chain fatty acids (VLCFAs) is often associated with the elaboration of highly specialized lipid pools like the extracellular cuticular lipids [36,37]. Finally, most double bonds of plant monounsaturated fatty acids appear to be in *cis* configuration.

A narrow spectrum of monounsaturated fatty acids can be found in membrane glycerolipids that includes the rather ubiquitous $18{:}1^{\Delta 9c}$ (oleic acid) and $16{:}1^{\Delta 9c}$ (palmitoleic acid) fatty acids [38], as well as a unique *trans* fatty acid, $16{:}1^{\Delta 3t}$, which is always esterified specifically at the *sn*-2 position of the glycerol backbone of phosphatidylglycerol (PG) and is only found in thylakoid membranes. $16{:}1^{\Delta 3t}$ has been detected throughout nearly the entire plant kingdom from green algae to land plants [39,40], but is absent in orchids [41] and cyanobacteria [42]. Sphingolipids represent another major structural component of membranes [43]. They share a common characteristic non-polar backbone made of a long-chain sphingoid base that can be *N*-acylated to a long-chain or a very-long-chain fatty acid, thus forming ceramides. The amide acyl residue is in a configurational position reflecting the *sn*-2 position of diacylglycerolipids, whereas the alkyl chain of the long-chain sphingoid base corresponds to the *sn*-1 substituent [44]. Both acyl chains can be monounsaturated. Double bonds are frequently present at position Δ4 (in the *trans* conformation) or Δ8 (either in the *cis* or *trans* conformation) of long-chain sphingoid bases [45-47]. In the plant kingdom, VLCFA components of ceramides are typically saturated, but ω9 monounsaturated acyl chains have been described in sphingolipids of Brassicaceae and some Poaceae species, as well as in selected species from other families [14,43,46,48-49].

Monounsaturated fatty acids found in seed and fruit oils comprise, among many others, oleic acid and its elongated ω9 derivatives $20{:}1^{\Delta 11c}$ (gondoic acid), $22{:}1^{\Delta 13c}$ (erucic acid), and $24{:}1^{\Delta 15c}$ (nervonic acid), as well as palmitoleic acid and its elongated ω7 derivatives $18{:}1^{\Delta 11c}$ (vaccenic acid) and $20{:}1^{\Delta 13c}$ (paullinic acid) [30,31] (Table 1). The seed oil of *Limnanthes* species is distinct from that of other plants because of its high content of $20{:}1^{\Delta 5c}$ and $22{:}1^{\Delta 5c}$ fatty acids [50,51], while $16{:}1^{\Delta 6c}$ (sapienic acid) accounts for more than 80% of seed fatty acids in *Thunbergia alata* [52] and $18{:}1^{\Delta 6c}$ (petroselinic acid) for up to 85% of total fatty acids in seeds of some Apiaceae, Araliaceae, and Garryaceae species [53,54].

With the exception of oleic acid, the biochemical characterization of monomer components of surface lipids (*e.g.* cutin, suberin, cuticular waxes) has mostly failed to identify monounsaturated fatty acids in the strictest meaning of the term. However, the occurrence of several monounsaturated fatty acid derivatives indicates that their fatty acid counterparts are synthesized at some points before efficient transformation. For example, monounsaturated 26:1, 28:1, and 30:1 primary alcohols having double bonds at position ω6 have been detected in the cuticular waxes of *Arabidopsis thaliana* inflorescence stems [55]. In leaves of *Poplar trichocarpa* (poplar), odd-numbered monounsaturated alkenes ranging in chain lengths from C23 to C31 and carrying a double bond between carbons 9 and 10 were detected [13], while longer (C33 to C37) 7- and 9-alkenes were observed in the leaf wax of *Arabidopsis* [56]. Other examples include 9-alkenes observed in *Agropyron intermedium*, *Hordeum*

vulgare, and *Ophrys sphegodes* [57-58], 7-alkenes described in *Ophrys exaltata* [59] and *Zea mays* [60], 12-alkenes in *Ophrys sphegodes* [58], 4-, 6-, and 10-alkenes in *Zea mays* [61].

3. Biosynthesis of monounsaturated acyl chains

3.1. Plant desaturases: one reaction mechanism, different actors

A desaturase is an oxygenase enzyme that can promote the removal of two protons linked to adjacent carbon atoms in a hydrocarbon chain, especially in a fatty acyl residue, resulting in the introduction of a C-C double bond in the [44,62,63]. Abstraction of hydrogens from unactivated methylene groups is thermodynamically demanding, C-H bond representing one of the most stable bonds in living systems with a dissociation energy reaching approximately 95 kcal.mol^{-1} [64]. This energy lying beyond the range of reactions usually catalyzed by amino acids alone, a metal cofactor harnesses the oxidative power of molecular oxygen to break this C-H bond and initiate the reaction [62]. It is most likely that all of the desaturases comprise an active-site di-iron cluster. Unlike standard oxygenases, which directly transfer oxygen to their substrate, desaturases use activated molecular oxygen to abstract hydrogens from the substrate [5,65]. In the end, a desaturation reaction consists in an oxidation reaction requiring two reducing equivalents (electrons) obtained from an electron transport chain to initiate the conversion of oxygen into a metal-bound electrophilic reagent with sufficient reactivity to perform the desired catalysis, the molecule of oxygen being completely reduced to water during the reaction (Figure 3) [66-68].

The detailed mechanism by which desaturases carry out their selective oxygen-dependent dehydrogenation chemistry has fascinated researchers for decades [68,69]. Despite increased knowledge gained through the characterization of related enzymes such as the methane monooxygenase [70-75], this mechanism remains partly speculative [76]. During catalysis, the di-iron complex is thought to go through a reaction cycle of cleaning, loading, activation, and firing [62]. A notable feature of this cycle is that the ligands of the di-iron complex permit substantial structural rearrangements during the course of catalysis. This conformational flexibility allows the di-iron center to optimize bonding interactions between metal ions and oxidant throughout the catalytic cycle [66]. In the stable resting form, the two oxidized (diferric or Fe^{III}-Fe^{III}) iron ions of the complex are coupled by a bridging oxygen atom ligand forming the μ-oxo-di-iron complex [77,78]. After removal of this oxygen atom by 2-electron reduction to produce the reduced (diferrous or Fe^{II}-Fe^{II}) form (cleaning), molecular oxygen binds to the iron center resulting in a μ-1,2 diferric(Fe^{III}) peroxo or P intermediate (loading) [78,79]. This intermediate may not be sufficiently oxidizing to carry out the desired substrate oxidation and therefore must undergo rearrangement to gain catalytic competence (activation) [80]. At some point during this sequence of molecular events, a molecule of water is formed, but the precise timing of this step remains unknown [62]. The new rearranged P' intermediate whose structure remains uncertain and may vary from one class of desaturase to another is kinetically competent to attack and cleave C-H bonds of the highest stability and represents the key oxidizing intermediate responsible for hydrogen abstraction (firing) [66]. This activated center catalyzes the stepwise abstraction of the two substrate hydrogens and their combination with one of the oxygen atoms to form a second molecule of

water, while the second oxygen atom is left behind as the μ-oxo-di-iron complex ready to start a new cycle [81]. Removal of the first substrate hydrogen would result in the formation of a radical intermediate. Removal of the second hydrogen would result in the formation of a transient diradical that would spontaneously recombine to form a C-C double bond in the substrate [62]. Importantly, hydrogen removal occurs in a stepwise manner, but with *syn* stereospecificity. The lifetime of the radical intermediate at the first carbon is indeed too short to allow a rotation of the C-C bond and the subsequent presentation of an originally *trans*-oriented proton to the di-iron center [44]. Accordingly, the stereochemical outcome of a desaturation reaction is not controlled by the actual reactivity of the di-iron center, but instead results from the conformation adopted by the hydrocarbon chain before reaction starts, this conformation being dictated by the geometry of the substrate hydrophobic cavity in the neighborhood of the di-iron center.

Two unrelated classes of desaturases are present in higher plants: soluble acyl-acyl carrier protein (ACP) desaturases and membrane-bound desaturases [82]. Both classes comprise di-iron-oxo enzymes exhibiting a dimeric quaternary structure [83,84]. Despite the similarities existing between the chemistry performed by these two classes of desaturases, they exhibit different rate-limiting steps. The limiting step for membrane-bound desaturases is the initial C-H bond-breaking [69]. That of soluble desaturases rather consists in the release of the desaturation product involving the energetically unfavorable solvation of hydrophobic acyl-ACP as the product leaves the hydrophobic cavity to enter the aqueous phase [5]. Then, the metal center of desaturase enzymes is kept in place by ligand shells composed of amino acid residues like histidine, glutamine, glutamic acid, and aspartic acid [81] and the two classes of desaturases possess distinct primary ligation spheres [2,85]. Soluble acyl-ACP desaturases exhibit a conserved protein fold consisting of a bundle of alpha helices, with sections of four helices providing the metal ligands required to assemble the di-iron complex [66]. In the primary sequence of these desaturases, the amino acid residues involved in binding the di-iron complex form the characteristic $EX_{(\sim 40)}$(D/E)EXRH-$X_{(\sim 100)}$-$EX_{(\sim 40)}$(D/E)EXRH dual motif [62]. In contrast to the soluble acyl-ACP desaturases, evidence for a di-iron active site in plant integral membrane desaturases is indirect, based on the presence of conserved histidine clusters defining the $HX_{(3\ or\ 4)}$H-$X_{(n)}$-$HX_{(2\ or\ 3)}$HH-$X_{(n)}$-(H/Q)$X_{(2\ or\ 3)}$HH motif [5,67,85]. These three histidine tracks, which are in equivalent positions with respect to potential membrane-spanning domains, are presumed to compose the Fe-binding active centers of the enzymes [86]. Assuming the formation of four transmembrane helices [67], the histidine boxes come to lie on the same side of the membrane, with scattered sequence parts not involved in the formation of the hydrophobic membrane anchor possibly building up a membrane-peripheral domain corresponding to the catalytic site [44]. Mutation of any single histidine residue in the motif causes complete loss of enzyme function [85]. These different motifs represent a convergent evolution of two unrelated types of proteins that used two iron ions and coordinated them by different ligation spheres, resulting in functionally equivalent di-iron centers able to catalyze desaturation reactions [44].

Desaturases can be located in different cell compartments and the electron transport systems that supply reducing equivalents to plastidial and microsomal desaturases are distinct, although comprising functionally equivalent components (Figure 3). Pairs of electrons from NADPH or NADH coenzymes

are firstly transferred to a flavoprotein. These electrons are then supplied one at a time to intermediate carrier proteins able to convey a single electron. Two reduced carrier proteins ultimately transfer electrons sequentially to the desaturase, allowing the two-electron reduction required for catalysis [62]. In the plastids, desaturase enzymes depend on the soluble 2Fe-2S protein ferredoxin as electron donor [87,88]. In photosynthetic tissues in the light, ferredoxin is reduced by photosystem I [89]. In photosynthetically inactive tissues and during desaturation in the dark in photosynthetic tissues, electrons are derived from NADPH via the soluble flavoprotein ferredoxin:NADP oxidoreductase [81] (Figure 3A). The extraplastidial microsomal desaturases use the small membrane-bound heme-binding protein cytochrome b_5 as an intermediate electron donor [90-92] (Figure 3B). *In vitro*, both NADH-cytochrome b_5 reductase and NADPH-cytochrome P450 reductase have the ability to reduce cytochrome b_5 and exhibit clear specificities in terms of the electron donor, NADH or NADPH, respectively [93]. But NADH-cytochrome b_5 reductase is regarded as the major electron-transfer component associated with desaturation reactions *in vivo* [81]. Surprisingly, genome sequencing programs identified cytochrome b_5 domains in various membrane-bound desaturases [94,95]. In this context, the NADH-cytochrome b_5 reductase can transfer electrons to the catalytic site of these fusion desaturases via their cytochrome b_5-like domain [96]. It was proposed that fusion of two components of the electron transport sequence may contribute to speed up electron transfer [96,97]. The existence of cytochrome b_5 fusion desaturases raises the question of the occurrence of fusions involving ferredoxins and desaturases that might operate in plastids. To date, no such fusion has been reported.

Desaturases able to catalyze the biosynthesis of monounsaturated acyl chains have been identified in the two known classes of plant desaturases (*i.e.* soluble and membrane-bound) (Figure 4). Soluble acyl-ACP desaturases all use saturated acyl-ACPs as substrates [82]. Membrane-bound desaturases introducing a first unsaturation in acyl-CoAs or acyl groups bound to various lipids form a common branching system split into different subgroups. The first one comprises acyl-CoA desaturase-like (ADS) enzymes that either introduce the first Δ7 double bond into palmitoyl residues at the *sn*-2 position of monogalactosyldiacylglycerol (MGDG) in the chloroplasts of so-called 16:3-plants, or desaturate very long-chain acyl-CoA thioesters in the endoplasmic reticulum (ER). The second subgroup comprises the plastid acyl-lipid desaturase FATTY ACID DESATURASE4 (FAD4) and related FAD4-like enzymes. It should be noted, however, that the histidine clusters within these enzymes do not correspond exactly with the consensus seen across other membrane desaturases, leaving an open question as to their evolutionary origin. Cytochrome b_5-containing desaturases from higher plants have been assigned with different types of enzymatic activities [65] and some of these desaturases were characterized as sphingolipid Δ8-desaturases that introduce a double bond on the long-chain base (LCB) moieties of sphingolipids without requiring previous desaturation (third subgroup) [98]. Finally, the fourth subgroup comprises sphingolipid Δ4-desaturases catalyzing the Δ4-*trans*-desaturation of sphinganine. Regardless of the class they belong to, these desaturases can be categorized according to their regioselectivity as Δ-counting desaturases introducing a double bond at position x referred to from the carboxyl end of the acyl chain, or ω-counting desaturases that introduce a double bond at position y referred to from the methyl end of the acyl chain [65].

3.2. Soluble acyl-ACP desaturases

Soluble acyl-ACP desaturases catalyze the insertion of C-C double bonds within the acyl chains of saturated fatty acids that are covalently attached by a thioester linkage to the 4′-phosphopantetheine prosthetic group of ACP [62]. These enzymes are found in photoauxotrophic *Euglena gracilis*, in the plastids of plants, and possibly in some Gram-positive bacteria and filamentous fungi [99,100]. Despite the essentially soluble nature of acyl-ACP desaturases, proteomic analyses have suggested that they could be associated to the thylakoids [101,102]. Such a tight association might favor efficient reductant supply to the enzyme since ferredoxin, the electron donor for this reaction, is reduced by photoreduction in photosynthetic organs [103]. In this context, reductant might be supplied in a form that would not necessarily equilibrate with the stromal pool of reductant [104]. This proposed suborganellar localization of the acyl-ACP desaturases remains to be confirmed though.

Δ9 stearoyl-ACP desaturases (SADs) efficiently desaturate 18:0 (stearic acid) to form $18{:}1^{\Delta 9c}$ [82,105]. Δ9 SADs represent the predominant isoforms of acyl-ACP desaturases in most plant tissues and are regarded as housekeeping enzymes. Although all plants require constitutive expression of *SAD* genes for the biosynthesis of oleic acid and its polyunsaturated derivatives, the exact phylogenetic origin of these archetype acyl-ACP desaturases remains unclear [44]. Complementary approaches have established that these desaturases are homodimeric di-iron proteins [105-107]. A more comprehensive understanding of the three-dimensional structure of the enzymes has been obtained by crystallization of the *Ricinus communis* (castor) Δ9 SAD more than twenty years ago [108]. The overall shape of each subunit is a compact cylinder. The secondary structure of each 41.6-kDa monomer is almost exclusively alpha-helical with nine helices forming an antiparallel helix bundle while the remaining two are capping each end [62] (Figure 5A). Ligands from four of the alpha-helices in the helix bundle coordinate the nonheme di-iron active site at the core of the monomer [108] (Figure 5C). One iron ion interacts with the side chain of glutamic acid 196 and histidine 232, while the second interacts with the side chains of glutamic acid 105 and histidine 146. In addition, the side chains of the glutamic acid residues 143 and 229 participate in the coordination of both iron ions [62]. The position of the di-iron cluster in the middle of the structure results in an isolated local environment suitable for reactive oxygen chemistry. The active site is positioned alongside a deep, bent, narrow hydrophobic cavity extending from the surface to the deep interior of each monomer, in which the substrate is bound during catalysis [5] (Figure 5B). The cavity bends at the di-iron cluster at a point corresponding to the insertion position of the double bond between carbons Δ9 and Δ10. The bend places constraint on the free rotation of the substrate during catalysis and explains the observed stereochemistry [62]. The dimer interface of the enzyme includes extensive contacts between helices and interdigitating loops [108]. However, the significant space separating the di-iron clusters of the two subunits suggests that each of the two monomers function independently from one another. What is more, recent experiments have shown that while the enzymes use a half-of-the-sites mechanism, they do not use an alternating subunit half-of-the-sites reactivity mechanism whereby substrate binding to one subunit is coordinated with product release from the other subunit [83].

The desaturation reaction requires the interaction of the ∆9 SAD with ACP bound to saturated acyl chain on one side, and with electron-donating cofactor ferredoxin on the other side [106]. 18:0-ACP binding precedes electron transfer, with occupation of the substrate channel by an 18:0 acyl chain possibly leading to conformational changes that optimize the ferredoxin binding site for efficient electron transfer [109]. Redox gating has been demonstrated in which binding of acyl-ACP substrate increases the desaturase redox potential by 0.1 volt favoring its reduction when substrate is bound [110]. This mechanism ensures that activation of oxygen only happens when substrate is in place. According to available ACP structures, the conserved central helix II of the carrier protein comprises negatively charged residues that play a dominant role in the interaction with ACP-dependent enzymes like ∆9 SADs. For this reason, this helix has been termed the 'recognition helix' of ACP [111]. Then, examination of the known structures of ACP-dependent enzymes has revealed a set of predominantly positively charged residues located near the opening of their substrate channel, which have been implicated in an electrostatic interaction with the helix II of ACP [3,111]. In unbound acyl-ACPs, the hydrophobic acyl chain is positioned in a pocket formed by a four-helix bundle. Upon docking to the desaturase, the hydrophobic segment of the acyl chain has to be released from the carrier protein to become available for insertion into desaturase, until the methyl end reaches the bottom of the substrate channel [81]. During transfer of the substrate, the acyl chain must overcome stabilizing hydrophobic interactions in the ACP binding pocket [112].

The proposed position of the ferredoxin binding site as supported by biochemical, catalytic, and computational approaches lies on the side of the desaturase monomer opposite to the ACP docking site [109]. This preferred binding site involves surface complementarity and electrostatic interactions between ferredoxin and desaturase. A triad of lysine residues on ∆9 SAD surface participates in the formation of the catalytic complex, and the substitution of all three lysine residues abolishes the ability of ∆9 SADs to recognize the ferredoxin as electron donor [109]. While two of the cysteines interacting with the [2Fe-2S] cluster in ferredoxin are solvent exposed, all of the ligands to the di-iron center of ∆9 SAD are buried within the four-helix bundle, eliminating the possibility of direct transfer of electrons from the ferredoxin to the di-iron center. Electrons therefore need to be transferred from the ferredoxin-docking surface to the internal di-iron cluster. From the three-dimensional structure of ∆9 SAD, two putative pathways for electron transfer have been put forward [108]. The pathway extending from the surface tryptophan 62 to the internal di-iron ligand histidine 146 seems the most plausible as the three lysine residues identified for the interaction with ferredoxin cluster near tryptophan 62 [109].

Aside from housekeeping Δ9 SADs, several plant species possess additional paralogous acyl-ACP desaturases exhibiting unconventional regiospecificity and/or chain-length selectivity. These additional desaturases have often been involved in the biosynthesis of unusual monounsaturated fatty acids used for triacylglycerol production in storage organs. For example, ∆9 palmitoyl-ACP desaturases (PADs) prefer 16:0 (palmitic acid) instead of 18:0 as a substrate and catalyze the formation of $16{:}1\Delta^{9c}$ (Figure 6). So far, Δ9 PAD isoforms have been identified in *Doxantha unguis-cati* [113] and *Arabidopsis* [114,115]. In *Arabidopsis*, the two genes coding for Δ9 PADs, named *AtAAD2* and *AtAAD3*, are transcriptionally activated by the endosperm-specific transcription factors AtMYB115 and AtMYB118 [115], explaining the specific enrichment in ω7 fatty acids observed in endosperm oil

compared to embryo oil [116-118]. Another unconventional acyl-ACP desaturase has been described in trichomes of *Pelargonium* x *hortorum*, where this Δ9 myristoyl-ACP desaturase uses 14:0 (myristic acid) substrate to form $14:1^{\Delta 9c}$ (myristoleic acid), a precursor in the production of compounds targeting pests and known as anacardic acids [119,120]. Despite their functional divergence, the acyl-ACP desaturases share a high degree of amino acid sequence similarity and a common structural fold [121]. Limited amino acid substitutions targeting residues lining the lower portion of the substrate channel of the enzymes were shown to be sufficient to shift chain-length selectivity while maintaining Δ9 regioselectivity [44,113]. The channel structure of the archetype Δ9 SADs is highly conserved among species. This channel is deep enough to accommodate 18:0 substrates. In Δ9 PADs, the distal end of the substrate channel is lined by residues with bulky lateral chains that reduce its depth and thus favor the binding of shorter substrates [113,115,122]. Notwithstanding similar enzymatic activities, plant Δ9 PADs described so far exhibit variations in the distal end of their substrate channels. These observations suggest that Δ9 PAD activity may have arisen independently in different species during the evolution of acyl-ACP desaturases, the diversification of which was probably favored by the emergence of multigene families within the genome of land plants followed by mutations of the archetype *SAD* sequence [115]. Interestingly, metabolic engineering based on combinatorial saturation mutagenesis and rational redesign of desaturases has allowed tailoring several original Δ9 PAD enzymes by reducing the depth of the substrate channel of Δ9 SAD enzymes [122-124]. Most of the combinations of amino acid substitutions yielding such a result involved the replacement of a residue lining the lower part of the substrate pocket by a bulkier one. While the molecular bases of the shift in selectivity toward shorter acyl chains have been unambiguously addressed, the reason why the Δ9 SADs are more active with 18:0 than with shorter substrates remains unclear. It has been hypothesized that interactions of the methyl end of the substrate with the bottom of the binding pocket may enhance rates of catalysis [100,123].

The isolation of genes encoding acyl-ACP desaturases with different regiospecificities represented an opportunity to investigate the molecular determinants of regioselectivity. For example, the seed oil of *Thunbergia alata* is enriched in $16:1^{\Delta 6c}$ produced by a Δ6 PAD [125]. Δ4 PAD producing $16:1^{\Delta 4c}$ were identified in *Coriandrum sativum* (coriander) [126-127] and *Hedera helix* (English ivy) [128]. Considering that acyl-ACP desaturases are Δ-counting enzymes, differences in regiospecificity may theoretically arise from variations in the length of the substrate binding channel from the surface of the enzyme to the di-iron cluster and/or from varying interactions between ACP and desaturase [62]. Comparative studies between the structures of the archetype Δ9 desaturase from *Ricinus communis* in complex with ACP on one side, and that of the Δ4 desaturase from *Hedera helix* and ACP on the other side, have paved the way for the elucidation of the remote control of regioselectivity in acyl-ACP desaturases [3]. The structures obtained revealed variations in ACP binding orientations potentially leading to insertion of the acyl chain into the substrate-binding cavity at different depths, yielding distinct regioselectivities. This approach identified a signature residue located at the entrance of the binding cavity of the desaturase that differs between the two enzymes. This residue appears to be the seminal determinant for the different binding modes of ACP with respect to the desaturase and favors either Δ9 or Δ4 desaturation via repulsion (asparagine with acidic side chain) or attraction (lysine with

positively charged side chain) of phospho-serine 38 of ACP, respectively [3]. But the precise shape and depth of the substrate channel below the di-iron cluster provide additional constraints that may also contribute to the high fidelity of product regioselectivity observed among the acyl-ACP desaturases.

Importantly, the acyl-ACP desaturases may not be the only determinants of monounsaturated acyl-ACP production. It was proposed that specialized ACP isoforms may partly control the production of unsaturated acyl-ACPs [129]. In the same vein, two general types of ferredoxins, often referred to as photosynthetic and heterotrophic, are known to occur in higher plants [130-131]. Photosynthetic ferredoxins are regulated by light and are predominantly found in photosynthetic tissues. Heterotrophic ferredoxins are independent of light regulation and exhibit a more ubiquitous tissue distribution [132-133]. It was shown that heterotrophic ferredoxin isoforms support higher rates of unusual acyl-ACP desaturase activities when compared with photosynthetic ferredoxins. This suggests that ferredoxin isoforms, through specific interactions with acyl-ACP desaturases, may also contribute to control the production of monounsaturated acyl-ACPs [134].

3.3. Membrane-bound desaturases

3.3.1. Acyl-CoA desaturase-like enzymes

The *ADS* genes encode proteins homologous to the ∆9 acyl-lipid desaturases of cyanobacteria and the ∆9 acyl-CoA desaturases of yeast and mammals [135-136]. While cDNAs encoding ADSs have been identified in several dicots, no homologous genes could be found in the genome of *Oryza sativa*, *Brachypodium distachyon*, or *Zea mays*, suggesting that *ADS* genes may be absent in monocots [137]. The *Arabidopsis ADS* family comprises nine highly related members (Figure 4). Their chromosomal location and similarity suggest that they arose through a series of gene duplication events [137]. Eight of these genes are located in clusters on chromosomes I and III, while the remaining gene is present on chromosome II [138]. Interestingly, the desaturase-like proteins encoded by this gene family exhibit different subcellular localizations. *AtADS3*/*FAD5* and a second closely related homologous gene designated *AtADS3.2* are predicted to encode proteins with a plastid transit peptide. The seven remaining members of the gene family have no characteristic plastid transit peptide and were designated as multipass membrane proteins located in the ER membrane. AtADS1 and AtADS2 contain a putative di-arginine (-RXR-) ER retrieval and retention motif [139] close to the C terminus, and when transiently expressed as yellow fluorescent protein-fusions in *Nicotiana benthamiana* leaves, they colocalize with ER membrane markers [137]. In the other five ADS proteins predicted to be ER-localized, the di-arginine motif is atypical, with arginine replaced with lysine residues (-KXK-) [140]. With the exception of AtADS4.2 [56], the actual subcellular localization of these ADS isoforms has not been experimentally confirmed yet.

The enzymatic and biological functions of the AtADS are only partially elucidated. Only one of the two plastidial isoforms has been characterized. *AtADS3/FAD5* encodes a plastidic palmitoyl-MGDG ∆7 desaturase, thus representing a glycerolipid-dependent activity [138] (Figure 6). Loss of AtADS3/FAD5 function results in failure to form $16{:}1^{\Delta 7c}$ on MGDG in the pathway leading to the production of $16{:}3^{\Delta 7c,19c,13c}$, a predominant leaf fatty acid [141,142].

In contrast, the seven extraplastidial *AtADS* gene products were proposed to have VLCFA-CoA desaturase activity and to exhibit different regiospecificities [137], even though the exact nature of the substrates used *in planta* by these desaturases often remains speculative, or even unknown. According to functional studies carried out in *Saccharomyces cerevisiae*, AtADS1 and AtADS2 catalyze introduction of double bonds relative to the methyl end of the substrate molecule at ω9 (ω9 desaturase activity). AtADS1.3 and AtADS4.2 display ω7 desaturase activity, AtADS4 displays ω6 desaturase activity, while AtADS1.2 and AtADS1.4 catalyze the introduction of double bonds relative to the carboxyl end of the substrate molecule at Δ9 (Δ9 desaturase activity). Reverse genetic approaches have established that AtADS2 is involved in the synthesis of the ω9 monounsaturated C24 and C26 components of different seed lipids such as the membrane lipids phosphatidylethanolamine (PE) and phospatidylserine, or sphingolipids [137] (Figure 7). Using forward and reverse genetic approaches, it was then proposed that AtADS4/ECERIFERUM17 (CER17) catalyzes the desaturation of C26, C28, and C30 VLCFA-CoAs, yielding ω6 monounsaturated very-long chain acyl-CoAs (Figure 7) that are ultimately converted into monounsaturated primary alcohols by the fatty acyl-CoA reductase AtCER4 [143] before accumulation in cuticular wax of inflorescence stem [55]. As for the product of the *AtADS4.2* gene, which is highly expressed in young leaves, it shows strong activity on acyl substrates longer than C32 and produces ω7 acyl-CoAs that are then converted into wax alkenes by AtCER1 and AtCER3 [56,144-145].

Interestingly, the subcellular localization of the ADSs was also shown to partly influence substrate specificity and regiospecificity of the enzymes, so that ADS activity seems to be influenced by metabolic context. It is thus possible to switch ADS enzyme specificity by alternate subcellular targeting [136]. For example, retargeting of the cytoplasmic VLCFA-CoA desaturases AtADS1 or AtADS2 to the plastid yields efficient desaturation of 16:0 on MGDG into $16{:}1^{\Delta 7c}$, so that expression of in-frame fusions between AtADS3 plastidial transit peptide (AtADS3 1-71) and the cytoplasmic desaturases AtADS1 or AtADS2 functionally complements the *ads3*/*fad5* phenotype [138]. These results suggest that AtADS3/FAD5 evolved from an ancestral cytosolic ADS by the addition of a plastidial transit peptide. The observation that the enzyme can still be active in two different cell compartments is somehow surprising considering the contrasted environments of the plastidial and cytoplasmic membranes and the presence of different electron donors (ferredoxin in the plastid versus cytochrome b_5 in the ER).

Homologs of the *Arabidopsis* ADS enzymes have been identified in other plant species, but very few have been functionally characterized. The biosynthesis of the unusual monounsaturated $20{:}1^{\Delta 5}$ in seeds of *Limnanthes* species (meadowfoam) involves a presumptive ER-bound ADS identified by random sequencing of an expressed sequence tag library prepared from *Limnanthes douglasii* seeds [146]. The substrate for this reaction is thought to be a 20:0-CoA [147]. Likewise, Δ5 desaturase activity on acyl chains has also been demonstrated for two ADS homologs isolated from developing seeds of *Anemone leveillei*, with indirect evidence suggesting that both enzymes utilize acyl-CoA substrates [148]. When expressed in *Arabidopsis*, one of these desaturases termed AL21 inserts Δ5 double bonds into both saturated (16:0 and 18:0) and unsaturated substrates ($18{:}2^{\Delta 9c,12c}$ and $18{:}3^{\Delta 9c,12c,15c}$), in the latter case in a non-methylene-interrupted manner, raising the possibility that this

desaturase may be responsible for the production of 16:1$^{\Delta 5c}$ and 18:1$^{\Delta 5c}$ detected in *Anemone leveillei* seed oil [148].

Whereas three dimensional structures of plant ADS are still missing, structures of mouse [149] and human stearoyl-CoA desaturases [150] are available. They show a fold comprising four long transmembrane alpha-helices presumably spanning the ER membrane and capped by a cytosolic domain. The acyl chain of the bound acyl-CoA substrate is inserted in a long, narrow tunnel buried into the mostly hydrophobic interior of the cytosolic domain of the protein. The conformation of this sharply kinked tunnel and the bound acyl chain provide a structural basis for the stereospecificity (induction of a *cis* conformation) and regioselectivity of the desaturation reaction [149]. A di-metal cluster coordinated by a unique spatial arrangement of conserved histidine residues sits at the kink in the substrate tunnel adjacent to carbons where the double bond is introduced and features the active site of the enzyme. All of the AtADS proteins display histidine clusters that are similar to those coordinating the two metal ion co-factors in the reference structure of the mammalian stearoyl-CoA desaturase, with almost identical spatial arrangement. Most hydrophobic amino acid residues lining the tunnel surface of mammalian and plant ADS appear to be well conserved, suggesting a rather good conservation of the enzyme structure. In a recent advance, the mechanism enabling ADS enzymes to desaturate VLCFA-CoA was reported. A tyrosine with bulky side chain forming the end of the substrate binding cavity for long chain desaturation is substituted for alanine or glycine, creating an opening in the end of the cavity that enables the methyl end of the substrate to exit the cavity and enter the lipid bilayer. Thus, various lengths of VLCFA-CoA can be accommodated with carbons Δ9 and Δ10 adjacent to the diiron site enabling Δ9 desaturation [151]. It would be equally interesting to observe how plastid-localized ADSs interact with the head group of MGDG and to elucidate how their acyl-lipid substrate initially buried in the lipid bilayer of a membranes accesses the catalytic domain of the desaturase.

3.3.2. FATTY ACID DESATURASE4 (FAD4)

In *Arabidopsis*, biosynthesis of 16:1$^{\Delta 3t}$ is catalyzed by FAD4, a plastid acyl-lipid desaturase involved in the formation of a *trans* double bond introduced close to the carboxyl group of 16:0, which is specifically esterified to the *sn*-2 position of the glycerol backbone of PG [152] (Figure 6). Identification and thorough characterization of this enzyme has confirmed results of labeling kinetics performed in algae suggesting that 16:0 esterified in PG is the substrate for the biosynthesis of 16:1$^{\Delta 3t}$ [153]. AtFAD4 is rather unusual in its evolutionary lineage and structural characteristics [44]. AtFAD4 does not appear evolutionarily related to other well-characterized FADs and is relatively smaller in size (37 kDa). Some algorithms predict four transmembrane domains for AtFAD4, but weak confidence scores, so that AtFAD4 may not adopt a transmembrane-spanning topology [154]. Instead, AtFAD4 is proposed to be associated with thylakoid membranes, facing the stroma, although the molecular mechanism underpinning this association remains to be elucidated [155]. AtFAD4 is a metalloenzyme whose protein sequence contains two histidine motifs (HAWAH and HAEHH) potentially coordinating a metal center involved in catalysis. Sequences and spacing of these motifs are reminiscent of, but not identical to conserved motifs in membrane-bound desaturases [85]. A third histidine motif potentially

involved in metal binding consists of QGHH [152]. Again, its sequence diverges from the third histidine motif present in membrane-bound desaturases. The *AtFAD4* gene has two closely related paralogs in *Arabidopsis*, *At1g62190* and *At2g22890*, whose functions remain uncharacterized [152].

AtFAD4 exhibits similarity with the CarF protein of the bacteria *Myxococcus xanthus*, which was initially thought to be involved in singlet oxygen signaling-mediated regulation of carotenoid biosynthesis [156]. More recently, CarF was shown to exhibit a plasmanylethanolamine desaturase activity which introduces the characteristic vinyl ether double bond into plasmalogen [157]. However, production of vinyl ether lipids could not be observed with AtFAD4 or AtFAD4-like paralogues, suggesting that these evolutionarily related enzymes have diverged in their structural and functional characteristics.

Interestingly, it was recently shown in *Arabidopsis* that production of $16{:}1^{\Delta 3t}$ also requires a thylakoid-associated redox protein termed PEROXIREDOXIN Q (PRXQ) [155]. The biochemical relationship between AtFAD4 and AtPRXQ appears to be very specific *in planta*, but the exact function of AtPRXQ remains uncertain. Despite a redox potential similar to that of plant ferredoxins, the absence of an iron-sulfur cluster in AtPRXQ makes it unlikely that the protein acts as the electron donor for AtFAD4. It was instead hypothesized that AtPRXQ may have a protective role for an oxidation-sensitive AtFAD4 enzyme. Given the proposed thylakoid location of AtFAD4, the desaturase might be susceptible to oxidation damage from photosynthesis-derived reactive oxygen species byproducts [155]. The protective role of AtPRXQ could be all the more important that $16{:}1^{\Delta 3t}$ synthesis was shown to be stimulated by high irradiance [158]. However, it is not clear why AtFAD4 expressed in yeast without AtPRXQ does not show any activity, when other FAD enzymes work well in the absence of additional redox-protective factors [155].

3.3.3. Cytochrome b_5 (Cb_5)-containing desaturases

A plant ∆8 LCB desaturase was first identified in *Helianthus annuus* (sunflower) as a desaturase-like enzyme containing an N-terminal cytochrome b_5 domain and conferring production of ∆8 unsaturated LCBs, when expressed in *Saccharomyces cerevisiae* [159-160]. Since then, homologs have been characterized in various species such as *Brassica napus* (rapeseed) [161], *Borago officinalis* [162], *Anemone leveillei* [123], *Nicotiana tabacum* [163], *Primula nivalis* and *Primula auricula* [9], *Ribes Nigrum* [164], *Aquilegia vulgaris*, *Sorghum bicolor*, *Triticum aestivum*, *Ricinus communis*, *Vitis vinifera*, *Glycine max* (soybean), *Populus tomentosa*, *Cucumis sativus*, and *Brachypodium distachyon* [165]. Thus, it seems that all higher plant species contain ∆8 LCB desaturases. In *Arabidopsis*, two paralogs, AtSPHINGOLIPID LCB ∆8 DESATURASE1 (SLD1) and AtSLD2, were identified and confirmed to be LCB ∆8 desaturases through yeast and *in planta* studies (Figure 4), AtSLD1 being the predominant contributor to LCB ∆8 unsaturation [161,166] (Figure 7). It is thought that sphingolipid ∆8-desaturases mostly use saturated LCBs bound in ceramides as substrates, rather than free LCBs [98,161]. Interestingly, the enzymes are stereo-unselective and insert both *cis* and *trans* double bonds at the C-8 position of their LCB substrates [49]. *Cis*/*trans* isomerism of the ∆8 unsaturation of LCBs is specific to plant sphingolipids [167]. When 20 genes encoding different LCB ∆8 desaturase isoforms originating from 12 plant species were expressed in *Saccharomyces cerevisiae* to elucidate the

relationship between the biochemical function and evolution of this enzyme, the isoforms could be divided into two groups on the basis of enzymatic characteristics: desaturase with a preference for a *trans*-isomer product and desaturase with a preference for a *cis*-isomer product. The conversion rate of the latter was generally lower than that of the former [165]. These *cis*/*trans* mixed stereospecificities were proposed to arise from alternative positioning of substrates in the active site of the desaturases [168], implying that their active site cavity is large or flexible enough to bind the substrate in two alternative conformations [44,98].

Cb_5-containing desaturases from higher plants display two main types of enzymatic activities. Whereas some of these were characterized as sphingolipid LCB Δ8 desaturases [98], others play key roles in the biosynthesis of very long-chain polyunsaturated fatty acids [65]. A study of the closely related Δ6 fatty acid desaturase and Δ8 LCB desaturase from *R. nigrum* showed that the N-terminal domains which contain cytochrome b_5 domains could be swapped without affecting the activity and substrate recognition of either enzyme [169]. As for substrate discrimination of the two types of enzymes, these experiments and others suggest that substrate specificity is not controlled by a specific stretch of amino acids but rather by residues dispersed distantly in the primary amino acid sequence of the protein [170,171]. To date, their identity and precise role remain unknown.

An intriguing characteristic of the Cb_5-containing desaturases is the replacement of the first histidine by glutamine in their third histidine box (Figure 4), when the structure of the active site appears rather invariant among membrane-bound desaturases [44]. The Cb_5-containing desaturases are usually limited in their regioselectivity to substrate positions along the substrate chain lying between carbons Δ2 and Δ10, that are close to the interfacial layers covering the hydrophobic core of the bilayer [172]. The di-iron complexes of desaturases being surrounded by sequences of intermediate polarity/hydrophobicity, it has been suggested that the active sites may be located near the membrane surface [81]. This position represents a compromise allowing optimization of the encounters with both the hydrophilic head of the electron donors and the hydrophobic substrate segments occasionally emerging from the membrane interior.

Surprisingly, a new atypical Cb_5-containing desaturase named PpSFD was recently described in *Physcomitrella patens* that catalyzes the introduction of double bonds at the ω8 position in VLCFAs of sphingolipids and some phospholipids like PE and phosphatidylcholine (PC) [173]. This activity being somehow reminiscent of that of the *Arabidopsis* AtADS2 acyl-CoA desaturase, the *PpSFD* gene was ectopically expressed in the cold sensitive *Arabidopsis* mutant *ads2*, defective in a methyl-end ω9 desaturase activity. The complementation of the mutant phenotype suggests that the slightly different double-bond insertion preference (ω9 in AtADS2 versus ω8 in PpSFD) does not affect the functionality of PpSFD in *Arabidopsis*. This remarkable convergence of sphingolipid VLCFA desaturation during plant and moss evolution invites to deepen our knowledge of the structure-function relationships among the Cb_5-containing desaturases.

3.3.4. Sphingolipid Δ4-desaturases

In *Arabidopsis*, sphingosine (d18:1$^{\Delta 4t}$) is synthesized via the Δ4-*trans*-desaturation of sphinganine (also known as dihydrosphingosine; d18:0) (Figure 7) [174]. The *Arabidopsis* genome contains a

unique dihydrosphingosine Δ4 desaturase (DSD)-coding gene that was identified by homology to analogous genes in mammals and filamentous fungi [174-175]. The exact nature of the substrate (*i.e*. LCB or ceramide) of related Δ4 desaturases in other organisms remains to be clarified, so that these enzymes are generally termed sphingolipid Δ4 desaturases. They define a class of desaturases evolutionary distinct from the sphingolipid Δ8 desaturases, and they do not contain a cytochrome b_5 domain [45,175] (Figure 4). They share only limited similarity with any other desaturases characterized by the histidine box motifs and form a clade distinct from other microsomal lipid desaturases [176].

4. Elongation of preexisting monounsaturated acyl chains

4.1. The fatty acid elongase complex

Not all of the monounsaturated acyl chains directly derive from the desaturation of saturated substrates. Instead, some monounsaturated fatty acids result from the elongation of shorter monounsaturated acyl chains. This is the case for very long-chain monounsaturated fatty acids produced by the ER-localized multienzyme fatty acid elongase complex [177]. A cycle of elongation involving four reactions adds two carbon units to a pre-existing acyl-CoA. Condensation of malonyl-CoA with a long chain acyl-CoA is catalyzed by a 3-ketoacyl-CoA synthase (KCS, condensing enzyme) [178-181]. The resulting 3-ketoacyl-CoA is reduced by the action of a β-ketoacyl-CoA reductase [182], yielding 3-hydroxyacyl-CoA that is then dehydrated to 2-enoyl-CoA by a 3-hydroxyacyl-CoA dehydratase [183-184]. A second reduction reaction catalyzed by an enoyl-CoA reductase reduces the enoyl-CoA, resulting in an elongated acyl-CoA [177]. The initial step in fatty acid elongation catalyzed by members of the KCS family is not only considered as rate limiting in the elongation process but also proposed to determine the substrate specificity and therefore the type of VLCFA produced [185]. By contrast, the other three enzyme activities of the elongase complex are thought to exhibit broad substrate specificities [186].

Plant genome sequencing has revealed large *KCS* families, with 21 *AtKCS* genes present in the *Arabidopsis* genome for example [179]. Functional characterization of known KCSs, though incomplete, has revealed contrasted substrate specificities applying not only to chain length, but also to the unsaturation level of the substrate [185]. Some isoforms, like AtKCS11 or AtKCS18/FATTY ACID ELONGASE1 (FAE1), are able to use both saturated and monounsaturated acyl chains, while AtKCS17 appears to be specific for saturated acyl-CoAs and PotriKCS1 for monounsaturated acyl chains [13]. The seed-specific *AtKCS18*/*FAE1* gene [187] and orthologs from different species like *Brassica napus* [188-191], *Crambe abyssinica* [181], *Teesdalia nudicaulis* [192], *Tropaeolum majus* [193] are responsible for the biosynthesis of C20 and C22 fatty acids incorporated in storage lipids, including the elongation of $18{:}1^{\Delta 9c}$ into $20{:}1^{\Delta 11c}$ and $22{:}1^{\Delta 13c}$. *Arabidopsis* FAE1 has more activity toward a C18 substrate than toward a C20 substrate, whereas the *Brassica napus* FAE1 enzyme exhibits similar activity toward both fatty acyl groups [185]. Hence the higher $22{:}1^{\Delta 13c}$-to-$20{:}1^{\Delta 11c}$ ratio observed in *Brassica napus* seed oil [194]. These ω9 very-long chain monounsaturated fatty acids can be further elongated to $24{:}1^{\Delta 15c}$ by other KCS isoforms [195]. The *KCS* genes involved in the biosynthesis of $24{:}1^{\Delta 15c}$ have been isolated from *Lunaria annua* [196], *Cardamine graeca* [197], and *Malania oleifera* [195]. Importantly, AtKCS18/FAE1 and orthologs can elongate both ω7 and ω9

monounsaturated substrates, as demonstrated by the concomitant loss of ω7 and ω9 very long-chain monounsaturated fatty acids in *fae1* mutants [114,198].

To form C-C bonds, KCS enzymes use a decarboxylating Claisen condensation mechanism relying on a cysteine-histidine-asparagine catalytic triad in which the cysteine residue forms an acyl-enzyme reaction intermediate with the substrate [199,200]. Acylation of the enzyme constitutes a prerequisite for the decarboxylation of the malonyl-CoA, with the histidine and asparagine of the catalytic triade participating in decarboxylation [201]. Despite the lack of crystal structure for KCS enzymes, several studies aimed at gaining insights into the structural bases for KCS catalysis and substrate specificity have been reported. Modeling studies using known structures of condensing enzymes showing similarity to the KCSs (such as the chalcone synthases) have proposed that KCS display a triangular shape with a prominent N-terminal arm [179]. The position, size, and hydrophobicity of this arm make it suitable for anchoring the enzyme in the ER membrane [201]. A cavity running throughout the enzyme then corresponds to a putative substrate-binding pocket, in accordance with bioinformatic predictions [179]. This pocket surrounds the active cysteine residue playing the role of the acyl acceptor in the first step of the condensation reaction [202,203]. Depending on the KCS modeled, different shapes and sizes for the predicted binding pocket were observed. It was hypothesized that these different topologies might be related to substrate preference [179], even though *in vivo* activities of KCS enzymes expressed in yeast suggest that the substrate-binding pocket is flexible [204]. Site-directed mutagenesis experiments have enlightened the importance of the N-terminal region of the protein, excluding the transmembrane domain, for imparting chain-length substrate specificity [204]. This region appears to be of particular heterogeneity among the plant KCS enzymes, in good agreement with the contrasted substrate specificities of these isoforms. The swapping of N-terminal domains between *Brassica napus* and *Arabidopsis* KCS18/FAE1 enzymes was sufficient to modify chain-length substrate specificity [204].

The condensation reaction of an acyl-CoA with a malonyl-CoA can also be catalyzed by elongases of the ELO family that are found in a wide range of organisms including plants [200]. However, these elongases that display no similarity in primary sequences or predicted three-dimensional structures with the KCS enzymes remain poorly characterized in plants and have not been associated with the elongation of monounsaturated acyl chains so far. In contrast, KCS-like 3-ketoacyl-ACP synthase II (KASII) enzymes were described in the Amazonian palm *Jessenia bataua* as well as in related palm species (*Elaeis guineensis* and *Elaeis oleifera*) that lack plastid-targeting signals and may be located in the microsomal fraction, although this subcellular location remains to be confirmed. Ectopic expression of one of these genes in *Arabidopsis* suggests that the corresponding 'KCS-like' enzyme may elongate both saturated and monounsaturated C18 chains [205]. Even though complementary approaches would be necessary to further characterize these enzymes, these results invite us to broaden the scope of the search for potential actors involved in the elongation of monounsaturated fatty acids.

4.2. The fatty acid synthase complex

In higher plants, *de novo* fatty acid biosynthesis is performed by a fatty acid synthase of type II, an easily dissociable multisubunit complex consisting of monofunctional enzymes [103,206,207]. Acetyl-CoA is used as the starting unit, and malonyl-ACP provides two-carbon units at each step of elongation. Cycles of acyl-ACP elongation are similar to that of acyl-CoA elongation catalyzed by the fatty acid elongase complex in the ER. Each cycle involves four enzymatic reactions catalyzed by 3-ketoacyl-ACP synthase (KAS), 3-ketoacyl-ACP reductase, hydroxyacyl-ACP dehydratase, and enoyl-ACP reductase [38]. Three KAS isoforms are required to produce 18-carbon fatty acids. The initial condensation reaction of acetyl-CoA and malonyl-ACP is catalyzed by KAS isoform III (KASIII), yielding a four-carbon product. Subsequent condensations (up to 16:0-ACP) require a second enzyme, namely KASI, whereas the final elongation of 16:0 to 18:0 is catalyzed by a third condensing enzyme, KASII [208,209]. If the fatty acid synthase complex is usually described as producing saturated acyl chains, it has been postulated that some KAS isoforms might be able to use $16{:}1^{\Delta 9c}$-ACP as substrate to form $18{:}1^{\Delta 11c}$-ACP. A KASII isoform was unambiguously assigned with such activity in *Escherichia coli* [210-211]. While a loss of function mutation affecting the *KASII* gene in *Arabidopsis* was shown to result in an embryo lethal phenotype [209,212], lines exhibiting decreased KASII contents as a consequence of a leaky mutation [208] or suppression strategies [198,209] were not sufficiently characterized to provide firm conclusions regarding the substrate specificity of this enzyme. More generally, the elongation of unusual monounsaturated acyl-ACP species in the plastids remains poorly characterized in plants. The only example of a KAS putatively involved in the elongation of a monounsaturated acyl-ACP is that of a KAS from *Coriandrum sativum* displaying a strong preference for the elongation of $16{:}1^{\Delta 4c}$-ACP *in vitro*, and hence regarded as a good candidate for the biosynthesis of $18{:}1^{\Delta 6c}$-ACP [213]. Direct proof of the function of this KAS is still missing however.

5. Known biological functions of plant monounsaturated fatty acids

One long-standing objective of plant lipid research is to link structure to function for particular molecular species in specific developmental and environmental contexts. Whereas the biological functions of the most common plant monounsaturated fatty acid species have gradually emerged through several decades of research combining biochemistry and functional genomics, the specific functions of most unusual monounsaturated fatty acids remain elusive.

5.1. Monounsaturated acyl chains as intermediates in lipid metabolism

Some monounsaturated fatty acid species do not seem to fulfill specific biological functions per se, but instead serve as precursors for the elaboration of further modified acyl chains. In this context, the first desaturation reaction can constitute a rate-limiting step or selectively channel acyl chain precursors in a given pathway. For example, $16{:}3^{\Delta 7c,10c,13c}$ is one of the most abundant fatty acids in the photosynthetic organs of so-called '16:3 plants'. This fatty acid is confined to the *sn*-2 position of MGDG and results from the sequential desaturation of 16:0 [214-215]. In *Arabidopsis*, a three-step desaturation pathway involving *AtFAD5* [141], *AtFAD6* [216], and *AtFAD7* [217] or *AtFAD8* [218]

sequentially introduces the Δ7, Δ10, and Δ13 double bonds (Figure 6). Mutant plants in which the initial AtFAD5-mediated Δ7 desaturation step is compromised exhibit growth defects and reduced leaf chlorophyll content [138,219], while recovery of PSII appears to be delayed after photoinhibition by high-light stress [142]. A high degree of fatty acid unsaturation associated with MGDG is thought to favor thylakoid assembly and constitutes a possible explanation for the *fad5* phenotypes [138,220].

In striking contrast with $16{:}1^{\Delta 7c}$, a fatty acid poorly abundant in plant tissues and almost exclusively used for synthesizing $16{:}3^{\Delta 7c,10c,13c}$, other monounsaturated fatty acids like $18{:}1^{\Delta 9c}$ were assigned multiple functions as such (see below), while also constituting the entry point to a variety of modification pathways. Oleoyl-CoA can be further elongated in the ER by the fatty acid elongase complex [177], yielding very long-chain monounsaturated fatty acyls like $20{:}1^{\Delta 11c}$ or $22{:}1^{\Delta 13c}$ (Figure 7). When bound to PC, $18{:}1^{\Delta 9c}$ can be successively desaturated by ER-localized FAD2 [221-222] and FAD3 desaturases [223], yielding $18{:}2^{\Delta 9c,12c}$ and $18{:}3^{\Delta 9c,12c,15c}$ polyunsaturated fatty acids (Figure 7). An equivalent desaturation sequence catalyzed by FAD6 and FAD7/FAD8 uses $18{:}1^{\Delta 9c}$ bound to plastidial glycerolipids to also produce $18{:}3^{\Delta 9c,12c,15c}$ [224] (Figure 6). This is but brief overview of the very large array of fatty acid species derived from $18{:}1^{\Delta 9c}$ that play multiple roles in plants as components of structural and storage lipids [31,225] or as signaling molecules [120,226].

Just like $18{:}1^{\Delta 9c}$, $18{:}1^{\Delta 11c}$ can be further elongated by the fatty acid elongase complex to produce $20{:}1^{\Delta 13c}$ and $22{:}1^{\Delta 15c}$ [114,227], while the double bond present at position Δ11 prevents further desaturation of the acyl chain by FAD2 or FAD6, therefore significantly reducing the number of $18{:}1^{\Delta 11c}$ derivatives. Interestingly, the first unsaturation introduced in acyl chains not only determines the type of further modifications that could target these acyl chains but, in some cases, also influences the channeling of unsaturated products during the elaboration of complex lipids. It was thus shown that LCB structure dictates downstream partitioning and ultimately determines the composition and content of specific sphingolipid classes [47]. *Arabidopsis sld1 sld2* double mutant lacking long-chain base Δ8 unsaturation exhibits a 50% reduction in glucosylceramides and a proportional increase in glycosyl inositol phosphoceramides (GIPCs), possibly due to the substrate specificity of glucosylceramide synthase [166]. Similarly, *Arabidopsis* mutants for the LCB Δ4 desaturase exhibit a 50% glucosylceramide reduction in pollen [174]. Altogether, these results exemplify how monounsaturation of LCBs contributes to metabolic partitioning of ceramides between glucosylceramide synthesis in the ER and GIPC synthesis in the Golgi.

5.2. Oleic acid - $18{:}1^{\Delta 9c}$

Classical biochemical analyses, complemented over the last decade by lipidomic analyses, have unambiguously designated oleic acid as one of the most ubiquitous fatty acid in plants [38,228]. Apparently occurring to some extent in all plant oils [30] (see below), oleic acid is also a common component of membrane glycerolipids, including PC, PE, phosphatidylinositol, PG, MGDG, digalactosyldiacylglycerol (DGDG), and sulfoquinovosyldiacylglycerol (SQDG) [38]. As such, oleic acid is found in every cell membrane and every cell compartment. Moreover, oleic acid can be present outside of certain cell types as a minor component of cutin and suberin polyester barriers [38]. Despite the ubiquitous presence of oleic acid and its derivatives in plants, and possibly due to this widespread

distribution among different lipid categories, the specific functions of oleic acid as a structural component of the plant cell have never been clearly elucidated. The characterization of simple and multiple mutants affected in Δ9 SAD-coding genes has revealed the importance of $18:1^{\Delta 9c}$ biosynthesis during vegetative development and seed formation. Nevertheless, the rather large fatty acid and lipid remodeling occurring in these mutant backgrounds has often prevented the authors from attributing the severe developmental phenotypes observed to precise biochemical modifications [229-231]. A specific function of $18:1^{\Delta 9c}$ as a signaling agent involved in plant immunity and participating in the crosstalk between salicylic acid and jasmonic acid signaling pathways during pathogen infection makes exception to this rule [232]. By physically interacting with NITRIC OXIDE ASSOCIATED1 (NAO1), plastid $18:1^{\Delta 9c}$ represses its activity, leading to the regulation of defense signaling via suppression of NO production [233]. This aspect has been extensively reviewed elsewhere [120,234,235].

5.3. *3E*-Hexadecenoic acid - $16:1^{\Delta 3t}$

The apparently universal occurrence of $16:1^{\Delta 3t}$ in the thylakoid membranes of green algae and higher plants has invited considerable speculation about a potential role of $16:1^{\Delta 3t}$-PG in photosynthetic membrane organization or function conferring some selective advantage [39,40,236]. Because $16:1^{\Delta 3t}$-PG is absent in etiolated tissues and accumulates in thylakoid membranes during light-induced chloroplast development, a specific role associated with the light reactions of photosynthesis was proposed [237]. Together with the galactolipids MGDG and DGDG, and the sulfolipid SQDG, PG indeed establishes the backbone of thylakoid membranes and is a structural component of the photosynthetic complexes. Approaches of X-ray crystallography have established that PG is present in photosystem I and II [238,239]. The lipid is essential for the stabilization of photosystem I trimers and photosystem II core dimers, which represent the functionally active forms of the photosystems *in planta* [240-244]. What is more, PG, which also contributes to the assembly and stabilization of light-harvesting complex II [245], might play a role in non-photochemical quenching of excess light [158]. However, *Arabidopsis fad4* mutants devoid of $16:1^{\Delta 3t}$ appear to grow normally under standard laboratory conditions. They show no obvious differences in grana development or in any major ultrastructural features of the chloroplast. Only minor effects of the *fad4* mutation on photosynthesis could be observed when compared with mutations affecting the biosynthesis of other chloroplast lipids [246]. These observations rule out the hypothesis of an obligatory involvement of $16:1^{\Delta 3t}$ in the development of thylakoid structure or in the light reactions of photosynthesis under normal growth conditions. Instead, the role of $16:1^{\Delta 3t}$-PG in photosynthetic tissues might be more subtle than previously suggested or manifest only under particular environmental conditions [246].

Surprisingly, whereas a specific function of $16:1^{\Delta 3t}$-PG in leaves has remained elusive, a possible role in seed triacylglycerol production has recently been attributed to this lipid species in *Arabidopsis* [247]. In essence, $16:1^{\Delta 3t}$ uniquely labels a small but biochemically active plastid PG pool in developing embryos, which is specifically recognized by a thylakoid-associated phospholipase A_1 termed PLASTID LIPASE1 (PLIP1). AtPLIP1 activity results in the release of polyunsaturated *sn*-1 acyl groups from $16:1^{\Delta 3t}$-PG for incorporation into triacylglycerol *via* the extraplastidic membranes,

thereby contributing a small fraction of the polyunsaturated fatty acids present in seed oil. Similar to the *plip1* mutants, the *fad4* mutants exhibit a nearly 10% reduction in total seed fatty acid content [247].

5.4. Monounsaturated acyl chains and membrane fluidity

While several environmental parameters, especially temperature, exert major effects on various physical properties of biological membranes and influence membrane fluidity, maintaining the integrity and fluidity of membranes is generally agreed to be of fundamental importance for plants to survive under extreme environmental conditions [248,249]. Temperature-induced changes involve membrane permeability to water, solutes, and protons [250], but also impacts the activity of membrane-associated proteins [251]. Plants were shown to balance these changes by regulating the level of saturation of membrane glycerolipids, as the introduction of an appropriate number of unsaturated bonds into the acyl chains of membrane glycerolipids decreases the phase-transition temperature from the gel (solid) to the liquid-crystalline phase and maintain the integrity and optimal fluidity of these membranes [67,252,253]. Unsaturated fatty acids display a lower transition temperature than their saturated counterparts because the steric hindrance imparted by the rigid kink of the double bond results in decreased packing of the acyl chains [63]. Interestingly, the biggest shift in melting properties occurs with the first double bond. When considering non-esterified C18 fatty acids for example, the transition from 18:0 to $18{:}1^{\Delta 9c}$ yields a 50°C decrease in melting temperature, whereas the downward shift accompanying the $18{:}1^{\Delta 9c}$-to-$18{:}2^{\Delta 9c,12c}$ transition is less than 20°C. The addition of a third unsaturation, yielding $18{:}3^{\Delta 9c,12c,15c}$, has almost negligible impact on melting properties (–5°C). Biophysical studies have established that the transition temperature of membrane lipids also depends on the position of the double bonds in the acyl chains as documented by the transition temperatures of PC molecules comprising two 18:0 (58°C), $18{:}1^{\Delta 5c}$ (10°C), $18{:}1^{\Delta 9c}$ (-20°C), or $18{:}1^{\Delta 13c}$ groups (0°C) [44,254]. In cold acclimated plants, the most saturated fatty acid species are therefore depleted [255,256], following the saturation grade principle, whereas high temperatures result in a reduction in the degree of unsaturation of fatty acids [252]. In photosynthetic tissues, galactolipids, which are the dominant component of thylakoid membranes, are major contributors to membrane unsaturation [257]. In these membranes, levels of $16{:}3^{\Delta 7c,10c,13c}$ and $18{:}3^{\Delta 9c,12c,15c}$ trienoic acids play a role of the utmost importance in maintaining membrane fluidity [256,258]. Monounsaturated C24 fatty acids comprised in various classes of membrane lipids may also play a role in membrane adaptation to varying temperatures, as suggested by the slower growth rate of *Arabidopsis ads2* mutants lacking monounsaturated C24 fatty acids [137]. In agreement with this hypothesis, *AtADS2* gene exhibits increased expression level in response to cold treatment [135].

But glycerolipids are not the only lipid components of cell membranes. Sterols and sphingolipids together form lipid raft microdomains that are important for recruiting receptor and signaling proteins [259], and small changes in sphingolipid content can have drastic effects on the formation of these microdomains. Whereas Δ8 unsaturation of LCB moieties of sphingolipids is not critical for growth under optimal conditions, a role for LCB unsaturation in chilling and freezing tolerance has been proposed [260-261]. The *Arabidopsis sld1 sld2* double mutant grown at 0°C develops a chlorotic

appearance and senesces prematurely with respect to wild-type plants [166], suggesting that LCB Δ8 desaturation contributes to the structural properties of the plasma membrane under environmental extremes [47]. These extremes not only include cold temperatures, since experimental approaches have shown that increasing the proportion of t18:1$^{\Delta 8c}$ LCB in sphingolipids was accompanied by improved tolerance towards elevated aluminum and gadolinium concentrations [262,263]. *Cis*-unsaturated glucosylceramides were proposed to maintain the membrane fluidity specifically associated with aluminum tolerance [167].

5.5. Monounsaturated acyl chains in surface lipids

Overall, the cuticle layer coating most aerial surfaces of land plants plays a major role in coordinating interactions between the plant and its environment, protecting the plant against adverse biotic and abiotic factors [144,264]. This hydrophobic barrier limits nonstomatal water loss, scatters UV radiations, and plays key roles in defense against insects and pathogens [265]. The cuticle is a composite structure comprising two lipid classes, the cutin polyester, a scaffold of long-chain fatty acid derivatives [266], and the non-polymerized cuticular waxes typically dominated by VLCFA derivatives like alkanes, alkenes, aldehydes, primary alcohols, secondary alcohols, ketones, and esters [56,267,268]. The use of monounsaturated fatty acids, in the strictest meaning of the term, for cuticle biosynthesis is rather limited [38]. By contrast, their monounsaturated derivatives can be fundamental components of cutin and cuticular waxes in certain plant species [38,55]. For example, monounsaturated alkenes have been described in the cuticular waxes of diverse plants [56,269,270]. Two complementary pathways contribute to the biosynthesis of different types of alkenes: one involving acyl-ACP desaturases, with desaturation of long chains occurring before elongation and removal of the carboxyl head group, the other involving acyl-CoA desaturases, with desaturation of very long chains occurring between elongation and head group removal. It seems likely that the presence of these alkenes affects the physical (texture and fluidity, as a function of temperature) and biological properties of the cuticular wax mixtures, even at relatively low concentrations, suggesting that they fulfill specific ecophysiological roles [271-273]. For example, the presence of wax alkenes in leaves of *Poplar trichocarpa* was associated with modified cuticle functions, such as enhanced resistance to leaf spot disease caused by an ascomycete [13]. Then, alkenes produced in the flower of some species of the Mediterranean orchid genus Ophrys participate in the chemistry of sexual deception, favoring plant pollination by hymenopterans [120]. Bioassays have emphasized the importance of the alkene unsaturation position for controlling pollinator preference [274]. Modeling approaches have illustrated how variations in acyl-ACP desaturase paralogs associated with alkene structure variations can drive evolutionary divergence between orchid species, with subsequent reproductive isolation allowing for rapid sympatric speciation by pollinator shift [120,275]. These examples emphasize the importance of initiating further studies to elucidate the ecological significance of monounsaturated compounds in surface lipids.

6. Monounsaturated fatty acids in storage lipids

Many land plants accumulate storage lipids, usually in the form of triacylglycerols, in seed and fruit tissues. Triacylglycerols stored in seeds are remobilized to fuel post-germinative seedling establishment, a period of the plant life cycle playing a crucial role in plant fitness [276]. During this process, and prior to initiation of photosynthesis in the seedling, nearly all nonparasitic angiosperms rely exclusively on reserves stored in seeds to meet two critical requirements: a source of carbon skeleton precursors and an energy source to assemble these precursors. Storage lipids efficiently fulfill these two requirements [118,277-279]. As for triacylglycerols stored in the oily mesocarp of certain fruits, they typically serve in the attraction of animals that consume these nutritious fruits, thus favoring seed dispersal [118,280,281]. Plants collectively display huge variation in the fatty acids they synthesize and store into seeds and fruits, including an array of common and unusual monounsaturated fatty acids. Many of these fatty acids have a great potential for food and chemical industries due to the particular physicochemical properties inherent in their structure [31].

6.1. Omega-9 monounsaturated fatty acids

6.1.1. Oleic acid - $18:1^{\Delta 9c}$

Oleic acid is very common in vegetable oils. Oils rich in oleic acid are desirable in the food industry for their considerable cooking and health benefits. Notably, oleic acid is oxidatively stable in comparison with its polyunsaturated derivatives [282]. For this reason, oils rich in oleic acid are more shelf-stable and their higher heat tolerance makes them optimal for deep-fat frying [283,284]. Moreover, oleic acid, the main fatty acid in olive oil, has been ascribed a number of health-beneficial properties. Noticeably, it reduces the risk of cardiovascular diseases [285] while suppressing tumorigenesis of inflammatory diseases [286]. Monounsaturated fatty acids like oleic acid also have significant industrial potential due to their higher thermal-oxidative stability and viscosity relative to other common fatty acids [287,288]. There is an increasing interest in the use of plant oils with high oleic acid as a renewable raw material in the production of biolubricants and biodiesel [289]. Finally, chemical cleavage of monounsaturated fatty acids at their double-bond yields monomers in high demand by the chemical industry. Oleic acid can thus be processed to yield azelaic acid (C9) monomers for nylon production [290].

For all these reasons, conventional breeding programs and biotechnological approaches have been implemented to increase the oleic acid content of oils in various oleaginous crops [290]. Characterization of the genetic diversity and mining of cultivar collections and lines developed by chemical mutagenesis have revealed the high degree of variability of oleic acid content in the fatty acid composition of oils. For example, *Olea europaea* (olive) cultivars exhibit an important phenotypic plasticity, with oleic acid accounting for 55 to 83% of total fatty acids in fruit mesocarp [291]. These approaches have contributed to identify germplasms of interest for conventional breeding programs aimed at developing high-oleic compositions. Characterization of lines with contrasted oleic acid content has also paved the way for the development of DNA markers linked to the loci determining oleic acid content that are useful for marker-assisted breeding [292]. Numerous linkage and association mapping studies were implemented [293-303]. The $18:1^{\Delta 9c}$ content appears to be a polygenic trait, and no stable quantitative trait loci have been reported except for *FAD2*, that encodes

the Δ12 desaturase catalyzing the conversion of 18:1$^{\Delta 9c}$ to 18:2$^{\Delta 9c,12c}$ [221] (Figure 8). To date, most of the high oleic acid germplasms available carry *fad2* knockout or mild alleles [301,304,305]. While genetically improved oils exhibiting 75 to 85% oleic acid levels are ideal for food uses, significant residual levels of polyunsaturated fatty acids cause problems in industrial and oleochemical applications [290]. Germplasms producing oils with high 18:1$^{\Delta 9c}$ and low 18:3$^{\Delta 9c,12c,15c}$ were therefore developed [292,304]. Unfortunately, the lines obtained by manipulating the *FAD2* gene family and exhibiting an extremely high oleic acid content (>80%) have revealed lower agronomic performance including lower seedling establishment and vigor, delayed flowering, reduced plant height at maturity, and reductions in total seed oil content under field conditions [306,307]. These poor agronomic characteristics are most noticeable when plants are grown at lower temperatures. They may be the consequence of an undesirable reduction in the levels of polyunsaturated fatty acids in cell membranes [306].

Aside from these breeding programs, biotechnological approaches have allowed the development of high-oleic oilseed crops by suppression of *FAD2* gene(s) through targeted genome mutagenesis by means of TALENs [308], CRISPR/Cas9-mediated gene editing [309-316], or TILLING [317]. However, these techniques potentially impact fatty acid metabolism in all parts of the plant so that very high oleic acid phenotypes are usually associated with undesirable pleiotropic effects on crop performance [310,316]. Alternatively, more targeted transgenic approaches relying on seed-specific silencing constructs have been developed by means of antisense RNA [318-321], RNAi strategies [322-327], or a combination of these technologies [328]. If some promising achievements were thus obtained, it should be noted that these technologies have disadvantages, such as instability, variability, and incomplete knockdown of target genes, yielding incomplete removal of polyunsaturated fatty acids that contribute to poor oxidative stability of seed oils.

Other actors of lipid metabolism were suppressed, most of the time together with *FAD2*, within the frame of biotechnological approaches aimed at developing high oleic lines (Figure 8). *FAD3* was thus suppressed concomitantly with *FAD2* in *Glycine max* [329-330]. *REDUCED OLEATE DESATURASE1* (*ROD1*) encodes a phosphatidylcholine:diacylglycerol choline phosphotransferase (PDCT), that transfers a phosphocholine head group between PC and diacylglycerol. ROD1 acts as a gatekeeper enzyme by directing 18:1$^{\Delta 9c}$ molecules for further desaturation occurring on PC and catalyzed by FAD2 and FAD3 [331,332]. Knockout mutations of *ROD1* and *FAD2* were efficiently combined in *Thlaspi arvense* to increase oleic acid content [333]. Mutation or suppression of the seed-specific *KCS18*/*FAE1* component of the fatty acid elongase complex, by impairing or limiting the production of very long-chain monounsaturated acyl-CoAs, can also contribute to increase the overall oleic acid content of seed oils [333]. Simultaneous down-regulation of *KCS18*/*FAE1* and *FAD2* proved to be an efficient strategy to obtain high levels of oleic acid in seed oils of *Camelina sativa* [334], *Crambe abyssinica* [335], *Brassica napus* [336], *Lepidium campestre* [337], or *Thlaspi arvense* [333]. Finally, a particularly successful approach aimed at developing superhigh oleic lines of *Glycine max* [338,339] and *Carthamus tinctorius* (safflower) [326] consisted in the concomitant suppression of *FAD2* and *FATB*, the latter preventing 16:0 release from the fatty acid synthase complex and subsequent accumulation of saturated fatty acids. No apparent adverse effects on agronomic performance were

associated with these modifications of fatty acid metabolism. What is more, the very low amounts of polyunsaturated remaining in the oils obtained and the stability of the constructs used over several generations seem to permit commercial release and open the way for new industrial applications of oleic acid as a chemical feedstock.

6.1.2. Erucic acid - $22:1^{\Delta 13c}$

Oilseeds of Brassicaceae species represent major sources of oil for nutritional purposes on a global scale. In the past, these oils often displayed high contents of erucic acid [340]. Presence of high erucic acid in edible oil makes it nutritionally undesirable for human and animal consumption. For instance, erucic acid consumption has been associated with myocardial lipidosis (triacylglycerol accumulates in the heart due to insufficient oxidation), in turn resulting in reduced contractility of the heart muscle [341,342]. To avoid potential public health issues, the erucic acid content in edible oils was regulated in many countries, with maximum levels set to 2% of total fatty acids [343,344]. Thus, reducing erucic acid content has become a major goal for rapeseed breeding programs in particular. The KCS18/FAE1 component of the fatty acid elongase complex controls erucic acid production in seeds of Brassicaceae. The diploid Brassica species (*Brassica nigra* and *Brassica rapa*) have one copy of *KCS18*/*FAE1* gene while the amphidiploid species (*Brassica napus* and *Brassica juncea*) have two copies with additive effect [345-347]. In *Brassica napus*, erucic acid is genetically controlled by two additive alleles, *E1* and *E2*, corresponding to the structural genes encoding BnFAE1.1 and BnFAE1.2 [348,349]. Elimination of erucic acid was therefore achieved by genetic limitation of acyl chain elongation due to variations in the sequence or expression level of the KCS-coding gene(s) *KCS18*/*FAE1* [346,350-353]. After the discovery of low erucic germplasms with naturally occurring mutations affecting *KCS18*/*FAE1*, major breeding efforts in the 1960s have led to the development of low erucic acid rapeseed (LEAR) varieties also termed Canola [354]. Nowadays, double zero (00) Canola cultivars with a low erucic acid content and a low glucosinolate content are predominantly being grown in most parts of the world [355]. More recently, biotechnological approaches such as the RNAi knockdown of *KCS18/FAE1* have provided alternative means for the development of LEAR lines [356].

On the other hand, plant oils rich in erucic acid are of interest for industrial purposes, so that high erucic acid types have retained some attention in a context of increasing demand for biodegradable and environmentally safe oil products. A major derivative of erucic acid is erucamide, which is used as slip agent for manufacturing plastic films like polyethylene. Aside from this role in the production of biodegradable plastics, erucic acid containing oils can be used for the production of high temperature lubricants, soaps, inks, emulsifiers, or surfactants [357,358]. Finally, high erucic oils have a high energy potential [359] that makes them desirable substrates for biofuel [360] and biodiesel production [361,362]. Today, the main feedstocks for erucic acid are high erucic acid rapeseeds (HEAR; *Brassica napus*) and mustards (*Brassica juncea*), that produce seed oils comprising 45-50% erucic acid. *Crambe abyssinica* represents a promising alternative feedstock with seed oil comprising 55-60% erucic acid and its inability to cause genetic cross-overs with edible oil crops [363,364]. Research aimed at maximizing erucic acid content in seed oil has been conducted. It was estimated that every

10% increase in the relative proportion of erucic acid in seed oil could theoretically reduce the production costs of erucamide by half. Conventional breeding in the Brassica genus relying on interspecific hybridizations allowing for the transfer of useful adaptive traits between species was extensively conducted to obtain varieties rich in erucic acid. For example, *Brassica carinata* lines with erucic acid levels close to 60% were developed through interspecific hybridization [365].

However, improvement of erucic acid content through conventional breeding is limited in the Brassicacae species because of the inability of endogenous lysophosphatidic acid acyltransferases (LPAATs) to use erucoyl-CoA as an acyl donor [366]. The exclusion of erucic acid from the *sn*-2 position of triacylglycerol sets up a threshold of 67% erucic acid in the seed oil that cannot be crossed by hybridization among the existing Brassica species. Biotechnological approaches relying on the expression of a gene from *Limnanthes douglasii* (*LdLPAAT*) encoding a lysophosphatidic acid acyltransferase able to insert erucic acid into the *sn*-2 position were thus implemented [366,367]. A gene stacking strategy has been applied in *Brassica napus* [355] and *Crambe abyssinica* [368] through overexpressing *LdLPAAT* and *BnFAE1* in a context where endogenous FAD2 activity was limited (using either a mutant background or a RNAi strategy), allowing to reach 73% erucic acid in seed oil of the best lines. Further research will be necessary to identify the bottlenecks that still limit the accumulation of trierucin in these lines [369].

6.1.3. Nervonic acid - $24{:}1^{\Delta 15c}$

First discovered in the brain of sharks, nervonic acid, also known as selacholeic acid, is very abundant in nervous system and brain tissues of vertebrate animals, where it is bound to sphingosine via amide linkage to form nervonyl sphingolipids [370]. These sphingolipids are the principal components of white matter and the myelin sheath of nerve fibers [371-373]. Nervonic acid therefore plays a vital role in developing and maintaining the brain [374] and is a natural component of maternal milk, that promotes infant growth during nervous system development [375,376]. In humans, abnormal nervonic acid levels are closely associated with a high risk of developing neurological disorders or mental illnesses such as psychosis, schizophrenia, or attention deficit disorder [377-380]. Dietary therapies with nervonic acid-containing fats and oils have met growing interest for preventing and treating neuro-degenerative diseases including X-linked adrenoleukodystrophy, Parkinson's disease, and multiple sclerosis [374,384], while the manufacture of supplement formulations for improving infant nutrition has developed. In addition, nervonic acid also functions as a non-competitive inhibitor of human immunodeficiency virus type-1 reverse transcriptase (HIV-1 RT) in a dose-dependent manner [385], further increasing the interest in production of nervonic acid for pharmaceutical and nutraceutical applications.

Animal nervonic acid mostly originates from marine organisms, where it is found in very low amounts. International ban on shark fishing has resulted in shortages of nervonic acid resources, therefore increasing the need for plant sources of nervonic acid to satisfy a strong market demand [373]. Nervonic acid is found in the seed oils of many plant species, although it usually represents less than 5% of total fatty acids. High levels of nervonic acid have been detected in relatively few species, as in *Malania oleifera* (40-67%) [386], *Tropaeolum speciosum* (40-45%) [387], or *Cardamine graeca*

(54%) [388]. However, long life cycles, narrow geographic distribution, or poor agronomic performance have hindered the use of these species as plant sources. *Lunaria annua* (14-24%), beyond its ornamental status, has been considered as a niche crop for future development and its oil has been used on a small scale as an industrial lubricant [197,389]. Breeding programs have even been intermittently ongoing in Europe to develop *Lunaria annua* accessions but only met little success [390]. The seed yields of this biennial herbaceous species vary greatly and harvesting difficulties due to seed shattering represent long-standing problems. What is more, due to its high erucic acid content (up to 50% of total fatty acids), *Lunaria annua* oil does not meet the nutraceutical and pharmaceutical requirements [373]. *Acer* species were also proposed as natural sources for commercial production of nervonic acid, despite the low abundance of this monounsaturated fatty acid in seed oils (5-6 % in *Acer truncatum*) [391,392].

Genetic engineering approaches have been implemented to obtain microorganisms, microalgae, and plants producing oils rich in nervonic acid suitable for nutraceutical and pharmacological applications [196,370,393]. Improvement of existing plant sources, especially in the Brassicaceae family, was considered to generate new elite cultivars. The adopted strategies all relied on the seed-specific overexpression of *KCS* genes selected chiefly from donor species naturally exhibiting high nervonic acid levels like *Lunaria annua* (*LaKCS*) [196,393], *Cardamine graeca* (*CgKCS*) [197], or *Malania oleifera* (*MoKCS11*) [195]. The host species were either cultivated Brassicaceae species accumulating high levels of erucic acid in their seed oils (*Brassica carinata* or *Brassica napus*), or related low-erucate species like *Arabidopsis* or *Camelina sativa*. While the majority of these approaches yielded significantly increased nervonic acid levels in seed oils, the nervonic acid levels attained varied considerably. These results illustrate the diversity of the KCS isoforms tested that obviously display contrasting enzymatic characteristics. The highest nervonic acid contents were obtained in transgenic *Brassica carinata* offspring expressing either *LaKCS* (30%) [196] or *CgKCS* (44%) [197]. Both KCS isoforms exploit the strong erucate production capacity of *Brassica carinata* to synthesize important amounts of nervonic acid, although not with the same efficiency. While *Brassica carinata* lines transformed with *LaKCS* produce oils still containing 29% of erucic acid, those transformed with *CgKCS* produce oils with significantly reduced erucid acid level (5.6%). By contrast, *MoKCS11* overexpression yielded low nervonic acid levels, with the highest concentrations obtained in low-erucate *Arabidopsis* and *Camelina sativa* seeds, suggesting a substrate preference of MoKCS11 for $20{:}1^{\Delta 11c}$ [195].

When systematically evaluating the combinatorial effects of *LaKCS* with *Arabidopsis* sequences coding for the three other enzymatic components of the fatty acid elongase complex on nervonic acid production in *Camelina sativa* seeds, it was observed that the nervonic acid contents from the *LaKCS*, *AtKCR* and *AtHCD* co-expressing lines were significantly higher than that of the *LaKCS* transgenic lines during the course of seed maturation [393]. However, the ultimate nervonic acid content measured in mature dry seeds did not change significantly.

6.2. Omega-7 monounsaturated fatty acids

Plant oils enriched in ω7 monounsaturated fatty acids like 16:1$^{\Delta 9c}$ and its elongation products 18:1$^{\Delta 11c}$ and 20:1$^{\Delta 13c}$ have a number of potential applications [31,394]. First, ω7 fatty acids have considerable insterest as a feedstock for the production of 1-octene by metathesis chemistry [395]. Olefin metathesis constitutes a powerful tool for polymer chemistry, and ethenolytic metathesis of ω7 fatty acids could potentially provide a competitive source of 1-octene to make linear low-density polyethylene [396]. In addition, ω7 monounsaturated fatty acids are attractive for biodiesel formulations with superior functional properties [397]. Last, ω7 monounsaturated fatty acids have been ascribed a number of beneficial health properties. In animals, adipose tissues use palmitoleic acid to communicate with distant organs and regulate systemic metabolic homeostasis [398]. Increasing evidence suggest that palmitoleic acid plays a key role in the pathophysiology of insulin resistance in humans, increasing muscle response to insulin [399]. Pharmaceutical companies therefore develop foods and nutraceuticals for health purposes enriched in ω7 sourced from vegetable oils. Aside from these nutritional aspects, palmitoleic acid also displays antioxidant, antimicrobial, and antiaging properties [394] that make it attractive for nonfood uses by the skin care industry.

Vegetable oils displaying high ω7 contents are infrequent. Foods and nutraceuticals enriched in ω7 monounsaturated fatty acids are often sourced from the berries of *Hippophae rhamnoides*, whose pulp oil contains up to 50% ω7 fatty acids, mostly in the form of 16:1$^{\Delta 9c}$ [400]. Seed oils enriched in ω7 fatty acids have also been described in *Doxantha unguis-cati* (75%) [401], *Entandrophragma cylindricum* (55%) [402], *Macadamia integrifolia* (35%) [403], *Roureopsis obliquifoliata* (30%) [404], or *Asclepias syriaca* (25%) [405], among others. However, these plants exhibit low yields and poor agronomical performances that preclude their use for industrial purposes.

Over the last decade, some biotechnological approaches have been implemented to develop specialized high-yielding cultivars through the metabolic engineering of oilseed crops. Species in the Brassicaceae family like *Camelina sativa* or *Brassica napus* often served as production platforms, owing both to their widespread cultivation and to the natural occurrence of ω7 monounsaturated fatty acids in their seed oils: ω7 fatty acids are poorly abundant in embryo oil but highly concentrated in endosperm oil [114,116,194,406]. The most efficient strategies described so far all rely on the seed-specific overexpression of *PAD* sequences either cloned from species producing ω7 fatty acids (*Doxantha unguis-cati, Arabidopsis*) or obtained through the engineering of archetypal *SAD* to achieve desired substrate specificity while retaining its stability and turnover characteristics [123]. Seed-specific overexpression of transcription factors (*e.g.* AtMYB115) able to activate the expression of endogenous PAD-coding genes in *Arabidopsis* also proved to significantly stimulate ω7 accumulation in seed oil, although not as efficiently as the direct overexpression of *PAD* sequences [227]. An elegant strategy initially validated in *Arabidopsis* [198], then adapted to *Camelina sativa* led to the production of seed oils comprising levels of ω7 fatty acids comparable with the highest levels found in natural plant sources [397] (Figure 9). This result was attained thanks to the use of an assembly of multiple seed-specific cassettes for co-expression of an engineered Δ^9 PAD coding-sequence and a Δ^9 16:0-CoA desaturase gene from *Caenorhabditis elegans*, plus concomitant RNAi suppression of genes coding for CsKASII and CsFatB aimed at enhancing substrate availability for the PADs. RNAi suppression of *CsFAE1* allowed a further, though limited, increase in ω7 production. A similar

approach was implemented with *Glycine max* but the amounts of ω7 monounsaturated fatty acids accumulated were considerably lower than that achieved in *Camelina sativa* seeds with the same transgene cassettes, yielding 16.5% ω7 fatty acids at most [397].

6.3. Delta-5 monounsaturated fatty acids

The close position of the double bond to the carboxy terminus in Δ5 monounsaturated fatty acids results in original chemical and physical properties. In particular, these monounsaturated fatty acids are more oxidatively stable than the widespread Δ9 monounsaturated fatty acids [407]. These properties make them interesting as industrial feedstocks. They can serve as chemical precursors for the synthesis of estolides and δ-lactones that can be used in turn for a range of industrial applications, including surfactants, lubricants, and plasticizers [408,409]. Oils rich in Δ5 monounsaturated fatty acids are also desirable for uses in cosmetics [410]. Seed oil of *Limnanthes alba* comprises 63% $20{:}1^{\Delta 5c}$ and 4% $22{:}1^{\Delta 5c}$ [411] and represents the richest known source of Δ5 monounsaturated fatty acids and presently the sole commercial source of Δ5 unsaturated VLCFAs. Domestication and breeding programs recently established meadowfoam as an oilseed rotation crop on limited acreage in the Pacific Northwest of the United States, despite a rather low seed oil content (20-25%) [412,413]. However, the relatively high price of meadowfoam oil limits its commercial use to primarily cosmetic applications [414]. Biotechnological approaches have been implemented to partially reconstruct the biosynthetic pathway of $20{:}1^{\Delta 5c}$ in established oilseed crops. Co-expression of *Limnanthes douglasii* cDNAs encoding specialized acyl-CoA desaturase (*LimDes5*) and KCS (*LimFAE1*), first in somatic embryos of *Glycine max* [146], then in seeds of *Glycine max* and *Brassica carinata* [414], resulted in the accumulation of $20{:}1^{\Delta 5c}$ to approximately 10% of the total fatty acids, failing to reproduce the high $20{:}1^{\Delta 5c}$ phenotype of meadowfoam oil [415]. It is very likely that other specific enzymes are required for high levels of synthesis and accumulation of this fatty acid, such as acyl-ACP thioesterases generating a large pool of 16:0 and acyltransferases efficiently acylating $20{:}1^{\Delta 5c}$ to the glycerol backbone of triacyglycerol.

6.4. Delta-6 monounsaturated fatty acids

In *Thunbergia alata*, a Δ6 PAD produces $16{:}1^{\Delta 6c}$, a major component of seed oil [52]. A Δ4 PAD identified in *Coriandrum sativum* produces $16{:}1^{\Delta 4c}$ that is further elongated to $18{:}1^{\Delta 6c}$ by a specialized KAS isoform [126,213]. Because of their Δ6 unsaturation, sapienic and petroselinic acids are of potential industrial significance. Their chemical cleavage by ozonolysis yields hexanedioic acid (adipic acid) and 10:0 (capric acid) or 12:0 (lauric acid), respectively. Adipic acid is one of the building blocks in 6,6-nylon. Lauric acid is a component of detergents and surfactants. Petroselinic acid has many prospective applications in functional foods and for the nutraceutical and pharmaceutical industries as well [416]. The melting point of petroselinic acid elevates to 33°C, when oleic acid melts at 12°C, meaning that petroselinic acid might provide the means to produce an unsaturated vegetable oil that is also a solid at room temperature and could therefore represent a healthy substitute for margarine and shortening in the food industry [417]. However, species storing a high percentage of these unusual monounsaturated fatty acids in their seed oils display low oil yields per hectare so that high-yielding

crops designed to produce these fatty acids would represent an economically favorable alternative [418]. Despite the identification of the acyl-ACP desaturases involved in the biosynthesis of these monounsaturated fatty acids, classical approaches of metabolic engineering by overexpression of the corresponding coding sequences yielded only low levels of the fatty acids of interest in seed oils [419]. More elaborated strategies will be required to efficiently channel these unusual fatty acids into triacylglycerol [416].

7. Conclusion and perspectives

While past research initiatives have already contributed to identify a broad range of plant monounsaturated fatty acids, many other structures remain to be discovered in the plant kingdom. This is firstly because plant oils, which have thus far constituted the primary source for the huge diversity in unusual fatty acids, have not been exhaustively characterized. It was estimated that 15% of plant orders and 40% of plant families were yet to be analyzed for fatty acid composition [30]. Then, steady progresses in analytical chemistry linked to advances in mass spectrometry have considerably improved the sensitivity of analyses, lowering detection limits and allowing the identification of molecular species poorly abundant in plant tissues or accumulated in very specific cell types. Lipidomic analyses of plants grown under various adverse environmental conditions will undoubtedly further increase the spectrum of known structures.

Approaches of functional genomics combined with structural analyses of desaturases have considerably improved our comprehension of monounsaturated fatty acid biosynthesis within the broader framework of plant lipid metabolism. Further knowledge in our understanding of the structure-function relationships of plant desaturases will certainly arise from the determination of the three-dimensional structures of membrane desaturases [5]. The structures of animal acyl-CoA desaturases already available [149,150] constitute a promising advance in this direction. In contrast, and despite recent progresses into the elucidation of the biological functions of some monounsaturated fatty acid species in specific developmental and environmental contexts, there remains a real lack of knowledge regarding the particular functions of many unusual monounsaturated fatty acids. Interdisciplinary research efforts now need to focus on the exploration of the links existing between molecular structures and biological functions. The knowledge gained will certainly improve our comprehension of fundamental physiological and developmental processes, and of plant interactions with a challenging environment.

Accession Numbers

Arabidopsis sequence data from this article can be found in the EMBL/GenBank data libraries under accession numbers: AtAAD2, At3g02610; AtAAD3, At5g16230; AtADS1, At1g06080; AtADS1.2, At1g06090; AtADS1.3, At1g06100; AtADS1.4, At1g06120; AtADS2; At2g31360; AtADS3/FAD5, At3g15850; AtADS3.2, At3g15870; AtADS4, At1g06350; AtADS4.2, At1g06360; AtDSD, At4g04930;

AtFAD2, At3g12120; AtFAD3, At2g29980; AtFAD4, At4g27030; AtFAD6, At4g30950; AtFAD7, At3g11170; AtFAD8, At5g05580; AtKASII/FAB1, At1g74960; AtKCS11, At2g26640; AtKCS17, At4g34510; AtKCS18/FAE1, At4g34520; AtMYB115, At5g40360; AtMYB118, At3g27785; AtPLIP1, At3g61680; AtPRXQ, At3g26060; AtSLD1, At3g61580; AtSLD2, At2g46210.

Acknowledgments

We are grateful to M. Miquel, P. Briozzo, and T. Chardot for helpful discussions about plant lipids. We apologize to those researchers whose work we were not able to cite in this review. The Institut Jean-Pierre Bourgin benefits from the support of the Labex Saclay Plant Sciences-SPS (grant number ANR-10-LABX-0040-SPS).

References

[1] Bloch K. Enzymatic synthesis of monounsaturated fatty acids. Acc Chem Res 1969;2:193-202.

[2] Guy JE, Whittle E, Kumaran D, Lindqvist Y, Shanklin J. The crystal structure of the ivy Δ^4-16:0-ACP desaturase reveals structural details of the oxidized active site and potential determinants of regioselectivity. J Biol Chem 2007;282:19863-71.

[3] Guy JE, Whittle E, Moche M, Lengqvist J, Lindqvist Y, Shanklin J. Remote control of regioselectivity in acyl-acyl carrier protein-desaturases. Proc Natl Acad Sci USA 2011;108:16594-9.

[4] Behrouzian B, Buist PH. Mechanism of fatty acid desaturation: a bioorganic perspective. Prostaglandins Leukot Essent Fatty Acids 2003;68:107-12.

[5] Shanklin J, Guy JE, Mishra G, Lindqvist Y. Desaturases: emerging models for understanding functional diversification of diiron-containing enzymes. J Biol Chem 2009;284;18559-63.

[6] Schuster S, Fichtner M, Sasso S. Use of Fibonacci numbers in lipidomics - Enumerating various classes of fatty acids. Sci Rep 2017;7:39821.

[7] Zhang JY, Yu QT, Liu BN, Huang ZH. Chemical modification in mass spectrometry IV—2-alkenyl-4,4-dimethyloxazolines as derivatives for the double bond location of long-chain olefinic acids. Biol Mass Spectrom 1988:15;33-44.

[8] Christie WW. Gas chromatography-mass spectrometry methods for structural analysis of fatty acids. Lipids 1998;33:343-53.

[9] Sun D, Froman BE, Orth RG, MacIsaac SA, Larosa T, Dong F, Valentin HE. Identification of plant sphingolipid desaturases using chromatography and mass spectrometry. J Chromatogr Sci 2009;47:895-901.

[10] Hamilton JT, Christie WW. Mechanisms for ion formation during the electron impact-mass spectrometry of picolinyl ester and 4,4-dimethyloxazoline derivatives of fatty acids. Chem Phys Lipids 2000;105:93-104.

[11] Christie WW, Robertson GW, McRoberts WC, Hamilton JTG. Mass spectrometry of the 4,4-dimethyloxazoline derivatives of isomeric octadecenoates (monoenes). Eur J Lipid Sci Technol 2000; 102:23-9.

[12] Buser HR, Arn H, Guerin P, Rauscher S. Determination of double bond position in mono-unsaturated acetates by mass spectrometry of dimethyl disulfide adducts. Anal Chem 1983:55;818-22.
[13] Gonzales-Vigil E, Hefer CA, von Loessl ME, La Mantia J, Mansfield SD. Exploiting natural variation to uncover an alkene biosynthetic enzyme in poplar. Plant Cell 2017;29:2000-15.
[14] Imai H, Yamamoto K, Shibahara A, Miyatani S, Nakayama T. Determining double-bond positions in monoenoic 2-hydroxy fatty acids of glucosylceramides by gas chromatography-mass spectrometry. Lipids 2000;35:233-6.
[15] Shibahara A, Yamamoto K, Kinoshita A, Anderson BL. An improved method for preparing dimethyl disulfide adducts for GC/MS analysis. J Am Oil Chem Soc 2008;85:93-4.
[16] Hancock SE, Poad BL, Batarseh A, Abbott SK, Mitchell TW. Advances and unresolved challenges in the structural characterization of isomeric lipids. Anal Biochem 2017;524:45-55.
[17] Rustam YH, Reid GE. Analytical challenges and recent advances in mass spectrometry based lipidomics. Anal Chem 2018;90:374-97.
[18] Porta Siegel T, Ekroos K, Ellis SR. Reshaping lipid biochemistry by pushing barriers in structural lipidomics. Angew Chem Int Ed Engl 2019;58:6492-501.
[19] Williams PE, Klein DR, Greer SM, Brodbelt JS. Pinpointing double bond and *sn*-positions in glycerophospholipids via hybrid 193 nm ultraviolet photodissociation (UVPD) mass spectrometry. J Am Chem Soc 2017;139:15681-90.
[20] Campbell JL, Baba T. Near-complete structural characterization of phosphatidylcholines using electron impact excitation of ions from organics. Anal Chem 2015;87:5837-45.
[21] Poad BLJ, Zheng X, Mitchell TW, Smith RD, Baker ES, Blanksby SJ. Online ozonolysis combined with ion mobility-mass spectrometry provides a new platform for lipid isomer analyses. Anal Chem 2018;90:1292-300.
[22] Zhang W, Zhang D, Chen Q, Wu J, Ouyang Z, Xia Y. Online photochemical derivatization enables comprehensive mass spectrometric analysis of unsaturated phospholipid isomers. Nat Commun 2019;10:79.
[23] Cao W, Ma X, Li Z, Zhou X, Ouyang Z. Locating carbon-carbon double bonds in unsaturated phospholipids by epoxidation reaction and tandem mass spectrometry. Anal Chem 2018;90:10286-92.
[24] Paine MRL, Poad BLJ, Eijkel GB, Marshall DL, Blanksby SJ, Heeren RMA, Ellis SR. Mass spectrometry imaging with isomeric resolution enabled by ozone-induced dissociation. Angew Chem Int Ed Engl 2018;57:10530-4.
[25] Wäldchen F, Spengler B, Heiles S. Reactive Matrix-assisted laser desorption/ionization mass spectrometry imaging using an intrinsically photoreactive Paternò-Büchi matrix for double-bond localization in isomeric phospholipids. J Am Chem Soc 2019;141:11816-20.
[26] Klein DR, Feider CL, Garza KY, Lin JQ, Eberlin LS, Brodbelt JS. Desorption electrospray ionization coupled with ultraviolet photodissociation for characterization of phospholipid isomers in tissue sections. Anal Chem 2018;90:10100-4.
[27] Chatgilialoglu C, Ferreri C, Melchiorre M, Sansone A, Torreggiani A. Lipid geometrical isomerism: from chemistry to biology and diagnostics. Chem Rev 2014;114:255-84.

[28] Voinov VG, Claeys M. Charge-remote fragmentation characteristics of monounsaturated fatty acids in resonance electron capture: differentiation between *cis* and *trans* isomers. Int J Mass Spectro 2001;205:57-64.
[29] Ji H, Voinov VG, Deinzer ML, Barofsky DF. Distinguishing between *cis*/*trans* isomers of monounsaturated fatty acids by FAB MS. Anal Chem 2007;79:1519-22.
[30] Ohlrogge J, Thrower N, Mhaske V, Stymne S, Baxter M, Yang W, Liu J, Shaw K, Shorrosh B, Zhang M, Wilkerson C, Matthäus B. PlantFAdb: a resource for exploring hundreds of plant fatty acid structures synthesized by thousands of plants and their phylogenetic relationships. Plant J 2018;96:1299-308.
[31] Baud S. Seeds as oil factories. Plant Reprod 2018;31:213-35.
[32] Millar AA, Smith MA, Kunst L. All fatty acids are not equal: discrimination in plant membrane lipids. Trends Plant Sci 2000;5:95-101.
[33] Aitzetmüller K; Matthäus B; Friedrich H. A new database for seed oil fatty acids-The database SOFA. Eur J Lipid Sci Technol 2003;105:92–103.
[34] Matthäus B. The database seed oil fatty acids (SOFA) is back on the internet! Eur J Lipid Sci Technol 2012;114:701-2.
[35] Knothe G, Dunn ROA. A comprehensive evaluation of the melting points of fatty acids and esters determined by differential scanning calorimetry. J Am Oil Chem Soc 2009;86:843-56.
[36] Kunst L, Samuels L. Plant cuticles shine: advances in wax biosynthesis and export. Curr Opin Plant Biol 2009;12:721-7.
[37] Delude C, Moussu S, Joubès J, Ingram G, Domergue F. Plant surface lipids and epidermis development. Subcell Biochem 2016;86:287-313.
[38] Li-Beisson Y, Shorrosh B, Beisson F, Andersson MX, Arondel V, Bates PD, Baud S, Bird D, Debono A, Durrett TP, Franke RB, Graham IA, Katayama K, Kelly AA, Larson T, Markham JE, Miquel M, Molina I, Nishida I, Rowland O, Samuels L, Schmid KM, Wada H, Welti R, Xu C, Zallot R, Ohlrogge J. Acyl-lipid metabolism. Arabidopsis Book. 2010;8:e0133.
[39] Dubacq J-P, Trémolières A. Occurrence and function of phosphatidylglycerol containing delta-3-*trans*-hexadecenoic acid in photosynthetic lamellae. Physiol Veg 1983;21:293-312.
[40] James AT, Nichols BW. Lipids of photosynthetic systems. Nature 1966;210:372-5.
[41] Roughan G. A simplified isolation of phosphatidylglycerol. Plant Sci 1986;43:57-62.
[42] Los DA, Mironov KS. Modes of fatty acid desaturation in cyanobacteria: an update. Life (Basel) 2015;5:554-67.
[43] Sperling P, Franke S, Lüthje S, Heinz E. Are glucocerebrosides the predominant sphingolipids in plant plasma membranes? Plant Physiol Biochem 2005;43:1031-8.
[44] Sperling P, Ternes P, Zank T, Heinz E. The evolution of desaturases. Prostaglandins Leukot Essent Fatty acids 2003;68:73-95.
[45] Napier JA, Michaelson LV, Dunn TM. A new class of lipid desaturase central to sphingolipid biosynthesis and signalling. Trends Plant Sci 2002;7:475-8.
[46] Lynch DV, Dunn TM. An introduction to plant sphingolipids and a review of recent advances in understanding their metabolism and function. New Phytol 2004;161:677-702.

[47] Markham JE, Lynch DV, Napier JA, Dunn TM, Cahoon EB. Plant sphingolipids: function follows form. Curr Opin Plant Biol 2013;16:350-7.
[48] Cahoon EB, Lynch DV. Analysis of glucocerebrosides of rye (*Secale cereale* L. cv Puma) leaf and plasma membrane. Plant Physiol 1991;95:58-68.
[49] Markham JE, Li J, Cahoon EB, Jaworski JG. Separation and identification of major plant sphingolipid classes from leaves. J Biol Chem 2006;281:22684-94.
[50] Miller RW, Daxenbichler ME, Earle FR, Gentry HS. Search for new industrial oils: VIII. The genus *Limnanthes*. J Am Oil Chem Soc 1964;41:167-9.
[51] Phillips BE, Smith CR, Tallent WH. Glycerides of *Limnanthes douglasii* seed oil. Lipids 1971;6:93-9.
[52] Cahoon EB, Becker CK, Shanklin J, Ohlrogge JB. cDNAs for isoforms of the Δ^9-stearoyl-acyl carrier protein desaturase from *Thunbergia alata* endosperm. Plant Physiol 1994;106:807-8.
[53] Wanner JKR, Dai DN, Huong LT, Hung NV, Schmidt E, Jirovetz L. Fatty acid methyl ester composition of some Turkish Apiaceae seed oils: New sources for petroselinic acid. Nat Prod Commun 2016;11:1697-700.
[54] Nguyen QH, Talou T, Evon P, Cerny M, Merah O. Fatty acid composition and oil content during coriander fruit development. Food Chem. 2020;326:127034.
[55] Yang X, Zhao H, Kosma DK, Tomasi P, Dyer JM, Li R, Liu X, Wang Z, Parsons EP, Jenks MA, Lü S. The acyl desaturase CER17 is involved in producing wax unsaturated primary alcohols and cutin monomers. Plant Physiol 2017;173:1109-24.
[56] Sun Y, Hegebarth D, Jetter R. Acyl-CoA desaturase ADS4.2 is involved in formation of characteristic wax alkenes in young Arabidopsis leaves. Plant Physiol 2021;186:1812-31.
[57] Tulloch AP, Hoffman LL. Epicuticular wax of *Agropyron intermedium*. Phytochemistry 1976;15: 1145-51.
[58] Schlüter PM, Xu S, Gagliardini V, Whittle E, Shanklin J, Grossniklaus U, Schiestl FP. Stearoyl-acyl carrier protein desaturases are associated with floral isolation in sexually deceptive orchids. Proc Natl Acad Sci USA 2011;108:5696-701.
[59] Sedeek KE, Whittle E, Guthörl D, Grossniklaus U, Shanklin J, Schlüter PM. Amino acid change in an orchid desaturase enables mimicry of the pollinator's sex pheromone. Curr Biol 2016;26:1505-11.
[60] Dennison T, Qin W, Loneman DM, Condon SGF, Lauter N, Nikolau BJ, Yandeau-Nelson MD. Genetic and environmental variation impact the cuticular hydrocarbon metabolome on the stigmatic surfaces of maize. BMC Plant Biol 2019;19:430.
[61] Bourgault R, Matschi S, Vasquez M, Qiao P, Sonntag A, Charlebois C, Mohammadi M, Scanlon MJ, Smith LG, Molina I. Constructing functional cuticles: analysis of relationships between cuticle lipid composition, ultrastructure and water barrier function in developing adult maize leaves. Ann Bot 2020;125:79-91.
[62] Shanklin J, Cahoon EB. Desaturation and related modifications of fatty acids. Annu Rev Plant Physiol Plant Mol Biol. 1998;49:611-41.
[63] Aguilar PS, de Mendoza D. Control of fatty acid desaturation: a mechanism conserved from bacteria to humans. Mol Microbiol 2006;62:1507-14.

[64] Fox BG, Lyle KS, Rogge CE. Reactions of the diiron enzyme stearoyl-acyl carrier protein desaturase. Acc Chem Res 2004;37:421-9.
[65] Meesapyodsuk D, Qiu X. The front-end desaturase: structure, function, evolution and biotechnological use. Lipids. 2012;47:227-37.
[66] Broadwater JA, Haas JA, Fox BG. The fundamental, versatile role of diiron enzymes in lipid metabolism. Fett/Lipid 1998;100:103-13.
[67] Los DA, Murata N. Structure and expression of fatty acid desaturases. Biochim Biophys Acta 1998;1394:3-15.
[68] Tocher DR, Leaver MJ, Hodgson PA. Recent advances in the biochemistry and molecular biology of fatty acyl desaturases. Prog Lipid Res 1998;37:73-117.
[69] Buist PH. Fatty acid desaturases: selecting the dehydrogenation channel. Nat Prod Rep 2004;21:249-62.
[70] Wallar BJ, Lipscomb JD. Dioxygen activation by enzymes containing binuclear non-heme iron clusters. Chem Rev 1996;96:2625-58.
[71] Shu L, Nesheim JC, Kauffmann K, Münck E, Lipscomb JD, Que L Jr. An $Fe_2^{IV}O_2$ diamond core structure for the key intermediate Q of methane monooxygenase. Science 1997;275:515-8.
[72] Torrent M, Musaev DG, Basch H, Morokuma K. Computational studies of reaction mechanisms of methane monooxygenase and ribonucleotide reductase. J Comput Chem 2002;23:59-76.
[73] Baik MH, Newcomb M, Friesner RA, Lippard SJ. Mechanistic studies on the hydroxylation of methane by methane monooxygenase. Chem Rev 2003;103:2385-419.
[74] Gherman BF, Baik MH, Lippard SJ, Friesner RA. Dioxygen activation in methane monooxygenase: a theoretical study. J Am Chem Soc 2004;126:2978-90.
[75] Banerjee R, Proshlyakov Y, Lipscomb JD, Proshlyakov DA. Structure of the key species in the enzymatic oxidation of methane to methanol. Nature 2015;518:431-4.
[76] Jasniewski AJ, Que L Jr. Dioxygen activation by nonheme diiron enzymes: Diverse dioxygen adducts, high-valent intermediates, and related model complexes. Chem Rev 2018;118:2554-92.
[77] Fox BG, Shanklin J, Ai J, Loehr TM, Sanders-Loehr J. Resonance Raman evidence for an Fe-O-Fe center in stearoyl-ACP desaturase. Primary sequence identity with other diiron-oxo proteins. Biochemistry 1994;33:12776-86.
[78] Ai J, Broadwater J, Loehr T, Sanders-Loehr J, Fox BG. Azide adducts of stearoyl-ACP desaturase: a model for μ-1,2 bridging by dioxygen in the binuclear iron active site. J Biol Inorgan Chem 1997;2:37-45.
[79] Broadwater JA, Achim C, Münck E, Fox BG. Mössbauer studies of the formation and reactivity of a quasi-stable peroxo intermediate of stearoyl-acyl carrier protein Δ9-desaturase. Biochemistry 1999; 38:12197-204.
[80] Chalupský J, Rokob TA, Kurashige Y, Yanai T, Solomon EI, Rulíšek L, Srnec M. Reactivity of the binuclear non-heme iron active site of Δ□ desaturase studied by large-scale multireference *ab initio* calculations. J Am Chem Soc 2014;136:15977-91.
[81] Sperling P, Heinz E. Desaturases fused to their electron donor. Eur J Lipid Sci Technol 2001;103:158-80.

[82] Shanklin J, Somerville C. Stearoyl-acyl-carrier-protein desaturase from higher plants is structurally unrelated to the animal and fungal homologs. Proc Natl Acad Sci USA 1991;88:2510-4.
[83] Liu Q, Chai J, Moche M, Guy J, Lindqvist Y, Shanklin J. Half-of-the-sites reactivity of the castor Δ9-18:0-acyl carrier protein desaturase. Plant Physiol 2015;169:432-41.
[84] Lou Y, Shanklin J. Evidence that the yeast desaturase Ole1p exists as a dimer *in vivo*. J Biol Chem 2010;285:19384-90.
[85] Shanklin J, Whittle E, Fox BG. Eight histidine residues are catalytically essential in a membrane-associated iron enzyme, stearoyl-CoA desaturase, and are conserved in alkane hydroxylase and xylene monooxygenase. Biochemistry 1994;33:12787-94.
[86] López Alonso D, García-Maroto F, Rodriguez-Ruiz J, Garrido JA, Vilches MA. Evolution of the membrane-bound fatty acid desaturases. Biochem Syst Ecol 2003;31:1111–24.
[87] Schmidt H, Heinz E. Involvement of ferredoxin in desaturation of lipid-bound oleate in chloroplasts. Plant Physiol 1990;94:214-20.
[88] Wada H, Schmidt H, Heinz E, Murata N. In vitro ferredoxin-dependent desaturation of fatty acids in cyanobacterial thylakoid membranes. J Bacteriol 1993;175:544-7.
[89] Jacobson BS, Jaworski JG, Stumpf PK. Fat metabolism in higher plants: LXII. Stearoyl-acyl carrier protein desaturase from spinach chloroplasts. Plant Physiol 1974;54:484-6.
[90] Dailey HA, Strittmatter P. Modification and identification of cytochrome b_5 carboxyl groups involved in protein-protein interaction with cytochrome b_5 reductase. J Biol Chem 1979;254:5388-96.
[91] Hackett CS, Strittmatter P. Covalent cross-linking of the active sites of vesicle-bound cytochrome b_5 and NADH-cytochrome b_5 reductase. J Biol Chem 1984;259:3275-82.
[92] Schenkman JB, Jansson I. The many roles of cytochrome b_5. Pharmacol Ther 2003;97:139-52.
[93] Fukuchi-Mizutani M, Mizutani M, Tanaka Y, Kusumi T, Ohta D. Microsomal electron transfer in higher plants: cloning and heterologous expression of NADH-cytochrome b_5 reductase from Arabidopsis. Plant Physiol 1999;119:353-62.
[94] Napier JA, Sayanova O, Stobart AK, Shewry PR. A new class of cytochrome b_5 fusion proteins. Biochem J 1997;328:717-8.
[95] Napier JA, Sayanova O, Sperling P, Heinz H. A growing family of cytochrome b_5-domain fusion. Trends Plant Sci 1999;4:2-4.
[96] Gostincar C, Turk M, Gunde-Cimerman N. The evolution of fatty acid desaturases and cytochrome b_5 in eukaryotes. J Membr Biol 2010;233:63-72.
[97] Mitchell AG, Martin CE. A novel cytochrome b_5-like domain is linked to the carboxyl terminus of the *Saccharomyces cerevisiae* Δ-9 fatty acid desaturase. J Biol Chem 1995;270:29766-72.
[98] Beckmann C, Rattke J, Oldham NJ, Sperling P, Heinz E, Boland W. Characterization of a Δ^8-sphingolipid desaturase from higher plants: a stereochemical and mechanistic study on the origin of *E*,*Z* isomers. Angew Chem Int Ed Engl 2002;41:2298-300.
[99] Nagai J, Bloch K. Enzymatic desaturation of stearyl acyl carrier protein. J Biol Chem 1968;243:4626-33.
[100] Haas JA, Fox BG. Fluorescence anisotropy studies of enzyme-substrate complex formation in stearoyl-ACP desaturase. Biochemistry 2002;41:14472-81.

[101] Ferro M, Brugière S, Salvi D, Seigneurin-Berny D, Court M, Moyet L, Ramus C, Miras S, Mellal M, Le Gall S, Kieffer-Jaquinod S, Bruley C, Garin J, Joyard J, Masselon C, Rolland N. AT_CHLORO, a comprehensive chloroplast proteome database with subplastidial localization and curated information on envelope proteins. Mol Cell Proteomics 2010;9:1063-84.

[102] Joyard J, Ferro M, Masselon C, Seigneurin-Berny D, Salvi D, Garin J, Rolland N. Chloroplast proteomics highlights the subcellular compartmentation of lipid metabolism. Prog Lipid Res 2010;49:128-58.

[103] Troncoso-Ponce MA, Nikovics K, Marchive C, Lepiniec L, Baud S. New insights on the organization and regulation of the fatty acid biosynthetic network in the model higher plant *Arabidopsis thaliana*. Biochimie 2016;120:3-8.

[104] Roughan PG, Ohlrogge JB. Evidence that isolated chloroplasts contain an integrated lipid-synthesizing assembly that channels acetate into long-chain fatty acids. Plant Physiol 1996;110:1239-47.

[105] McKeon TA, Stumpf PK. Purification and characterization of the stearoyl-acyl carrier protein desaturase and the acyl-acyl carrier protein thioesterase from maturing seeds of safflower. J Biol Chem 1982;257:12141-7.

[106] Thompson GA, Scherer DE, Foxall-Van Aken S, Kenny JW, Young HL, Shintani DK, Kridl JC, Knauf VC. Primary structures of the precursor and mature forms of stearoyl-acyl carrier protein desaturase from safflower embryos and requirement of ferredoxin for enzyme activity. Proc Natl Acad Sci USA 1991;88:2578-82.

[107] Fox BG, Shanklin J, Somerville C, Münck E. Stearoyl-acyl carrier protein Δ^9 desaturase from *Ricinus communis* is a diiron-oxo protein. Proc Natl Acad Sci USA 1993;90:2486-90.

[108] Lindqvist Y, Huang W, Schneider G, Shanklin J. Crystal structure of Δ^9 stearoyl-acyl carrier protein desaturase from castor seed and its relationship to other di-iron proteins. EMBO J 1996;15:4081-92.

[109] Sobrado P, Lyle KS, Kaul SP, Turco MM, Arabshahi I, Marwah A, Fox BG. Identification of the binding region of the [2Fe-2S] ferredoxin in stearoyl-acyl carrier protein desaturase: insight into the catalytic complex and mechanism of action. Biochemistry 2006;45:4848-58.

[110] Reipa V, Shanklin J, Vilker V. Substrate binding and the presence of ferredoxin affect the redox properties of the soluble plant Δ^9-18:0-acyl carrier protein desaturase. Chem Commun 2004;2406-7.

[111] Zhang YM, Marrakchi H, White SW, Rock CO. The application of computational methods to explore the diversity and structure of bacterial fatty acid synthase. J Lipid Res 2003;44:1-10.

[112] Baer MD, Shanklin J, Raugei S. Atomistic insight on structure and dynamics of spinach acyl carrier protein with substrate length. Biophys J 2021:S0006-3495(21)00161-2.

[113] Cahoon EB, Shah S, Shanklin J, Browse J. A determinant of substrate specificity predicted from the acyl-acyl carrier protein desaturase of developing cat's claw seed. Plant Physiol 1998;117:593-8.

[114] Bryant FM, Munoz-Azcarate O, Kelly AA, Beaudoin F, Kurup S, Eastmond PJ. ACYL-ACYLCARRIER PROTEIN DESATURASE2 and 3 are responsible for making omega-7 fatty acids in the Arabidopsis aleurone. Plant Physiol 2016;172:154-62.

[115] Troncoso-Ponce MA, Barthole G, Tremblais G, To A, Miquel M, Lepiniec L, Baud S. Transcriptional activation of two delta-9 palmitoyl-ACP desaturase genes by MYB115 and MYB118 is critical for biosynthesis of omega-7 monounsaturated fatty acids in the endosperm of Arabidopsis seeds. Plant Cell 2016;28:2666-82.

[116] Penfield S, Rylott EL, Gilday AD, Graham S, Larson TR, Graham IA. Reserve mobilization in the Arabidopsis endosperm fuels hypocotyl elongation in the dark, is dependent of abscisic acid, and requires *PHOSPHOENOLPYRUVATE CARBOXYKINASE1*. Plant Cell 2004;16:2705-18.

[117] Barthole G, To A, Marchive C, Brunaud V, Soubigou-Taconnat L, Berger N, Dubreucq B, Lepiniec L, Baud S. MYB118 represses endosperm maturation in seeds of *Arabidopsis*. Plant Cell 2014;26:3519-37.

[118] Miray R, Kazaz S, To A, Baud S. Molecular control of oil metabolism in the endosperm of seeds. Int J Mol Sci 2021;22:1621.

[119] Schultz DJ, Cahoon EB, Shanklin J, Craig R, Cox-Foster DL, Mumma RO, Meford JI. Expression of a Δ9 14:0-acyl carrier protein fatty acid desaturase gene is necessary for the production of ω5 anacardic acids found in pest-resistant geranium (*Pelargonium xhortorum*). Proc Natl Acad Sci USA 1996;93:8771-5.

[120] Kazaz S, Miray R, Baud S. Acyl-acyl carrier protein desaturases and plant biotic interactions. Cells 2021;10:674.

[121] Kachroo A, Shanklin J, Whittle E, Lapchyk L, Hildebrand D, Kachroo P. The Arabidopsis stearoyl-acyl carrier protein-desaturase family and the accumulation of leaf isoforms to oleic acid synthesis. Plant Mol Biol 2007;63:257-71.

[122] Cahoon EB, Lindqvist Y, Schneider G, Shanklin J. Redesign of soluble fatty acid desaturases from plants for altered substrate specificity and double bond position. Proc Natl Acad Sci USA 1997;94: 4872-7.

[123] Whittle E, Shanklin J. Engineering Δ^9-16:0-acyl carrier protein (ACP) desaturase specificity based on combinatorial saturation mutagenesis and logical redesign of the castor Δ^9-18:0-ACP desaturase. J Biol Chem 2001; 276:21500-5.

[124] Cahoon EB, Shanklin J. Substrate-dependent mutant complementation to select fatty acid desaturase variants for metabolic engineering of plant seed oils. Proc Natl Acad Sci USA 2000;97: 12350-5.

[125] Cahoon EB, Cranmer AM, Shanklin J, Ohlrogge JB. Δ^6 Hexadecenoic acid is synthesized by the activity of a soluble Δ^6 palmitoyl-acyl carrier protein desaturase in *Thunbergia alata* endosperm. J Biol Chem 1994;269:27519-26.

[126] Cahoon EB, Shanklin J, Ohlrogge JB. Expression of a coriander desaturase results in petroselinic acid production in transgenic tobacco. Proc Natl Acad Sci USA 1992;89:11184-8.

[127] Cahoon EB, Ohlrogge JB. Metabolic evidence for the involvement of a Δ^4-palmitoyl-acyl carrier protein desaturase in petroselinic acid synthesis in coriander endosperm and transgenic tobacco cells. Plant Physiol 1994;104:827-37.

[128] Whittle E, Cahoon EB, Subrahmanyam S, Shanklin J. A multifunctional acyl-acyl carrier protein desaturase from *Hedera helix* L. (English ivy) can synthesize 16- and 18-carbon monoene and diene products. J Biol Chem 2005;280:28169-76.
[129] Suh MC, Schultz DJ, Ohlrogge JB. Isoforms of acyl carrier protein involved in seed-specific fatty acid synthesis. Plant J 1999;17:679-88.
[130] Kamide K, Sakai H, Aoki K, Sanada Y, Wada K, Green LS, Yee BC, Buchanan BB. Amino acid sequences of heterotrophic and photosynthetic ferredoxins from the tomato plant (*Lycopersicon esculentum* Mill.). Photosynth Res 1995;46:301-8.
[131] Aoki K, Yamamoto M, Wada K. Photosynthetic and heterotrophic ferredoxin isoproteins are colocalized in fruit plastids of tomato. Plant Physiol 1998;118:439-49.
[132] Kimata Y, Hase T. Localization of ferredoxin isoproteins in mesophyll and bundle sheath cells in maize leaf. Plant Physiol 1989;89:1193-7.
[133] Hase T, Kimata Y, Yonekura K, Matsumura T, Sakakibara H. Molecular cloning and differential expression of the maize ferredoxin gene family. Plant Physiol 1991;96:77-83.
[134] Schultz DJ, Suh MC, Ohlrogge JB. Stearoyl-acyl carrier protein and unusual acyl-acyl carrier protein desaturase activities are differentially influenced by ferredoxin. Plant Physiol 2000;124:681-92.
[135] Fukuchi-Mizutani M, Tasaka Y, Tanaka Y, Ashikari T, Kusumi T, Murata N. Characterization of ∆9 acyl-lipid desaturase homologues from *Arabidopsis thaliana*. Plant Cell Physiol 1998;39:247-53.
[136] Heilmann I, Pidkowich MS, Girke T, Shanklin J. Switching desaturase enzyme specificity by alternate subcellular targeting. Proc Natl Acad Sci USA 2004;101:10266-71.
[137] Smith MA, Dauk M, Ramadan H, Yang H, Seamons LE, Haslam RP, Beaudoin F, Ramirez-Erosa I, Forseille L. Involvement of Arabidopsis ACYL-COENZYME A DESATURASE-LIKE2 (At2g31360) in the biosynthesis of the very-long-chain monounsaturated fatty acid components of membrane lipids. Plant Physiol 2013;161:81-96.
[138] Heilmann I, Mekhedov S, King B, Browse J, Shanklin J. Identification of the Arabidopsis palmitoyl-monogalactosyldiacylglycerol ∆7-desaturase gene *FAD5*, and effects of plastidial retargeting of Arabidopsis desaturases on the *fad5* mutant phenotype. Plant Physiol 2004;136:4237-45
[139] Zerangue N, Schwappach B, Jan YN, Jan LY. A new ER trafficking signal regulates the subunit stoichiometry of plasma membrane K(ATP) channels. Neuron 1999;22:537-48.
[140] Benghezal M, Wasteneys GO, Jones DA. The C-terminal dilysine motif confers endoplasmic reticulum localization to type I membrane proteins in plants. Plant Cell 2000;12:1179-201.
[141] Kunst L, Browse J, Somerville C. A mutant of Arabidopsis deficient in desaturation of palmitic acid in leaf lipids. Plant Physiol 1989;90:943-7.
[142] Vijayan P, Browse J. Photoinhibition in mutants of Arabidopsis deficient in thylakoid unsaturation. Plant Physiol 2002;129:876-85.
[143] Rowland O, Zheng H, Hepworth SR, Lam P, Jetter R, Kunst L. *CER4* encodes an alcohol-forming fatty acyl-coenzyme A reductase involved in cuticular wax production in Arabidopsis. Plant Physiol 2006;142:866-77.
[144] Bourdenx B, Bernard A, Domergue F, Pascal S, Léger A, Roby D, Pervent M, Vile D, Haslam RP, Napier JA, Lessire R, Joubès J. Overexpression of Arabidopsis *ECERIFERUM1* promotes wax

very-long-chain alkane biosynthesis and influences plant response to biotic and abiotic stresses. Plant Physiol 2011;156:29-45.
[145] Bernard A, Domergue F, Pascal S, Jetter R, Renne C, Faure JD, Haslam RP, Napier JA, Lessire R, Joubès J. Reconstitution of plant alkane biosynthesis in yeast demonstrates that *Arabidopsis* ECERIFERUM1 and ECERIFERUM3 are core components of a very-long-chain alkane synthesis complex. Plant Cell 2012;24:3106-18.
[146] Cahoon EB, Marillia E-F, Stecca KL, Hall SE, Taylor DC, Kinney AJ. Production of fatty acid components of meadowfoam oil in somatic soybean embryos. Plant Physiol 2000;124:243-51.
[147] Pollard MR, Stumpf PK. Biosynthesis of C_{20} and C_{22} fatty acids by developing seeds of *Limnanthes alba*. Chain elongation and Δ5 desaturation. Plant Physiol 1980;66:649-55.
[148] Sayanova O, Haslam R, Venegas Caleron M, Napier JA. Cloning and characterization of unusual fatty acid desaturases from *Anemone leveillei*: identification of an acyl-coenzyme A C_{20} Δ^5-desaturase responsible for the synthesis of sciadonic acid. Plant Physiol 2007;144:455-67.
[149] Bai Y, McCoy JG, Levin EJ, Sobrado P, Rajashankar KR, Fox BG, Zhou M. X-ray structure of a mammalian stearoyl-CoA desaturase. Nature 2015;524:252-6.
[150] Wang H, Klein MG, Zou H, Lane W, Snell G, Levin I, Li K, Sang BC. Crystal structure of human stearoyl-coenzyme A desaturase in complex with substrate. Nat Struct Mol Biol 2015;22:581-5.
[151] Cai Y, Yu XH, Chai J, Liu CJ, Shanklin J. A conserved evolutionary mechanism permits Δ9 desaturation of very-long-chain fatty acyl lipids. J Biol Chem 2020;295:11337-11345.
[152] Gao J, Ajjawi I, Manoli A, Sawin A, Xu C, Froehlich JE, Last RL, Benning C. FATTY ACID DESATURASE4 of Arabidopsis encodes a protein distinct from characterized fatty acid desaturases. Plant J 2009;60:832-9.
[153] Ohnishi M, Thompson GA Jr. Biosynthesis of the unique *trans*-delta3-hexadecenoic acid component of chloroplast phosphatidylglycerol: evidence concerning its site and mechanism of formation. Arch Biochem Biophys 1991;288:591-9.
[154] Schwacke R, Schneider A, van der Graaff E, Fischer K, Catoni E, Desimone M, Frommer WB, Flügge UI, Kunze R. ARAMEMNON, a novel database for Arabidopsis integral membrane proteins. Plant Physiol 2003;131:16-26.
[155] Horn PJ, Smith MD, Clark TR, Froehlich JE, Benning C. PEROXIREDOXIN Q stimulates the activity of the chloroplast 16:1$^{\Delta 3trans}$ FATTY ACID DESATURASE4. Plant J 2020;102:718-29.
[156] Galbis-Martínez M, Padmanabhan S, Murillo FJ, Elías-Arnanz M. CarF mediates signaling by singlet oxygen, generated via photoexcited protoporphyrin IX, in *Myxococcus xanthus* light-induced carotenogenesis. J Bacteriol 2012;194:1427-36.
[157] Gallego-García A, Monera-Girona AJ, Pajares-Martínez E, Bastida-Martínez E, Pérez-Castaño R, Iniesta AA, Fontes M, Padmanabhan S, Elías-Arnanz M. A bacterial light response reveals an orphan desaturase for human plasmalogen synthesis. Science 2019;366:128-32.
[158] Gray GR, Ivanov AG, Król M, Williams JP, Kahn MU, Myscich EG, Huner NP. Temperature and light modulate the *trans*-delta3-hexadecenoic acid content of phosphatidylglycerol: light-harvesting complex II organization and non-photochemical quenching. Plant Cell Physiol 2005;46:1272-82.

[159] Sperling P, Schmidt H, Heinz E. A cytochrome-b_5-containing fusion protein similar to plant acyl lipid desaturases. Eur J Biochem 1995;232:798-805.
[160] Sperling P, Blume A, Zähringer U, Heinz E. Further characterization of ∆8-sphingolipid desaturases from higher plants. Biochem Soc Trans 2000;28:638-41.
[161] Sperling P, Zähringer U, Heinz E. A sphingolipid desaturase from higher plants. Identification of a new cytochrome b5 fusion protein. J Biol Chem 1998;273:28590-6.
[162] Sperling P, Libisch B, Zähringer U, Napier JA, Heinz E. Functional identification of a Δ^8-sphingolipid desaturase from *Borago officinalis*. Arch Biochem Biophys 2001;388:293-8.
[163] García-Maroto F, Garrido-Cárdenas JA, Michaelson LV, Napier JA, Alonso DL. Cloning and molecular characterisation of a Δ^8-sphingolipid-desaturase from *Nicotiana tabacum* closely related to Δ^6-acyl-desaturases. Plant Mol Biol 2007;64:241-50.
[164] Song LY, Lu WX, Hu J, Zhang Y, Yin WB, Chen YH, Hao ST, Wang BL, Wang RR, Hu ZM. Identification and functional analysis of the genes encoding Δ^6-desaturase from *Ribes nigrum*. J Exp Bot 2010;61:1827-38.
[165] Li SF, Zhang GJ, Zhang XJ, Yuan JH, Deng CL, Hu ZM, Gao WJ. Genes encoding Δ^8-sphingolipid desaturase from various plants: identification, biochemical functions, and evolution. J Plant Res 2016;129:979-87.
[166] Chen M, Markham JE, Cahoon EB. Sphingolipid Δ8 unsaturation is important for glucosylceramide biosynthesis and low-temperature performance in Arabidopsis. Plant J 2012;69:769-81.
[167] Sato M, Nagano M, Jin S, Miyagi A, Yamaguchi M, Kawai-Yamada M, Ishikawa T. Plant-unique *cis*/*trans* isomerism of long-chain base unsaturation is selectively required for aluminum tolerance resulting from glucosylceramide-dependent plasma membrane fluidity. Plants 2019;9:19.
[168] Habel A, Sperling P, Bartram S, Heinz E, Boland W. Conformational studies on the Δ^8(*E*,*Z*)-sphingolipid desaturase from *Helianthus annuus* with chiral fluoropalmitic acids as mechanistic probes. J Org Chem 2010;75:4975-82.
[169] Song LY, Zhang Y, Li SF, Hu J, Yin WB, Chen YH, Hao ST, Wang BL, Wang RR, Hu ZM. Identification of the substrate recognition region in the Δ□-fatty acid and Δ□-sphingolipid desaturase by fusion mutagenesis. Planta. 2014;239:753-63.
[170] Libisch B, Michaelson LV, Lewis MJ, Shewry PR, Napier JA. Chimeras of Δ^6-fatty acid and Δ^8-sphingolipid desaturases. Biochem Biophys Res Commun. 2000;279:779-85.
[171] Na-Ranong S, Laoteng K, Kittakoop P, Tanticharoen M, Cheevadhanarak S. Targeted mutagenesis of a fatty acid Δ^6-desaturase from *Mucor rouxii*: role of amino acid residues adjacent to histidine-rich motif II. Biochem Biophys Res Commun 2006;339:1029-34.
[172] White SH, Wimley WC. Membrane protein folding and stability: physical principles. Annu Rev Biophys Biomol Struct 1999;28:319-65.
[173] Resemann HC, Herrfurth C, Feussner K, Hornung E, Ostendorf AK, Gömann J, Mittag J, van Gessel N, Vries J, Ludwig-Müller J, Markham J, Reski R, Feussner I. Convergence of sphingolipid desaturation across over 500 million years of plant evolution. Nat Plants 2021;7:219-32.

[174] Michaelson LV, Zäuner S, Markham JE, Haslam RP, Desikan R, Mugford S, Albrecht S, Warnecke D, Sperling P, Heinz E, Napier JA. Functional characterization of a higher plant sphingolipid Δ4-desaturase: defining the role of sphingosine and sphingosine-1-phosphate in Arabidopsis. Plant Physiol 2009;149:487-98.
[175] Ternes P, Franke S, Zähringer U, Sperling P, Heinz E. Identification and characterization of a sphingolipid delta 4-desaturase family. J Biol Chem 2002;277:25512-8.
[176] Hashimoto K, Yoshizawa AC, Okuda S, Kuma K, Goto S, Kanehisa M. The repertoire of desaturases and elongases reveals fatty acid variations in 56 eukaryotic genomes. J Lipid Res 2008;49:183-91.
[177] Haslam TM, Kunst L. Extending the story of very-long-chain fatty acid elongation. Plant Sci 2013;210:93-107.
[178] Chen Y, Kelly EE, Masluk RP, Nelson CL, Cantu DC, Reilly PJ. Structural classification and properties of ketoacyl synthases. Protein Sci 2011;20:1659-67.
[179] Joubès J, Raffaele S, Bourdenx B, Garcia C, Laroche-Traineau J, Moreau P, Domergue F, Lessire R. The VLCFA elongase gene family in *Arabidopsis thaliana*: phylogenetic analysis, 3D modelling and expression profiling. Plant Mol Biol 2008;67:547-66.
[180] Jasinski S, Lécureuil A, Miquel M, Loudet O, Raffaele S, Froissard M, Guerche P. Natural variation in seed very long chain fatty acid content is controlled by a new isoform of KCS18 in Arabidopsis thaliana. PLoS One 2012;7:e49261.
[181] Mietkiewska E, Brost JM, Giblin EM, Barton DL, Taylor DC. Cloning and functional characterization of the *fatty acid elongase 1* (*FAE1*) gene from high erucic *Crambe abyssinica* cv. Prophet. Plant Biotechnol J 2007;5:636-45.
[182] Beaudoin F, Wu X, Li F, Haslam RP, Markham JE, Zheng H, Napier JA, Kunst L. Functional characterization of the Arabidopsis beta-ketoacyl-coenzyme A reductase candidates of the fatty acid elongase. Plant Physiol 2009;150:1174-91.
[183] Domergue F, Chevalier S, Créach A, Cassagne C, Lessire R. Purification of the acyl-CoA elongase complex from developing rapeseed and characterization of the 3-ketoacyl-CoA synthase and the 3-hydroxyacyl-CoA dehydratase. Lipids 2000;35:487-94.
[184] Bach L, Michaelson LV, Haslam R, Bellec Y, Gissot L, Marion J, Da Costa M, Boutin JP, Miquel M, Tellier F, Domergue F, Markham JE, Beaudoin F, Napier JA, Faure JD. The very-long-chain hydroxy fatty acyl-CoA dehydratase PASTICCINO2 is essential and limiting for plant development. Proc Natl Acad Sci USA 2008;105:14727-31.
[185] Blacklock BJ, Jaworski JG. Substrate specificity of Arabidopsis 3-ketoacyl-CoA synthases. Biochem Biophys Res Commun 2006;346:583-90.
[186] Millar AA, Kunst L. Very-long-chain fatty acid biosynthesis is controlled through the expression and specificity of the condensing enzyme. Plant J 1997;12:121-31.
[187] Rossak M, Smith M, Kunst L. Expression of the *FAE1* gene and *FAE1* promoter activity in developing seeds of *Arabidopsis thaliana*. Plant Mol Biol 2001;46:717-25.

[188] Han J, Lühs W, Sonntag K, Zähringer U, Borchardt DS, Wolter FP, Heinz E, Frentzen M. Functional characterization of beta-ketoacyl-CoA synthase genes from *Brassica napus* L. Plant Mol Biol 2001;46:229-39.
[189] Puyaubert J, Garbay B, Costaglioli P, Dieryck W, Roscoe TJ, Renard M, Cassagne C, Lessire R. Acyl-CoA elongase expression during seed development in *Brassica napus*. Biochim Biophys Acta 2001;1533:141-52.
[190] Puyaubert J, Dieryck W, Costaglioli P, Chevalier S, Breton A, Lessire R. Temporal gene expression of 3-ketoacyl-CoA reductase is different in high and in low erucic acid *Brassica napus* cultivars during seed development. Biochim Biophys Acta 2005;1687:152-63.
[191] Chiron H, Wilmer J, Lucas MO, Nesi N, Delseny M, Devic M, Roscoe TJ. Regulation of *FATTY ACID ELONGATION1* expression in embryonic and vascular tissues of *Brassica napus*. Plant Mol Biol 2015;88:65-83.
[192] Mietkiewska E, Brost JM, Giblin EM, Barton DL, Taylor DC. A *Teesdalia nudicaulis FAE1* complements the *fae1* mutation in transgenic *Arabidopsis thaliana* plants and shows a preference for elongating oleic acid to eicosenoic acid. Plant Sci 2007;173:198-205.
[193] Mietkiewska E, Giblin EM, Wang S, Barton DL, Dirpaul J, Brost JM, Katavic V, Taylor DC. Seed-specific heterologous expression of a nasturtium FAE gene in Arabidopsis results in a dramatic increase in the proportion of erucic acid. Plant Physiol 2004;136:2665-75.
[194] Li Y, Beisson F, Ohlrogge J. Oil content of Arabidopsis seeds: the influence of seed anatomy, light and plant-to-plant variation. Phytochemistry 2006;67:904-15.
[195] Li Z, Ma S, Song H, Yang Z, Zhao C, Taylor D, Zhang M. A *3-ketoacyl-CoA synthase* 11 (KCS11) homolog from *Malania oleifera* synthesizes nervonic acid in plants rich in 11Z-eicosenoic acid. Tree Physiol 2021;41:331-42.
[196] Guo Y, Mietkiewska E, Francis T, Katavic V, Brost JM, Giblin M, Barton DL, Taylor DC. Increase in nervonic acid content in transformed yeast and transgenic plants by introduction of a *Lunaria annua* L. *3-ketoacyl-CoA synthase* (*KCS*) gene. Plant Mol Biol 2009;69:565-75.
[197] Taylor DC, Francis T, Guo Y, Brost JM, Katavic V, Mietkiewska E, Michael Giblin E, Lozinsky S, Hoffman T. Molecular cloning and characterization of a *KCS* gene from *Cardamine graeca* and its heterologous expression in *Brassica* oilseeds to engineer high nervonic acid oils for potential medical and industrial use. Plant Biotechnol J 2009;7:925-38.
[198] Nguyen HT, Mishra G, Whittle E, Pidkowich MS, Bevan SA, Merlo AO, Walsh TA, Shanklin J. Metabolic engineering of seeds can achieve levels of ω-7 fatty acids comparable with the highest levels found in natural plant sources. Plant Physiol 2010;154:1897-904.
[199] Heath RJ, Rock CO. The Claisen condensation in biology. Nat prod Rep 2002;19:581-96.
[200] Blacklock BJ. Fatty acid elongation by ELOVL condensing enzymes depends on a histidine nucleophile. Nat Struct Mol Biol 2021;28:462-4.
[201] Ghanevati M, Jaworski JG. Engineering and mechanistic studies of the *Arabidopsis* FAE1 beta-ketoacyl-CoA synthase, FAE1 KCS. Eur J Biochem 2002;269:3531-9.
[202] Lassner MW, Lardizabal K, Metz JG. A jojoba ß-Ketoacyl-CoA synthase cDNA complements the canola fatty acid elongation mutation in transgenic plants. Plant Cell 1996;8:281-92.

[203] Ghanevati M, Jaworski JG. Active-site residues of a plant membrane-bound fatty acid elongase ß-ketoacyl-CoA synthase, FAE1 KCS. Biochim Biophys Acta 2001;1530:77-85.
[204] Blacklock BJ, Jaworski JG. Studies into factors contributing to substrate specificity of membrane-bound 3-ketoacyl-CoA synthases. Eur J Biochem 2002;269:4789-98.
[205] Teh OK, Ramli US. Characterization of a KCS-like KASII from *Jessenia bataua* that elongates saturated and monounsaturated stearic acids in *Arabidopsis thaliana*. Mol Biotechnol 2011;48:97-108.
[206] Brown AP, Affleck V, Fawcett T, Slabas AR. Tandem affinity purification tagging of fatty acid biosynthetic enzymes in *Synechocystis* sp. PCC6803 and *Arabidopsis thaliana*. J Exp Bot 2006;57:1563-71.
[207] Marchive C, Kinovics K, To A, Lepiniec L, Baud S. Transcriptional regulation of fatty acid production in higher plants: Molecular bases and biotechnological outcomes. Eur J Lipid Sci Technol 2014;116:1332-43.
[208] Carlsson AS, LaBrie ST, Kinney AJ, von Wettstein-Knowles P, Browse J. A *KAS2* cDNA complements the phenotypes of the Arabidopsis *fab1* mutant that differs in a single residue bordering the substrate binding pocket. Plant J 2002;29:761-70.
[209] Pidkowich MS, Nguyen HT, Heilmann I, Ischebeck T, Shanklin J. Modulating seed ß-ketoacyl-acyl carrier protein synthase II level converts the composition of a temperate seed oil to that of a palm-like tropical oil. Proc Natl Acad Sci USA 2007;104:4742-7.
[210] Magnuson K, Jackowski S, Rock CO, Cronan JE Jr. Regulation of fatty acid biosynthesis in *Escherichia coli*. Microbiol Rev 1993;57:522-42.
[211] Huang W, Jia J, Edwards P, Dehesh K, Schneider G, Lindqvist Y. Crystal structure of ß-ketoacyl-acyl carrier protein synthase II from *E. coli* reveals the molecular architecture of condensing enzymes. EMBO J 1998;17:1183-91.
[212] Gao J, Wallis JG, Browse J. Mutations in the prokaryotic pathway rescue the *fatty acid biosynthesis1* mutant in the cold. Plant Physiol 2015;169:442-52.
[213] Mekhedov S, Cahoon EB, Ohlrogge J. An unusual seed-specific 3-ketoacyl-ACP synthase associated with the biosynthesis of petroselinic acid in coriander. Plant Mol Biol 2001;47:507-18.
[214] Siebertz H, Heinz E. Labelling experiments on the origin of hexa-and octa-decatrienoic acids in galactolipids from leaves. Z Naturforsch 1977;32:193-205.
[215] Browse J, Warwick N, Somerville CR, Slack CR. Fluxes through the prokaryotic and eukaryotic pathways of lipid synthesis in the '16:3' plant *Arabidopsis thaliana*. Biochem J 1986;235:25-31.
[216] Falcone DL, Gibson S, Lemieux B, Somerville C. Identification of a gene that complements an Arabidopsis mutant deficient in chloroplast omega 6 desaturase activity. Plant Physiol 1994;106:1453-9.
[217] Iba K, Gibson S, Nishiuchi T, Fuse T, Nishimura M, Arondel V, Hugly S, Somerville C. A gene encoding a chloroplast omega-3 fatty acid desaturase complements alterations in fatty acid desaturation and chloroplast copy number of the *fad7* mutant of *Arabidopsis thaliana*. J Biol Chem. 1993;268:24099-105.
[218] McConn M, Hugly S, Browse J, Somerville C. A mutation at the *fad8* locus of *Arabidopsis* identifies a second chloroplast ω-3 Desaturase. Plant Physiol 1994;106:1609-14.

[219] Hugly S, Somerville C. A role for membrane lipid polyunsaturation in chloroplast biogenesis at low temperature. Plant Physiol 1992;99:197-202.
[220] Simidjiev I, Stoylova S, Amenitsch H, Javorfi T, Mustardy L, Laggner P, Holzenburg A, Garab G. Self-assembly of large, ordered lamellae from non-bilayer lipids and integral membrane proteins in vitro. Proc Natl Acad Sci USA 2000;97:1473-6.
[221] Okuley J, Lightner J, Feldmann K, Yadav N, Lark E, Browse J. Arabidopsis *FAD2* gene encodes the enzyme that is essential for polyunsaturated lipid synthesis. Plant Cell 1994;6:147-58.
[222] Kang J, Snapp AR, Lu C. Identification of three genes encoding microsomal oleate desaturases (FAD2) from the oilseed crop *Camelina sativa*. Plant Physiol Biochem 2011;49:223-9.
[223] Arondel V, Lemieux B, Hwang I, Gibson S, Goodman HM, Somerville CR. Map-based cloning of a gene controlling omega-3 fatty acid desaturation in Arabidopsis. Science 1992;258:1353-5.
[224] Román Á, Hernández ML, Soria-García Á, López-Gomollón S, Lagunas B, Picorel R, Martínez-Rivas JM, Alfonso M. Non-redundant contribution of the plastidial FAD8 ω-3 desaturase to glycerolipid unsaturation at different temperatures in Arabidopsis. Mol Plant 2015;8:1599-611.
[225] Napier JA. The production of unusual fatty acids in transgenic plants. Annu Rev Plant Biol 2007;58:295-319.
[226] Jeon JE, Kim JG, Fischer CR, Mehta N, Dufour-Schroif C, Wemmer K, Mudgett MB, Sattely E. A pathogen-responsive gene cluster for highly modified fatty acids in tomato. Cell 2020;180:176-87.
[227] Ettaki H, Troncoso-Ponce MA, To A, Barthole G, Lepiniec L, Baud S. Overexpression of *MYB115*, *AAD2*, or *AAD3* in *Arabidopsis thaliana* seeds yields contrasting omega-7 contents. PLoS One 2018;13:e0192156.
[228] Kehelpannala C, Rupasinghe T, Pasha A, Esteban E, Hennessy T, Bradley D, Ebert B, Provart NJ, Roessner U. An Arabidopsis lipid map reveals differences between tissues and dynamic changes throughout development. Plant J 2021;107:287-302.
[229] Lightner J, Wu J, Browse J. A mutant of Arabidopsis with increased levels of stearic acid. Plant Physiol 1994;106:1443-51.
[230] Lightner J, Lark E, James D, Browse J. Novel mutations affecting leaf stearate content and plant size in Arabidopsis. Theor Appl Genet 1997;94:975-81.
[231] Kazaz S, Barthole G, Domergue F, Ettaki H, To A, Vasselon D, De Vos D, Belcram K, Lepiniec L, Baud S. Differential activation of partially redundant Δ9 stearoyl-ACP desaturase genes is critical for omega-9 monounsaturated fatty acid biosynthesis during seed development in Arabidopsis. Plant Cell 2020;32:3613-37.
[232] Kachroo P, Shanklin J, Shah J, Whittle EJ, Klessig DF. A fatty acid desaturase modulates the activation of defense signaling pathways in plants. Proc Natl Acad Sci USA 2001;98:9448-53.
[233] Mandal MK, Chandra-Shekara AC, Jeong RD, Yu K, Zhu S, Chanda B, Navarre D, Kachroo A, Kachroo P. Oleic acid-dependent modulation of NITRIC OXIDE ASSOCIATED1 protein levels regulates nitric oxide-mediated defense signaling in Arabidopsis. Plant Cell 2012;24:1654-74.
[234] Walley JW, Kliebenstein DJ, Bostock RM, Dehesh K. Fatty acids and early detection of pathogens. Curr Opin Plant Biol 2013;16:520-6.

[235] Lim GH, Singhal R, Kachroo A, Kachroo P. Fatty acid- and lipid-mediated signaling in plant defense. Annu Rev Phytopathol 2017;55:505-36.
[236] Boudière L, Michaud M, Petroutsos D, Rébeillé F, Falconet D, Bastien O, Roy S, Finazzi G, Rolland N, Jouhet J, Block MA, Maréchal E. Glycerolipids in photosynthesis: composition, synthesis and trafficking. Biochim Biophys Acta 2014;1837:470-80.
[237] Mackender RO. Galactolipid and chlorophyll synthesis and changes in fatty acid composition during the greening of etiolated maize leaf segments of different ages. Plant Sci Lett 1979;16:101-9.
[238] Jordan P, Fromme P, Witt HT, Klukas O, Saenger W, Krauss N. Three-dimensional structure of cyanobacterial photosystem I at 2.5 Å resolution. Nature 2001;411:909-17.
[239] Loll B, Kern J, Saenger W, Zouni A, Biesiadka J. Towards complete cofactor arrangement in the 3.0 Å resolution structure of photosystem II. Nature 2005;438:1040-4.
[240] Kruse O, Hankamer B, Konczak C, Gerle C, Morris E, Radunz A, Schmid GH, Barber J. Phosphatidylglycerol is involved in the dimerization of photosystem II. J Biol Chem 2000;275:6509-14.
[241] Sakurai I, Hagio M, Gombos Z, Tyystjarvi T, Paakkarinen V, Aro EM, Wada H. Requirement of phosphatidylglycerol for maintenance of photosynthetic machinery. Plant Physiol 2003;133:1376-84.
[242] Sakurai I, Shen JR, Leng J, Ohashi S, Kobayashi M, Wada H. Lipids in oxygen-evolving photosystem II complexes of cyanobacteria and higher plants. J Biochem 2006;140:201-9.
[243] Domonkos I, Malec P, Sallai A, Kovács L, Itoh K, Shen G, Ughy B, Bogos B, Sakurai I, Kis M, Strzalka K, Wada H, Itoh S, Farkas T, Gombos Z. Phosphatidylglycerol is essential for oligomerization of photosystem I reaction center. Plant physiol 2004;134:1471-8.
[244] Zhou Y, Hölzl G, vom Dorp K, Peisker H, Melzer M, Frentzen M, Dörmann P. Identification and characterization of a plastidial phosphatidylglycerophosphate phosphatase in *Arabidopsis thaliana*. Plant J 2017;89:221-34.
[245] Trémolières A, Dubacq J-P, Ambard-Bretteville F, Rémy R. Lipid composition of chlorophyll-protein complexes. Specific enrichment in *trans*-hexadecenoic acid of an oligomeric form of light-harvesting chlorophyll a/b protein. FEBS Lett 1981;130:27-31.
[246] Browse J, McCourt P, Somerville C. A mutant of *Arabidopsis* lacking a chloroplast-specific lipid. Science 1985;227:763-5.
[247] Wang K, Froehlich JE, Zienkiewicz A, Hersh HL, Benning C. A plastid phosphatidylglycerol lipase contributes to the export of acyl groups from plastids for seed oil biosynthesis. Plant Cell 2017;29:1678-96.
[248] Lyons JM. Chilling injury in plants. Annu Rev Plant Physiol 1973;24:445-66.
[249] Wallis JG, Browse J. Mutants of Arabidopsis reveal many roles for membrane lipids. Prog Lipid Res 2002;41:254-78.
[250] Lande MB, Donovan JM, Zeidel ML. The relationship between membrane fluidity and permeabilities to water, solutes, ammonia, and protons. J Gen Physiol 1995;106:67-84.
[251] Whiting KP, Restall CJ, Brain PF. Steroid hormone-induced effects on membrane fluidity and their potential roles in non-genomic mechanisms. Life Sci 2000;67:743-57.
[252] Nishida I, Murata N. Chilling sensitivity in plants and cyanobacteria: The crucial contribution of membrane lipids. Annu Rev Plant Physiol Plant Mol Biol 1996;47:541-68.

[253] Burgos A, Szymanski J, Seiwert B, Degenkolbe T, Hannah MA, Giavalisco P, Willmitzer L. Analysis of short-term changes in the *Arabidopsis thaliana* glycerolipidome in response to temperature and light. Plant J 2011;66:656-68.
[254] Barton PG, Gunstone FD. Hydrocarbon chain packing and molecular motion in phospholipid bilayers formed from unsaturated lecithins. Synthesis and properties of sixteen positional isomers of 1,2-dioctadecenoyl-*sn*-glycero-3-phosphorylcholine. J Biol Chem 1975;250:4470-6.
[255] Gerloff ED, Richardson T, Stahmann MA. Changes in fatty acids of alfalfa roots during cold hardening. Plant Physiol 1966;41:1280-4.
[256] Routaboul JM, Fischer SF, Browse J. Trienoic fatty acids are required to maintain chloroplast function at low temperatures. Plant Physiol 2000;124:1697-705.
[257] Zheng G, Tian B, Zhang F, Tao F, Li W. Plant adaptation to frequent alterations between high and low temperatures: remodelling of membrane lipids and maintenance of unsaturation levels. Plant Cell Environ 2011;34:1431-42.
[258] Degenkolbe T, Giavalisco P, Zuther E, Seiwert B, Hincha DK, Willmitzer L. Differential remodeling of the lipidome during cold acclimation in natural accessions of *Arabidopsis thaliana*. Plant J 2012;72:972-82.
[259] Mamode Cassim A, Gouguet P, Gronnier J, Laurent N, Germain V, Grison M, Boutté Y, Gerbeau-Pissot P, Simon-Plas F, Mongrand S. Plant lipids: Key players of plasma membrane organization and function. Prog Lipid Res 2019;73:1-27.
[260] Tarazona P, Feussner K, Feussner I. An enhanced plant lipidomics method based on multiplexed liquid chromatography-mass spectrometry reveals additional insights into cold- and drought-induced membrane remodeling. Plant J 2015;84:621-33.
[261] Zhou Y, Zeng L, Fu X, Mei X, Cheng S, Liao Y, Deng R, Xu X, Jiang Y, Duan X, Baldermann S, Yang Z. The sphingolipid biosynthetic enzyme *Sphingolipid delta8 desaturase* is important for chilling resistance of tomato. Sci Rep 2016;6:38742.
[262] da Silva AL, Sperling P, Horst W, Franke S, Ott C, Becker D, Stass A, Lörz H, Heinz E. A possible role of sphingolipids in the aluminum resistance of yeast and maize. J Plant Physiol 2006;163:26-38.
[263] Ryan PR, Liu Q, Sperling P, Dong B, Franke S, Delhaize E. A higher plant Δ8 sphingolipid desaturase with a preference for (*Z*)-isomer formation confers aluminum tolerance to yeast and plants. Plant Physiol. 2007 Aug;144:1968-77.
[264] Yeats TH, Rose JK. The formation and function of plant cuticles. Plant Physiol 2013;163:5-20.
[265] Bernard A, Joubès J. Arabidopsis cuticular waxes: advances in synthesis, export and regulation. Prog Lipid Res 2013;52:110-29.
[266] Pollard M, Beisson F, Li Y, Ohlrogge JB. Building lipid barriers: biosynthesis of cutin and suberin. Trends Plant Sci 2008;13:236-46.
[267] Samuels L, Kunst L, Jetter R. Sealing plant surfaces: cuticular wax formation by epidermal cells. Annu Rev Plant Biol 2008;59:683-707.
[268] Busta L, Jetter R. Moving beyond the ubiquitous: the diversity and biosynthesis of specialty compounds in plant cuticular waxes. Phytochem Rev 2018;17:1275-304

[269] Perera MA, Qin W, Yandeau-Nelson M, Fan L, Dixon P, Nikolau BJ. Biological origins of normal-chain hydrocarbons: a pathway model based on cuticular wax analyses of maize silks. Plant J 2010;64:618-32.
[270] Qin P, Tu B, Wang Y, Deng L, Quilichini TD, Li T, Wang H, Ma B, Li S. ABCG15 encodes an ABC transporter protein, and is essential for post-meiotic anther and pollen exine development in rice. Plant Cell Physiol. 2013;54:138-54.
[271] Small DM. Lateral chain packing in lipids and membranes. J Lipid Res 1984;25:1490-500.
[272] Gibbs A, Pomonis JG. Physical properties of insect cuticular hydrocarbons: the effects of chain length, methyl-branching and unsaturation. Comp Biochem Physiol B, Biochem Mol Biol 1995:112;243-9
[273] Gibbs AG. Lipid melting and cuticular permeability: new insights into an old problem. J Insect Physiol 2002;48:391-400.
[274] Xu S, Schlüter PM, Grossniklaus U, Schiestl FP. The genetic basis of pollinator adaptation in a sexually deceptive orchid. PLoS Genet 2012;8:e1002889.
[275] Xu S, Schlüter PM. Modeling the two-locus architecture of divergent pollinator adaptation: how variation in SAD paralogs affects fitness and evolutionary divergence in sexually deceptive orchids. Ecol Evol 2015;5:493-502.
[276] Westoby M, Jurado E, Leishman M. Comparative evolutionary ecology of seed size. Trends Ecol Evol 1992;7:368-72.
[277] Graham IA. Seed storage oil mobilization. Annu Rev Plant Biol 2008;59:115-42.
[278] Baud S, Lepiniec L. Physiological and developmental regulation of seed oil production. Prog Lipid Res 2010;49:235-49.
[279] Sanyal A, Lenoir J, O'Neill C, Dubois F, Decocq G. Intraspecific and interspecific adaptive latitudinal cline in Brassicaceae seed oil traits. Am J Bot 2018;105:85-94.
[280] Onstein RE, Baker WJ, Couvreur TLP, Faurby S, Herrera-Alsina L, Svenning JC, Kissling WD. To adapt or go extinct? The fate of megafaunal palm fruits under past global change. Proc Biol Sci 2018;285:20180882.
[281] Guerin C, Serret J, Montúfar R, Vaissayre V, Bastos-Siqueira A, Durand-Gasselin T, Tregear J, Morcillo F, Dussert S. Palm seed and fruit lipid composition: phylogenetic and ecological perspectives. Ann Bot 2020;125:157-72.
[282] O'Keefe VA, Wiley V A, Knauft DA. Comparison of oxidative stability of high- and normal-oleic peanut oils. J Am Oil Chem Soc 1993:70;489-92.
[283] Warner K, Knowlton S. Frying quality and oxidative stability of high-oleic corn oils. J Am Oil Chem Soc 1997;74:1317-22.
[284] Barth CA. Nutritional value of rapeseed oil and its high oleic/low linolenic variety–A call for differentiation. Eur J Lipid Sci Technol 2009;111:953-6.
[285] Sales-Campos H, Souza PR, Peghini BC, da Silva JS, Cardoso CR. An overview of the modulatory effects of oleic acid in health and disease. Mini Rev Med Chem 2013;13:201-10.

[286] Yamaki T, Nagamine I, Fukumoto T, Yano T, Miyahara M, Sakurai H. High oleic peanut oil modulates promotion stage in lung tumorigenesis of mice treated with methyl nitrosourea. Food Sci Technol Res 2005;11:231-5.
[287] Smith SA, King RE, Min DB. Oxidative and thermal stabilities of genetically modified high oleic sunflower oil. Food Chem 2007;102:1208-13.
[288] Davis JP, Dean LO, Faircloth WH, Sanders TH. Physical and chemical characterizations of normal and high-oleic oils from nine commercial cultivars of peanut. J Am Oil Chem Soc 2008;85:235-43.
[289] Durrett TP, Benning C, Ohlrogge JB. Plant triacylglycerols as feedstocks for the production of biofuels. Plant J 2008;54:593-607.
[290] Vanhercke T, Wood CC, Stymne S, Singh SP, Green AG. Metabolic engineering of plant oils and waxes for use as industrial feedstocks. Plant Biotechnol J 2013;11:197-210.
[291] Hernández ML, Sicardo MD, Belaj A, Martínez-Rivas JM. The oleic/linoleic acid ratio in olive (*Olea europaea* L.) fruit mesocarp is mainly controlled by *OeFAD2-2* and *OeFAD2-5* genes together with the different specificity of extraplastidial acyltransferase enzymes. Front Plant Sci 2021;12:653997.
[292] Spasibionek S, Mikołajczyk K, Ćwiek-Kupczyńska H, Piętka T, Krótka K, Matuszczak M, Nowakowska J, Michalski K, Bartkowiak-Broda I. Marker assisted selection of new high oleic and low linolenic winter oilseed rape (*Brassica napus* L.) inbred lines revealing good agricultural value. PLoS One 2020;15:e0233959.
[293] Burns MJ, Barnes SR, Bowman JG, Clarke MH, Werner CP, Kearsey MJ. QTL analysis of an intervarietal set of substitution lines in *Brassica napus*: (i) Seed oil content and fatty acid composition. Heredity 2003;90:39-48.
[294] Hu X, Sullivan-Gilbert M, Gupta M, Thompson SA. Mapping of the loci controlling oleic and linolenic acid contents and development of *fad2* and *fad3* allele-specific markers in canola (*Brassica napus* L.). Theor Appl Genet 2006;113:497-507.
[295] Smooker AM, Wells R, Morgan C, Beaudoin F, Cho K, Fraser F, Bancroft I. The identification and mapping of candidate genes and QTL involved in the fatty acid desaturation pathway in *Brassica napus*. Theor Appl Genet 2011;122:1075-90.
[296] Yang Q, Fan C, Guo Z, Qin J, Wu J, Li Q, Fu T, Zhou Y. Identification of *FAD2* and *FAD3* genes in *Brassica napus* genome and development of allele-specific markers for high oleic and low linolenic acid contents. Theor Appl Genet 2012;125:715-29.
[297] Körber N, Bus A, Li J, Parkin IA, Wittkop B, Snowdon RJ, Stich B. Agronomic and seed quality traits dissected by genome-wide association mapping in *Brassica napus*. Front Plant Sci 2016;7:386.
[298] Qu C, Jia L, Fu F, Zhao H, Lu K, Wei L, Xu X, Liang Y, Li S, Wang R, Li J. Genome-wide association mapping and identification of candidate genes for fatty acid composition in *Brassica napus* L. using SNP markers. BMC Genomics 2017;18:232.
[299] Bao B, Chao H, Wang H, Zhao W, Zhang L, Raboanatahiry N, Wang X, Wang B, Jia H, Li M. Stable, environmental specific and novel QTL identification as well as genetic dissection of fatty acid metabolism in *Brassica napus*. Front Plant Sci 2018;9:1018.

[300] Chen F, Zhang W, Yu K, Sun L, Gao J, Zhou X, Peng Q, Fu S, Hu M, Long W, Pu H, Chen S, Wang X, Zhang J. Unconditional and conditional QTL analyses of seed fatty acid composition in *Brassica napus* L. BMC Plant Biol 2018;18:49.
[301] Zhao Q, Wu J, Cai G, Yang Q, Shahid M, Fan C, Zhang C, Zhou Y. A novel quantitative trait locus on chromosome A9 controlling oleic acid content in *Brassica napus*. Plant Biotechnol J 2019;17:2313-24.
[302] Liu X, Qin D, Piersanti A, Zhang Q, Miceli C, Wang P. Genome-wide association study identifies candidate genes related to oleic acid content in soybean seeds. BMC Plant Biol 2020;20:399.
[303] Zafar S, Tang MQ, Wang YK, Sarwar R, Liu SY, Tan XL. Candidate genes-association study to identify loci related to oleic acid in *Brassica napus* using SNP markers and their heterologous expression in yeast. Plant Physiol Biochem 2020;146:294-302.
[304] Pham AT, Lee JD, Shannon JG, Bilyeu KD. Mutant alleles of *FAD2-1A* and *FAD2-1B* combine to produce soybeans with the high oleic acid seed oil trait. BMC Plant Biol 2010;10:195.
[305] Shockey J, Dowd M, Mack B, Gilbert M, Scheffler B, Ballard L, Frelichowski J, Mason C. Naturally occurring high oleic acid cottonseed oil: identification and functional analysis of a mutant allele of *Gossypium barbadense fatty acid desaturase-2*. Planta 2017;245:611-22.
[306] Kinney AJ. Genetic modification of the storage lipids of plants. Curr Opin Biotechnol 1994;5:144-51.
[307] Bai S, Engelen S, Denolf P, Wallis JG, Lynch K, Bengtsson JD, Van Thournout M, Haesendonckx B, Browse J. Identification, characterization and field testing of *Brassica napus* mutants producing high-oleic oils. Plant J 2019;98:33-41.
[308] Haun W, Coffman A, Clasen BM, Demorest ZL, Lowy A, Ray E, Retterath A, Stoddard T, Juillerat A, Cedrone F, Mathis L, Voytas DF, Zhang F. Improved soybean oil quality by targeted mutagenesis of the *fatty acid desaturase 2* gene family. Plant Biotechnol J 2014;12:934-40.
[309] Jiang WZ, Henry IM, Lynagh PG, Comai L, Cahoon EB, Weeks DP. Significant enhancement of fatty acid composition in seeds of the allohexaploid, *Camelina sativa*, using CRISPR/Cas9 gene editing. Plant Biotechnol J 2017;15:648-57.
[310] Morineau C, Bellec Y, Tellier F, Gissot L, Kelemen Z, Nogué F, Faure JD. Selective gene dosage by CRISPR-Cas9 genome editing in hexaploid *Camelina sativa*. Plant Biotechnol J 2017;15:729-39.
[311] Abe K, Araki E, Suzuki Y, Toki S, Saika H. Production of high oleic/low linoleic rice by genome editing. Plant Physiol Biochem 2018;131:58-62.
[312] Okuzaki A, Ogawa T, Koizuka C, Kaneko K, Inaba M, Imamura J, Koizuka N. CRISPR/Cas9-mediated genome editing of the *fatty acid desaturase 2* gene in *Brassica napus*. Plant Physiol Biochem 2018;131:63-9.
[313] Do PT, Nguyen CX, Bui HT, Tran LTN, Stacey G, Gillman JD, Zhang ZJ, Stacey MG. Demonstration of highly efficient dual gRNA CRISPR/Cas9 editing of the homeologous *GmFAD2-1A* and *GmFAD2-1B* genes to yield a high oleic, low linoleic and α-linolenic acid phenotype in soybean. BMC Plant Biol 2019;19:311.

[314] Huang H, Cui T, Zhang L, Yang Q, Yang Y, Xie K, Fan C, Zhou Y. Modifications of fatty acid profile through targeted mutation at *BnaFAD2* gene with CRISPR/Cas9-mediated gene editing in *Brassica napus*. Theor Appl Genet 2020;133:2401-11.
[315] Bahariah B, Masani MYA, Rasid OA, Parveez GKA. Multiplex CRISPR/Cas9-mediated genome editing of the *FAD2* gene in rice: a model genome editing system for oil palm. J Genet Eng Biotechnol 2021;19:86.
[316] Lee KR, Jeon I, Yu H, Kim SG, Kim HS, Ahn SJ, Lee J, Lee SK, Kim HU. Increasing monounsaturated fatty acid contents in hexaploid *Camelina sativa* seed oil by *FAD2* gene knockout using CRISPR-Cas9. Front Plant Sci 2021;12:702930.
[317] Lakhssassi N, Lopes-Caitar VS, Knizia D, Cullen MA, Badad O, El Baze A, Zhou Z, Embaby MG, Meksem J, Lakhssassi A, Chen P, AbuGhazaleh A, Vuong TD, Nguyen HT, Hewezi T, Meksem K. TILLING-by-sequencing+ reveals the role of novel fatty acid desaturases (GmFAD2-2s) in increasing soybean seed oleic acid content. Cells 2021;10:1245.
[318] Sivaraman I, Arumugam N, Sodhi YS, Gupta V, Mukhopadhyay A, Pradhan AK, Burma PK, Pental D. Development of high oleic and low linoleic acid transgenics in a zero erucic acid *Brassica juncea* L. (Indian mustard) line by antisense suppression of the *fad2* gene. Mol Breed 2004:13:365-75.
[319] Mroczka A, Roberts PD, Fillatti JJ, Wiggins BE, Ulmasov T, Voelker T. An intron sense suppression construct targeting soybean *FAD2-1* requires a double-stranded RNA-producing inverted repeat T-DNA insert. Plant Physiol 2010;153:882-91.
[320] Jung JH, Kim H, Go YS, Lee SB, Hur CG, Kim HU, Suh MC. Identification of functional *BrFAD2-1* gene encoding microsomal delta-12 fatty acid desaturase from *Brassica rapa* and development of *Brassica napus* containing high oleic acid contents. Plant Cell Rep 2011;30:1881-92.
[321] Zhang L, Yang XD, Zhang YY, Yang J, Qi GX, Guo DQ, Xing GJ, Yao Y, Xu WJ, Li HY, Li QY, Dong YS. Changes in oleic acid content of transgenic soybeans by antisense RNA mediated posttranscriptional gene silencing. Int J Genomics 2014;2014:921950.
[322] Wagner N, Mroczka A, Roberts PD, Schreckengost W, Voelker T. RNAi trigger fragment truncation attenuates soybean *FAD2-1* transcript suppression and yields intermediate oil phenotypes. Plant Biotechnol J 2011;9:723-8.
[323] Zaplin ES, Liu Q, Li Z, Butardo VM, Blanchard CL, Rahman S. Production of high oleic rice grains by suppressing the expression of the *OsFAD2-1* gene. Funct Plant Biol 2013;40:996-1004.
[324] Chen Y, Zhou XR, Zhang ZJ, Dribnenki P, Singh S, Green A. Development of high oleic oil crop platform in flax through RNAi-mediated multiple *FAD2* gene silencing. Plant Cell Rep 2015;34:643-53.
[325] Tiwari GJ, Liu Q, Shreshtha P, Li Z, Rahman S. RNAi-mediated down-regulation of the expression of *OsFAD2-1*: effect on lipid accumulation and expression of lipid biosynthetic genes in the rice grain. BMC Plant Biol 2016;16:189.
[326] Wood CC, Okada S, Taylor MC, Menon A, Mathew A, Cullerne D, Stephen SJ, Allen RS, Zhou XR, Liu Q, Oakeshott JG, Singh SP, Green AG. Seed-specific RNAi in safflower generates a superhigh oleic oil with extended oxidative stability. Plant Biotechnol J 2018;16:1788-96.

[327] Yang J, Xing G, Niu L, He H, Guo D, Du Q, Qian X, Yao Y, Li H, Zhong X, Yang X. Improved oil quality in transgenic soybean seeds by RNAi-mediated knockdown of *GmFAD2-1B*. Transgenic Res 2018;27:155-66.
[328] Lee KR, Kim EH, Roh KH, Kim JB, Kang HC, Go YS, Suh MC, Kim HU. High-oleic oilseed rapes developed with seed-specific suppression of *FAD2* gene expression. Appl Biol Chem 2016:59;669-76.
[329] Pham AT, Shannon JG, Bilyeu KD. Combinations of mutant *FAD2* and *FAD3* genes to produce high oleic acid and low linolenic acid soybean oil. Theor Appl Genet 2012;125:503-15.
[330] Demorest ZL, Coffman A, Baltes NJ, Stoddard TJ, Clasen BM, Luo S, Retterath A, Yabandith A, Gamo ME, Bissen J, Mathis L, Voytas DF, Zhang F. Direct stacking of sequence-specific nuclease-induced mutations to produce high oleic and low linolenic soybean oil. BMC Plant Biol 2016;16:225.
[331] Lu C, Xin Z, Ren Z, Miquel M, Browse J. An enzyme regulating triacylglycerol composition is encoded by the *ROD1* gene of Arabidopsis. Proc Natl Acad Sci USA 2009;106:18837-42.
[332] Bates PD. Understanding the control of acyl flux through the lipid metabolic network of plant oil biosynthesis. Biochim Biophys Acta 2016;1861:1214-25.
[333] Jarvis BA, Romsdahl TB, McGinn MG, Nazarenus TJ, Cahoon EB, Chapman KD, Sedbrook JC. CRISPR/Cas9-induced *fad2* and *rod1* mutations stacked with *fae1* confer high oleic acid seed oil in Pennycress (*Thlaspi arvense* L.). Front Plant Sci 2021;12:652319.
[334] Nguyen HT, Silva JE, Podicheti R, Macrander J, Yang W, Nazarenus TJ, Nam JW, Jaworski JG, Lu C, Scheffler BE, Mockaitis K, Cahoon EB. Camelina seed transcriptome: a tool for meal and oil improvement and translational research. Plant Biotechnol J 2013;11:759-69
[335] Li X, Mei D, Liu Q, Fan J, Singh S, Green A, Zhou XR, Zhu LH. Down-regulation of crambe fatty acid desaturase and elongase in Arabidopsis and crambe resulted in significantly increased oleic acid content in seed oil. Plant Biotechnol J 2016;14:323-31.
[336] Peng Q, Hu Y, Wei R, Zhang Y, Guan C, Ruan Y, Liu C. Simultaneous silencing of *FAD2* and *FAE1* genes affects both oleic acid and erucic acid contents in *Brassica napus* seeds. Plant Cell Rep 2010;29:317-25.
[337] Ivarson E, Ahlman A, Lager I, Zhu LH. Significant increase of oleic acid level in the wild species *Lepidium campestre* through direct gene silencing. Plant Cell Rep 2016;35:2055-63.
[338] Buhr T, Sato S, Ebrahim F, Xing A, Zhou Y, Mathiesen M, Schweiger B, Kinney A, Staswick P, Clemente T. Ribozyme termination of RNA transcripts down-regulate seed fatty acid genes in transgenic soybean. Plant J 2002;30:155-63.
[339] Graef G, LaVallee BJ, Tenopir P, Tat M, Schweiger B, Kinney AJ, Van Gerpen JH, Clemente TE. A high-oleic-acid and low-palmitic-acid soybean: agronomic performance and evaluation as a feedstock for biodiesel. Plant Biotechnol J 2009;7:411-21.
[340] Lu S, Aziz M, Sturtevant D, Chapman KD, Guo L. Heterogeneous distribution of erucic acid in *Brassica napus* seeds. Front Plant Sci 2020;10:1744.
[341] Bremer J, Norum KR. Metabolism of very long-chain monounsaturated fatty acids (22:1) and the adaptation to their presence in the diet. J Lipid Res 1982;23:243-56.
[342] Badawy IH, Atta B, Ahmed WM. Biochemical and toxicological studies on the effect of high and low erucic acid rapeseed oil on rats. Nahrung 1994;38:402-11.

[343] Abbott P, Baines J, Fox P, Graf L, Kelly L, Stanley G, Tomaska L. Review of the regulations for contaminants and natural toxicants. Food Control 2003;14:383-9.
[344] Wendlinger C, Hammann S, Vetter W. Various concentrations of erucic acid in mustard oil and mustard. Food Chem 2014;153:393-7.
[345] Gupta V, Mukhopadhyay A, Arumugam N, Sodhi YS, Pental D, Pradhan AK. Molecular tagging of erucic acid trait in oilseed mustard (*Brassica juncea*) by QTL mapping and single nucleotide polymorphisms in *FAE1* gene. Theor Appl Genet 2004;108:743-9.
[346] Yan G, Li D, Cai M, Gao G, Chen B, Xu K, Li J, Li F, Wang N, Qiao J, Li H, Zhang T, Wu X. Characterization of *FAE1* in the zero erucic acid germplasm of *Brassica rapa* L. Breed Sci 2015;65:257-64.
[347] Saini N, Singh N, Kumar A, Vihan N, Yadav S, Vasudev S, Yadava DK. Development and validation of functional CAPS markers for the FAE genes in *Brassica juncea* and their use in marker-assisted selection. Breed Sci 2016;66:831-7.
[348] Fourmann M, Barret P, Renard M, Pelletier G, Delourme R, Brunel D. The two genes homologous to Arabidopsis *FAE1* co-segregate with the two loci governing erucic acid content in *Brassica napus*. Theor Appl Genet 1998;96:852-8.
[349] Cao Z, Tian F, Wang N, Jiang C, Lin B, Xia W, Shi J, Long Y, Zhang C, Meng J. Analysis of QTLs for erucic acid and oil content in seeds on A8 chromosome and the linkage drag between the alleles for the two traits in *Brassica napus*. J Genet Genomics 2010;37:231-40.
[350] Roscoe TJ, Lessire R, Puyaubert J, Renard M, Delseny M. Mutations in the *fatty acid elongation 1* gene are associated with a loss of ß-ketoacyl-CoA synthase activity in low erucic acid rapeseed. FEBS Lett 2001;492:107-11.
[351] Katavic V, Mietkiewska E, Barton DL, Giblin EM, Reed DW, Taylor DC. Restoring enzyme activity in nonfunctional low erucic acid *Brassica napus* fatty acid elongase 1 by a single amino acid substitution. Eur J Biochem. 2002;269:5625-31.
[352] Lei WU, Yan-li JIA, Gang WU, Chang-ming LU. Molecular evidence for blocking erucic acid synthesis in rapeseed (*Brassica napus* L.) by a two-base-pair deletion in *FAE1* (*fatty acid elongase 1*), J Integr Agric 2015;14:1251-60.
[353] Vetter W, Darwisch V, Lehnert K. Erucic acid in *Brassicaceae* and salmon – An evaluation of the new proposed limits of erucic acid in food. NFS J 2020;19:9-15.
[354] Stefansson BR, Hougen EW, Downey RK. Note on the isolation of rape plants with seed oil free from erucic acid. Can J Plant Sci 1961;41:218-9.
[355] Nath UK, Wilmer JA, Wallington EJ, Becker HC, Möllers C. Increasing erucic acid content through combination of endogenous low polyunsaturated fatty acids alleles with *Ld-LPAAT* + *Bn-fae1* transgenes in rapeseed (*Brassica napus* L.). Theor Appl Genet 2009;118:765-73.
[356] Shi J, Lang C, Wu X, Liu R, Zheng T, Zhang D, Chen J, Wu G. RNAi knockdown of *fatty acid elongase1* alters fatty acid composition in *Brassica napus*. Biochem Biophys Res Commun 2015;466:518-22.
[357] Leonard C. Sources and commercial applications of high erucic vegetable oils. Lipid Tech 1994;4: 79-83.

[358] Piazza GJ, Foglia TA. Rapeseed oil for oleochemical uses. Eur J Lipid Sci Technol 2001;103:405-54.
[359] Semenov VG, Semenova DU, Slipushenko VP. Calculation of the high heat value of biofuels. Chem Tech Fuels Oil 2006;42:144-9.
[360] Zhao X, Weim L, Cheng S, Kadis E, Cao Y, Boakye E, Gu Z, Julson J. Hydroprocessing of carinata oil for hydrocarbon biofuel over Mo-Zn/Al_2O_3. Appl Catal B 2016:196;41-9.
[361] Vicente G, Martínez M, Aracil J. Optimization of *Brassica carinata* oil methanolysis for biodiesel production. J Amer Oil Chem Soc 2005;82:899-904.
[362] Claver A, Rey R, López MV, Picorel R, Alfonso M. Identification of target genes and processes involved in erucic acid accumulation during seed development in the biodiesel feedstock Pennycress (*Thlaspi arvense* L.). J Plant Physiol 2017;208:7-16.
[363] Vargas-Lopez JM, Wiesenborn D, Tostenson K, Cihacek L. Processing of Crambe for oil and isolation of erucic acid. J Am Chem Oil Soc 1999;76:801-9.
[364] Zorn K, Oroz-Guinea I, Bornscheuer UT. Strategies for enriching erucic acid from *Crambe abyssinica* oil by improved *Candida antarctica* lipase A variants. Process Biochem 2019;79:65-73.
[365] Roslinsky V, Falk KC, Gaebelein R, Mason AS, Eynck C. Development of *B. carinata* with super-high erucic acid content through interspecific hybridization. Theor Appl Genet 2021
[366] Cao YZ, Oo KC, Huang AH. Lysophosphatidate acyltransferase in the microsomes from maturing seeds of meadowfoam (*Limnanthes alba*). Plant Physiol 1990;94:1199-206.
[367] Brough CL, Coventry JM, Christie WW, Kroon JTM, Brown AR, Barsby TL, Slabas AR. Towards the genetic engineering of triacylglycerols of defined fatty acid composition: major changes in erucic acid content at the *sn*-2 position affected by the introduction of a 1-acyl-*sn*-glycerol-3-phosphate acyltransferase from *Limnanthes douglasii* into oil seed rape. Mol Breed 1996;2:133-42.
[368] Li X, van Loo EN, Gruber J, Fan J, Guan R, Frentzen M, Stymne S, Zhu LH. Development of ultra-high erucic acid oil in the industrial oil crop *Crambe abyssinica*. Plant Biotechnol J 2012;10:862-70.
[369] Guan R, Lager I, Li X, Stymne S, Zhu LH. Bottlenecks in erucic acid accumulation in genetically engineered ultrahigh erucic acid *Crambe abyssinica*. Plant Biotechnol J 2014;12:193-203.
[370] Fan Y, Meng HM, Hu GR, Li FL. Biosynthesis of nervonic acid and perspectives for its production by microalgae and other microorganisms. Appl Microbiol Biotechnol 2018;102:3027-35.
[371] Merrill AH Jr, Schmelz EM, Wang E, Dillehay DL, Rice LG, Meredith F, Riley RT. Importance of sphingolipids and inhibitors of sphingolipid metabolism as components of animal diets. J Nutr 1997;127:830S-3S.
[372] Martínez M, Mougan I. Fatty acid composition of human brain phospholipids during normal development. J Neurochem 1998;71:2528-33.
[373] Liu F, Wang P, Xiong X, Zeng X, Zhang X, Wu G. A review of nervonic acid production in plants: prospects for the genetic engineering of high nervonic acid cultivars plants. Front Plant Sci 2021;12:626625.
[374] Sargent JR, Coupland K, Wilson R. Nervonic acid and demyelinating disease. Med Hypotheses 1994 ;42:237-42.

[375] Ntoumani E, Strandvik B, Sabel KG. Nervonic acid is much lower in donor milk than in milk from mothers delivering premature infants-Of neglected importance? Prostaglandins Leukot Essent Fatty Acids 2013;89:241-4.
[376] Yu J, Yuan T, Zhang X, Jin Q, Wei W, Wang X. Quantification of nervonic acid in human milk in the first 30 days of lactation: Influence of lactation stages and comparison with infant formulae. Nutrients 2019;11:1892.
[377] Chen JR, Hsu SF, Hsu CD, Hwang LH, Yang SC. Dietary patterns and blood fatty acid composition in children with attention-deficit hyperactivity disorder in Taiwan. J Nutr Biochem 2004;15:467-72.
[378] Pamplona R, Dalfó E, Ayala V, Bellmunt MJ, Prat J, Ferrer I, Portero-Otín M. Proteins in human brain cortex are modified by oxidation, glycoxidation, and lipoxidation. Effects of Alzheimer disease and identification of lipoxidation targets. J Biol Chem 2005;280:21522-30.
[379] Amminger GP, Schäfer MR, Klier CM, Slavik JM, Holzer I, Holub M, Goldstone S, Whitford TJ, McGorry PD, Berk M. Decreased nervonic acid levels in erythrocyte membranes predict psychosis in help-seeking ultra-high-risk individuals. Mol Psychiatry 2012;17:1150-2.
[380] Kageyama Y, Deguchi Y, Hattori K, Yoshida S, Goto YI, Inoue K, Kato T. Nervonic acid level in cerebrospinal fluid is a candidate biomarker for depressive and manic symptoms: A pilot study. Brain Behav 2021;11:e02075.
[381] Tanaka K, Shimizu T, Ohtsuka Y, Yamashiro Y, Oshida K. Early dietary treatments with Lorenzo's oil and docosahexaenoic acid for neurological development in a case with Zellweger syndrome. Brain Dev 2007;29:586-9.
[382] Lewkowicz N, Piątek P, Namiecińska M, Domowicz M, Bonikowski R, Szemraj J, Przygodzka P, Stasiołek M, Lewkowicz P. Naturally occurring nervonic acid ester improves myelin synthesis by human oligodendrocytes. Cells 2019;8:786.
[383] Hu D, Cui Y, Zhang J. Nervonic acid amends motor disorder in a mouse model of Parkinson's disease. Transl Neurosci 2021;12:237-46.
[384] Umemoto H, Yasugi S, Tsuda S, Yoda M, Ishiguro T, Kaba N, Itoh T. Protective effect of nervonic acid against 6-hydroxydopamine-induced oxidative stress in PC-12 cells. J Oleo Sci 2021;70:95-102.
[385] Kasai N, Mizushina Y, Sugawara F, Sakaguchi K. Three-dimensional structural model analysis of the binding site of an inhibitor, nervonic acid, of both DNA polymerase beta and HIV-1 reverse transcriptase. J Biochem 2002;132:819-28.
[386] Tang TF, Liu XM, Ling M, Lai F, Zhang L, Zhou YH, Sun RR. Constituents of the essential oil and fatty acid from *Malania oleifera*. Ind Crops Prod 2013;43:1-5.
[387] Litchfield C. *Tropaeolum speciosum* seed fat: a rich source of *cis*-15-tetracosenoic and *cis*-17-hexacosenoic acids. Lipids 1970;5:144-6.
[388] Jart A. The fatty acid composition of various Cruciferous seeds. J Am Oil Chem Soc 1978;55:873-5.
[389] Meier zu Beerentrup H, Röbbelen G. Screening for European production of oilseeds with unusual fatty acids. Angew Botanik 1987;61:287-303.

[390] Mastebroek HD, Marvin HJP. Breeding prospects of *Lunaria annua* L. Ind. Crop Prod 2000;11: 139-43

[391] Ma Q, Sun T, Li S, Wen J, Zhu L, Yin T, Yan K, Xu X, Li S, Mao J, Wang YN, Jin S, Zhao X, Li Q. The *Acer truncatum* genome provides insights into nervonic acid biosynthesis. Plant J 2020;104:662-78.

[392] He X, Li DZ, Tian B. Diversity in seed oil content and fatty acid composition in *Acer* species with potential as sources of nervonic acid. Plant Divers 2020;43:86-92.

[393] Huai D, Zhang Y, Zhang C, Cahoon EB, Zhou Y. Combinatorial effects of fatty acid elongase enzymes on nervonic acid production in *Camelina sativa*. PLoS One 2015;10:e0131755.

[394] Wu Y, Li R, Hildebrand DF. Biosynthesis and metabolic engineering of palmitoleate production, an important contributor to human health and sustainable industry. Prog Lipid Res. 2012; 51: 240-9.

[395] Meier MAR. Metathesis with oleochemicals: new approaches for the utilization of plant oils as renewable resources in polymer science. Macromol Chem Phys 2009;210:1073-9.

[396] Rybak A, Fokou PA, Meier MAR. Metathesis as a versatile tool in oleochemistry. Eur J Lipid Sci Technol 2008;110:797-804.

[397] Nguyen HT, Park H, Koster KL, Cahoon RE, Nguyen HTM, Shanklin J, Clemente TE, Cahoon EB. Redirection of metabolic flux for high levels of omega-7 monounsaturated fatty acid accumulation in camelina seeds. Plant Biotechnol J 2015;13:38-50.

[398] Cao H, Gerhold K, Mayers JR, Wiest MM, Watkins SM, Hotamisligil GS. Identification of a lipokine, a lipid hormone linking adipose tissue to systemic metabolism. Cell 2008;134:933-44.

[399] Stefan N, Kantartzis K, Celebi N, Staiger H, Machann J, Schick F, Cegan A, Elcnerova M, Schleicher E, Fritsche A, Häring HU. Circulating palmitoleate strongly and independently predicts insulin sensitivity in humans. Diabetes Care 2010;33:405-7.

[400] Fatima T, Snyder CL, Schroeder WR, Cram D, Datla R, Wishart D, Weselake RJ, Krishna P. Fatty acid composition of developing sea buckthorn (*Hippophae rhamnoides* L.) berry and the transcriptome of the mature seed. PLOS ONE 2012;7:e34099.

[401] Bondaruk M, Johnson S, Degafu A, Boora P, Bilodeau P, Morris J, Wiehler W, Foroud N, Weselake R, Shah S. Expression of a cDNA encoding palmitoyl-acyl carrier protein desaturase from cat's claw (*Doxantha unguis-cati* L.) in *Arabidopsis thaliana* and *Brassica napus* leads to accumulation of unusual unsaturated fatty acids and increased stearic acid content in the seed oil. Plant Breed 2007;126:186-94.

[402] Kleiman R, Payne-Wahl KL. Fatty acid composition of seed oils of the meliaceae, including one genus rich in *cis*-vaccenic acid. J Am Oil Chem Soc 1984;61:1836-8.

[403] Gummeson PO, Lenman M, Lee M, Singh S, Stymne S. Characterisation of acyl-ACP desaturases from *Macadamia integrifolia* Maiden & Betche and *Nerium oleander* L. Plant Sci 2000;154:53-60.

[404] Spencer GF, Kleiman R. Palmitoleic acid in *Roureopsis obliquifoliata* (Connaraceae) seed oil. J Am Oil Chem Soc 1978;55:689.

[405] Badami RC, Patil KB. Structure and occurrence of unusual fatty acids in minor seed oils. Prog Lipid Res 1980;19:119-53.

[406] Barthet VJ. (n-7) and (n-9) *cis*-monounsaturated fatty acid contents of 12 Brassica species. Phytochemistry 2008;69:411-7.
[407] Isbell T. Development of meadowfoam as an industrial crop through novel fatty acid derivatives. Lipid Technol 1997;9:140-4.
[408] Burg DA, Kleiman R. Preparation of meadowfoam dimer acids and dimer esters and their use as lubricants. J Am Oil Chem Soc 1991;68:600-3.
[409] Erhan SM, Kleiman R, Isbell TA. Estolides from meadowfoam oil fatty acids and other monounsaturated acyl moieties in developing seeds. J Am Oil Chem Soc 1993;70:460-5.
[410] Wohlman A. Meadowfoam derivatives: technologically advanced cosmetic ingredients. J Cosmet Sci 2001;52:149-50.
[411] Knapp SJ, Crane JM. Fatty acid diversity of section Inflexae *Limnanthes* (meadowfoam). Ind Crops Prod 1995;4:219-27.
[412] Knapp SJ, Crane JM. Breeding advances and germplasm resources in meadowfoam: a very long chain oilseed. In: Janick J, ed. Perspectives on new crops and new uses. Alexandria: ASHS Press, p225-233. 1999;225-33.
[413] Knapp SJ, Crane JM, Brunick R. Registration of 'Ross' meadowfoam. Crop Sci 2005;45:407
[414] Jadhav A, Marillia E-F, Babic V, Giblin EM, Cahoon EB, Kinney AJ, Mietkiewska E, Brost JM, Taylor DC. Production of 22:2$^{\Delta 5,\Delta 13}$ and 20:1$^{\Delta 5}$ in *Brassica carinata* and soybean breeding lines via introduction of *Limnanthes* genes. Mol Breed 2005;15:157-67
[415] Slabaugh MB, Cooper LD, Kishore VK, Knapp SJ, Kling JG. Genes affecting novel seed constituents in *Limnanthes alba* Benth: transcriptome analysis of developing embryos and a new genetic map of meadowfoam. PeerJ 2015;3:e915.
[416] Yang Z, Li C, Jia Q, Zhao C, Taylor DC, Li D, Zhang M. Transcriptome analysis reveals candidate genes for petroselinic acid biosynthesis in fruits of *Coriandrum sativum* L. J Agric Food Chem 2020;68:5507-20.
[417] Ohlrogge JB. Design of new plant products: engineering of fatty acid metabolism. Plant Physiol 1994;104:821-6.
[418] Carlsson AS, Yilmaz JL, Green AG, Stymne S, Hofvander P. Replacing fossil oil with fresh oil - with what and for what? Eur J Lipid Sci Technol 2011;113:812-31.
[419] Suh MC, Schultz DJ, Ohlrogge JB. What limits production of unusual monoenoic fatty acids in transgenic plants? Planta 2002;215:584-95.

Figure legends

Figure 1. Structure of 9-octadecenoic acid and some derivatives used for structural analyses

(A) Structure of two 9-octadecenoic acid isomers differing by the configuration of their C-C double bond. Carbon atoms are numbered according to the delta nomenclature, in green, and to the ω nomenclature, in blue.

(B-F) Fatty acid derivates used for structural analyses. The figure displays the structure of a methyl ester derivative of (9*E*)-octadecenoic acid, commonly used for gas chromatography analyses (B).

Structures of pyrrolidine (C), picolynil (D), 4,4-dimethyloxazoline (DMOX) derivatives (E), and dimethyl disulfide (DMDS) adducts (F) used for structural characterization are presented too.

Figure 2. Structural diversity of plant monounsaturated fatty acids

A. Table of monounsaturated fatty acids. All possible structures of monounsaturated fatty acids ranging from C3 (top) to C34 (bottom) are displayed as squares. Squares corresponding to monounsaturated fatty acid structures already identified in land plants are highlighted in purple, with their C-C double bond configuration specified as *c* (*cis*) or *t* (*trans*). For a given chain length, a yellow square at the left end of the row means that no monounsaturated fatty acid has been identified so far, while a pink color indicates that at least one structure has been characterized. The data displayed in this table mostly originate from the PlantFA database (https://plantfadb.org/).

B. Partitioning of characterized monounsaturated fatty acids according to the length of their acyl chain. Dark green, odd-numbered (all *cis*) fatty acid; light green, even-numbered and *cis* fatty acid; orange, even-numbered and *trans* fatty acid.

C. Venn diagram presenting the partitioning of characterized monounsaturated fatty acid structures according to carbon number and configuration of the C-C double bond. Same color code as in B.

Figure 3. Enzymatic reaction catalyzed by desaturases and associated electron transport chains

For the formation of a C-C double bond in the acyl chain of a fatty acid, two electrons are required to initiate the conversion of oxygen into a metal-bound electrophilic reagent. Reducing equivalents are supplied by different electron transport chains depending on the subcellular location of the enzyme.

(a) In the plastids, the electron transport chain involves a ferredoxin-NADP reductase (FNR) and ferredoxins (Fdx). In photosynthetic tissues in the light, reducing equivalents arising from photosystem I can be directly transferred to ferredoxin, bypassing the FNR.

(b) In the endoplasmic reticulum, the flavoprotein is cytochrome b_5 reductase, and the electron carrier is cytochrome b_5 (Cyt b_5)**.**

Figure 4. Diversity of plant desaturases using saturated acyl chains as substrates in *Arabidopsis thaliana*

The different classes of desaturase enzymes catalyzing the biosynthesis of monounsaturated acyl chains are displayed, together with their subcellular location and enzymatic characteristics. They belong to two distinct categories of unrelated proteins: the soluble and membrane-bound desaturases. In the case of soluble acyl-acyl carrier protein desaturase, conserved amino acid residues involved in binding the di-iron complex have been unambiguously identified and are presented on the schematic. In the case of membrane-bound desaturases, conserved histidine clusters presumed to compose the Fe-binding active centers of the enzymes are schematized. Vertical yellow bars represent putative ER retrieval and retention motifs.

AAD, acyl-acyl carrier protein desaturase; ADS, acyl-CoA desaturase-like; Cb_5, cytochrome b_5 domain; cTP, chloroplast transit peptide; FAD4, FATTY ACID DESATURASE4 and related proteins;

LCB, long-chain base; MGDG, monogalactosyldiacylglycerol; PG, phosphatidylglycerol; SLCB, sphingoid long-chain base; SLD, sphingolipid long-chain base Δ8 desaturase; DSD, dihydrosphingosine Δ4 desaturase; Stereo., stereospecificity.

Figure 5. Structure of the Δ9 acyl-acyl carrier protein desaturase from *Ricinus communis*

(a) Three-dimensional structure of the protein dimer viewed along different axes. The two subunits are colored blue and green, and red spheres represent irons.

(b) Internal view of a monomer. In this mesh surface model, the substrate binding pocket is highlighted in yellow, with a black arrow pointing the entry of the cavity. Red spheres represent irons.

(c) Stereo view of a di-iron center with ligands. The lateral chains of the six labelled amino acid residues coordinating the di-iron center are presented as sticks with carbon atoms as green, oxygen as orange, and nitrogen as blue. Red spheres represent irons.

All figures were produced using PyMol and were adapted from [108]; Protein Data Bank 1AFR.

Figure 6. Overview of fatty acid and acyl lipid metabolism in the plastids of *Arabidopsis thaliana*

The scheme depicts the different pathways involved in the biosynthesis of fatty acids and the elaboration of membrane lipids in the plastids of *A. thaliana*. Production of monounsaturated acyl chains by desaturases is highlighted. Unless otherwise specified, the C-C double bonds of the acyl chains presented are all in the *cis* configuration. Symbols on the right side of the schematic represent connections with the metabolic pathways depicted in figure 7.

ACP, acyl carrier protein; CDP-DAG, cytidinediphosphate-diacylglycerol; DAG, diacylglycerol; CDP-DAGS, cytidinediphosphate-diacylglycerol synthase; DGDG, digalactosyldiacylglycerol; DGDGS, digalactosyldiacylglycerol synthase; FAD, fatty acid desaturase; G3P, glycerol-3-phosphate; FAT, acyl-acyl carrier protein thioesterase; GPAT, glycerol-3-phosphate acyltransferase; KAS, fatty acid synthase complex comprising a 3-ketoacyl-ACP synthase; LPA, lysophosphatidic acid; LPAAT, lysophosphatidic acid acyltransferase; MGDG, monogalactosyldiacylglycerol; MGDGS, monogalactosyldiacylglycerol synthase; NEFA, non-esterified fatty acids; PA, phosphatidic acid; PAP, phosphatidic acid phosphatase; PAD, Δ9 palmitoyl–acyl carrier protein desaturase; PG, phosphatidylglycerol; PGP, phosphatidylglycerol-phosphate; PGPP, phosphatidylglycerol-phosphate phosphatase; PGPS, phosphatidylglycerol-phosphate synthase; SAD, Δ9 stearoyl–acyl carrier protein desaturase; SQD2, UDP-sulfoquinovose:diacylglycerol sulfoquinovosyltransferase; SQDG, sulfoquinovosyldiacylglycerol.

Figure 7. Simplified overview of extraplastidial acyl lipid metabolism in *Arabidopsis thaliana*

Production of monounsaturated acyl chains by desaturases is highlighted. Unless otherwise specified, the C-C double bonds of the acyl chains presented are all in the *cis* configuration. Symbols on the right side of the schematic represent connections with the metabolic pathways depicted in figure 6.

ADS, acyl-CoA desaturase-like; Cer, ceramide; CoA, coenzyme A; CPT, cytidine diphosphate-choline:diacylglycerol choline phosphotransferase; CS, ceramide synthase; d18:0, sphinganine; Dn

DAG, *de novo* synthesized diacylglycerol; DGAT, acyl-coenzyme A:diacylglycerol acyltransferase; DSD, dihydrosphingosine Δ4 desaturase; FAD, fatty acid desaturase; FAE1, fatty acid elongase complex comprising the 3-ketoacyl-CoA synthase FATTY ACID ELONGASE1; FAH, fatty acid α-hydroxylase; GIPC, glycosyl inositol phosphoceramide; GlcCer, glucosylceramide; G3P, glycerol-3-phosphate; GPAT, glycerol-3-phosphate acyltransferase; KCS, 3-ketoacyl-coenzyme A synthase; KSR, 3-ketosphinganine reductase; LACS, long-chain acyl-coenzyme A synthetase; LCB, long-chain base; LPA, lysophosphatidic acid; LPAAT, lysophosphatidic acid acyltransferase; LPC, lysophosphatidylcholine; LPCAT, acyl-coenzyme A:lysophosphatidylcholine acyltransferase; NEFA, non-esterified fatty acid; PA, phosphatidic acid; PAP, phosphatidic acid phosphatase; PC, phosphatidylcholine; PCd DAG, phosphatidylcholine-derived diacylglycerol; PDAT, phospholipid:diacylglycerol acyltransferase; PDCT, phosphatidylcholine:diacylglycerol choline phosphotransferase; PLA2, phospholipase A2; PLD, phospholipase D; SBH, sphingobase C4-hydroxylase ; SLD, sphingolipid long-chain base Δ8 desaturase; SPT, serine palmitoyltransferase; t18:0, 4-hydroxysphinganine; TAG, triacylglycerol; VLCFA, very long-chain fatty acid.

Figure 8. Production of oleic acids in seeds of transgenic lines

The scheme depicts the main pathways comprising fatty acid, acyl-CoA, and acyl-lipid metabolism in seeds of transgenic lines engineered to produce oils rich in oleic acid. For the sake of clarity, different pathways have been omitted such as the production of ω7 fatty acids or the biosynthesis of triacylglycerol by phospholipid:diacylglycerol acyltransferases. Red arrows linked with sight symbols represent metabolic steps that have been down-regulated, alone or in combination, to increase oleic acid content in seed oil. Metabolites under accumulated in transgenic lines with respect to the wild type appear in red, those over accumulated in green. The C-C double bonds of the acyl chains presented are all in the *cis* configuration.

ACP, acyl carrier protein; CoA, coenzyme A; CPT, cytidine diphosphate-choline:diacylglycerol choline phosphotransferase ; DAG, diacylglycerol; DGAT, acyl-coenzyme A:diacylglycerol acyltransferase; FAD, fatty acid desaturase; FAE1, fatty acid elongase complex comprising the 3-ketoacyl-CoA synthase FATTY ACID ELONGASE1; FAT, acyl-acyl carrier protein thioesterase; G3P, glycerol-3-phosphate; GPAT, glycerol-3-phosphate acyltransferase; KAS, fatty acid synthase complex comprising a 3-ketoacyl-ACP synthase; LACS, long-chain acyl-coenzyme A synthetase; LPA, lysophosphatidic acid; LPAAT, lysophosphatidic acid acyltransferase; LPC, lysophosphatidylcholine; LPCAT, acyl-coenzyme A:lysophosphatidylcholine acyltransferase; NEFA, non-esterified fatty acid; PA, phosphatidic acid; PAP, phosphatidic acid phosphatase; PC, phosphatidylcholine; PDCT, phosphatidylcholine:diacylglycerol choline phosphotransferase; PLA_2, phospholipase A_2; SAD, Δ9 stearoyl-acyl carrier protein desaturase; TAG, triacylglycerol.

Figure 9. Production of omega-7 fatty acids in seeds of transgenic lines of *Camelina sativa*

The scheme depicts the different pathways comprising fatty acid and acyl-CoA metabolism in seeds of transgenic *Camelina sativa* lines engineered to produce oils rich in ω7 fatty acids [397]. Blue arrows represent exogenous enzymes introduced into the metabolic system: the mutant Δ9 16:0-ACP

desaturase (PAD) Com25 and the *Caenorhabditis elegans* ∆9 16:0-CoA-specific desaturase (ADS) Fat5. Red arrows linked with sight symbols represent endogenous down-regulated metabolic steps. The identity of the 3-ketoacyl-ACP synthase responsible for the elongation of $16:1^{\Delta 9c}$ into $18:1^{\Delta 9c}$ remains unclear. Metabolites over accumulated in transgenic lines appear in green, those under accumulated in red. The C-C double bonds of the acyl chains presented are all in the *cis* configuration. ACP, acyl carrier protein; ADS, acyl-coenzyme A desaturase; CoA, coenzyme A; FAE1, fatty acid elongase complex comprising the 3-ketoacyl-CoA synthase FATTY ACID ELONGASE1; FAT, acyl-acyl carrier protein thioesterase; KAS, fatty acid synthase complex comprising a 3-ketoacyl-ACP synthase; LACS, long-chain acyl-coenzyme A synthetase; NEFA, non-esterified fatty acid; PAD, ∆9 palmitoyl-acyl carrier protein desaturase; SAD, ∆9 stearoyl-acyl carrier protein desaturase.

Table 1. List of monounsaturated fatty acids found in seed oils and described in this review

Δ Notation	ω	Systematic name	Common name	Examples of plant sources
$16:1^{\Delta 6c}$	10	(6*Z*)-Hexadecenoic acid	Sapienic acid	*Thunbergia alata*
$16:1^{\Delta 9c}$	7	(9*Z*)-Hexadecenoic acid	Palmitoleic acid	*Doxantha unguis-cati*
$18:1^{\Delta 6c}$	12	(6*Z*)-Octadecenoic acid	Petroselinic acid	*Coriandrum sativum*, *Hedera helix*
$18:1^{\Delta 9c}$	9	(9*Z*)-Octadecenoic acid	Oleic acid	*Carthamus tinctorius*, *Olea europaea*
$18:1^{\Delta 11c}$	7	(11*Z*)-Octadecenoic acid	Vaccenic acid	*Hippophae rhamnoides*, *Doxantha unguis-cati*
$20:1^{\Delta 5c}$	15	(5*Z*)-Eicosaenoic acid	-	*Limnanthes alba*, *Limnanthes douglasii*
$20:1^{\Delta 11c}$	9	(11*Z*)-Eicosaenoic acid	Gondoic acid	*Simmondsia chinensis*
$20:1^{\Delta 13c}$	7	(13*Z*)-Eicosaenoic acid	Paullinic acid	*Paullinia elegans*
$22:1^{\Delta 5c}$	17	(5*Z*)-Docosenoic acid	-	*Limnanthes alba*, *Limnanthes douglasii*
$22:1^{\Delta 13c}$	9	(13*Z*)-Docosenoic acid	Erucic acid	*Tropaeolum majus*, *Brassica rapa*
$24:1^{\Delta 15c}$	9	(5*Z*)-Tetracosenoic acid	Nervonic acid	*Cardamine graeca*, *Lunaria annua*, *Malania oleifera*

A

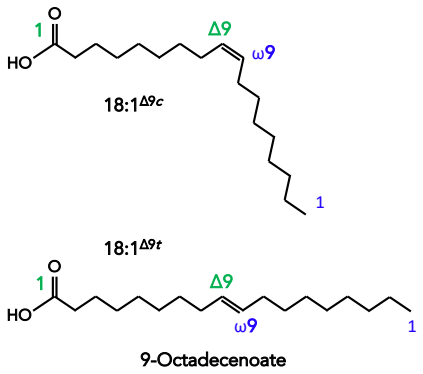

9-Octadecenoate

B

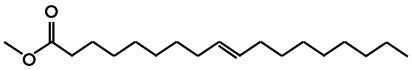

Methyl 9-octadecenoate

C

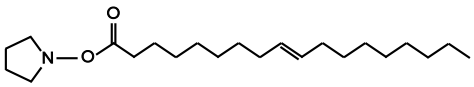

N-Octadec-9-enoyl pyrrolidine

D

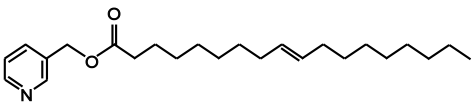

3-Pyridylcarbinyl 9-octadecenoate

E

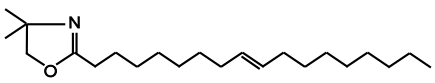

DMOX derivative of methyl 9-octadecenoate

F

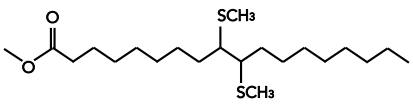

DMDS adduct of methyl 9-octadecenoate

Figure 1

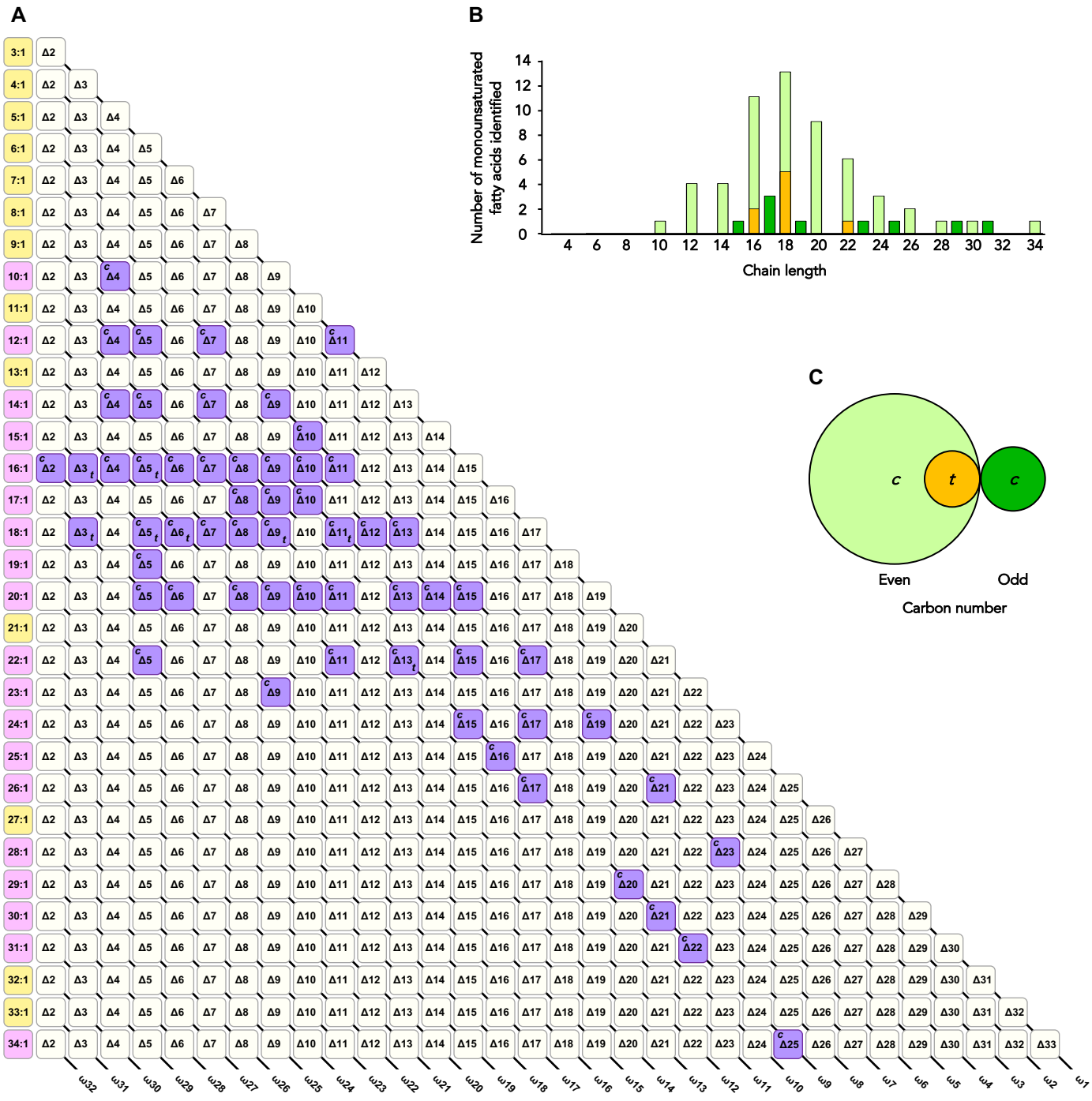
A
B
Number of monounsaturated fatty acids identified
Chain length
C
c
t
c
Even
Odd
Carbon number

Figure 2

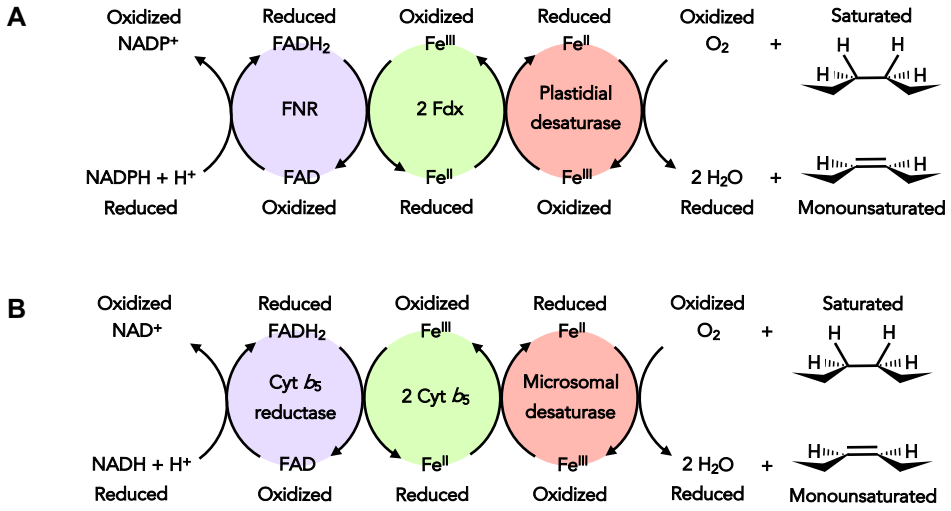
A
Oxidized
NADP+
Reduced
FADH2
Oxidized
FeIII
Reduced
FeII
Oxidized
O2
+
Saturated
FNR
2 Fdx
Plastidial
desaturase
NADPH + H+
Reduced
FAD
Oxidized
FeII
Reduced
FeIII
Oxidized
2 H2O
Reduced
+
Monounsaturated
B
Oxidized
NAD+
Reduced
FADH2
Oxidized
FeIII
Reduced
FeII
Oxidized
O2
+
Saturated
Cyt b5
reductase
2 Cyt b5
Microsomal
desaturase
NADH + H+
Reduced
FAD
Oxidized
FeII
Reduced
FeIII
Oxidized
2 H2O
Reduced
+
Monounsaturated

Figure 3

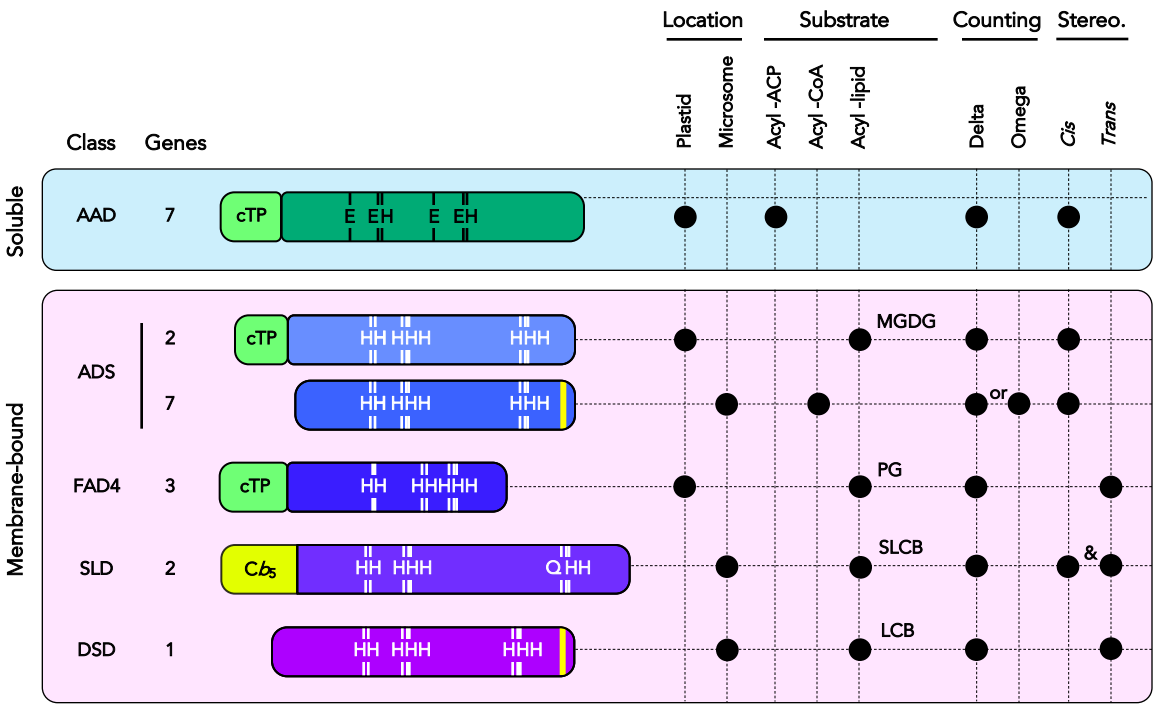
Location
Substrate
Counting
Stereo.
Plastid
Microsome
Acyl -ACP
Acyl -CoA
Acyl -lipid
Delta
Omega
Cis
Trans
Class
Genes
Soluble
AAD
7
cTP
E EH E EH
Membrane-bound
ADS
2
7
cTP
HH HHH HHH
MGDG
or
FAD4
3
cTP
HH HHHHH
PG
SLD
2
Cb5
HH HHH QHH
SLCB
&
DSD
1
HH HHH HHH
LCB

Figure 4

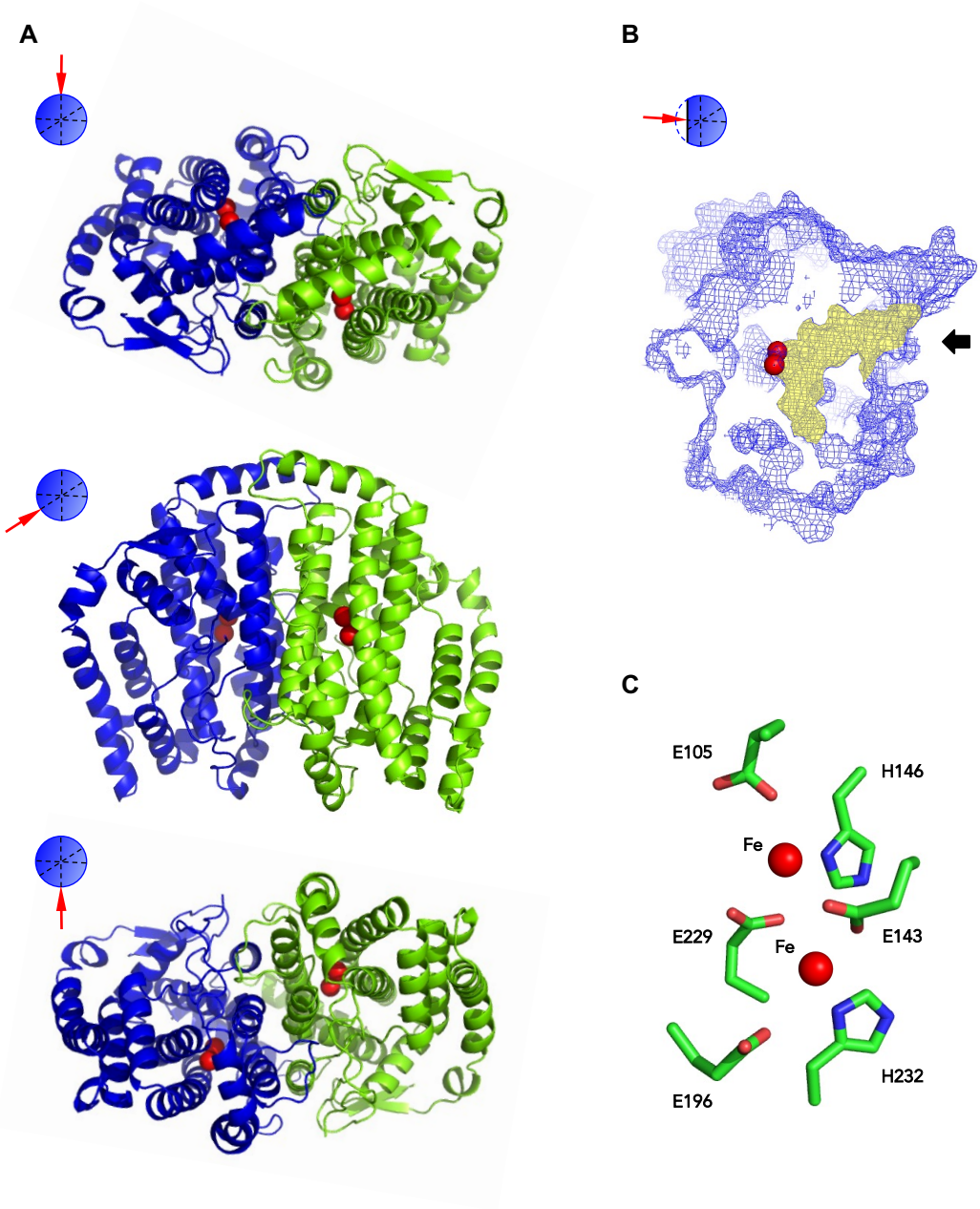

Figure 5

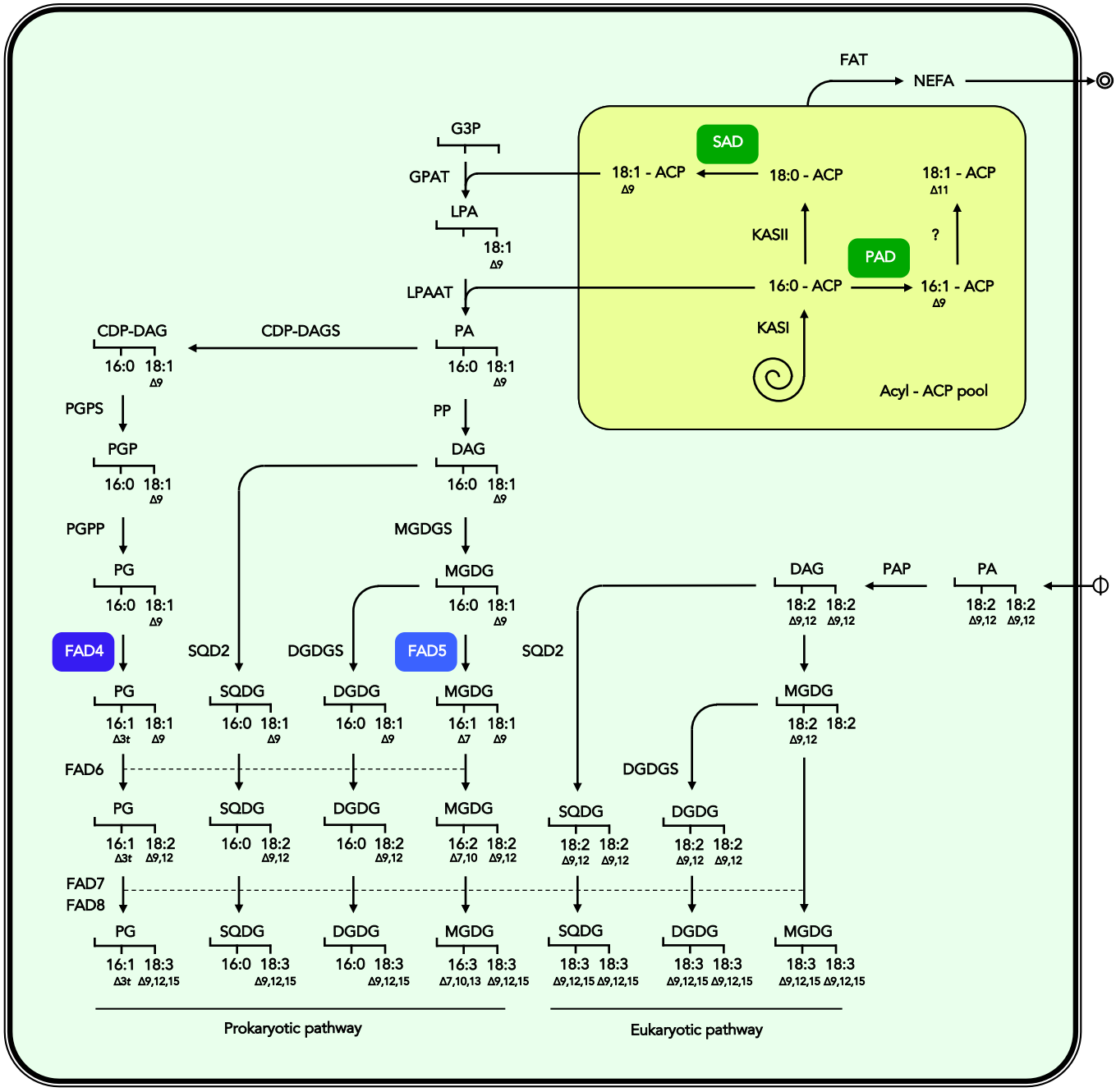
FAT
NEFA
G3P
GPAT
LPA
18:1 Δ9
LPAAT
SAD
18:1 - ACP Δ9
18:0 - ACP
18:1 - ACP Δ11
KASII
?
PAD
16:0 - ACP
16:1 - ACP Δ9
KASI
Acyl - ACP pool
CDP-DAG
CDP-DAGS
PA
16:0 18:1 Δ9
PGPS
PP
PGP
DAG
PGPP
MGDGS
PG
MGDG
FAD4
SQD2
DGDGS
FAD5
SQD2
SQDG
DGDG
FAD6
FAD7
FAD8
PAP
16:0 18:1 Δ9
16:1 18:1 Δ3t Δ9
16:1 Δ7 Δ9
16:0 18:2 Δ9,12
16:1 18:2 Δ3t Δ9,12
16:2 18:2 Δ7,10 Δ9,12
18:2 18:2 Δ9,12
16:1 18:3 Δ3t Δ9,12,15
16:0 18:3 Δ9,12,15
16:3 18:3 Δ7,10,13 Δ9,12,15
18:3 18:3 Δ9,12,15
Prokaryotic pathway
Eukaryotic pathway

Figure 6

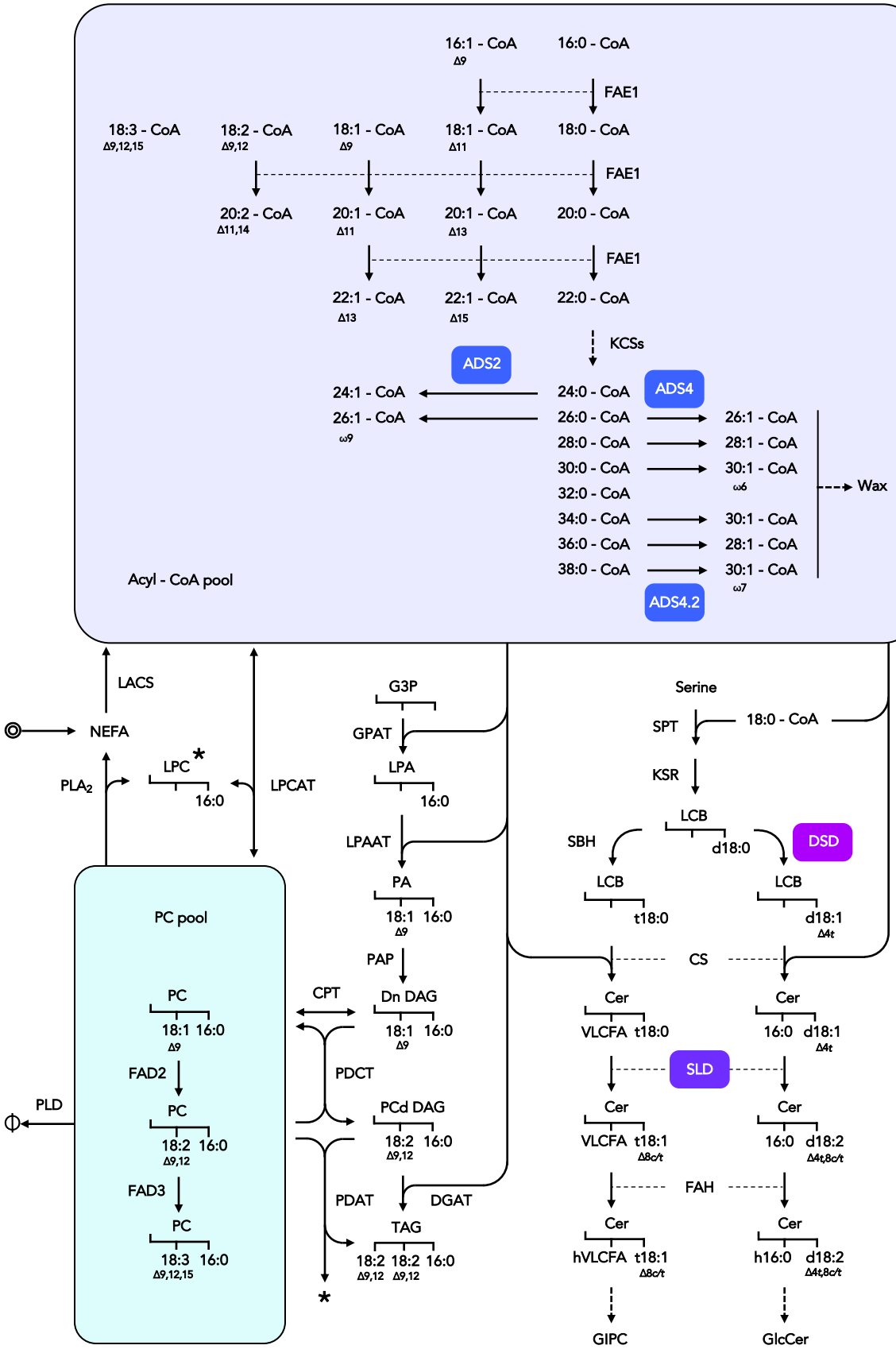
16:1 - CoA
Δ9
16:0 - CoA
FAE1
18:3 - CoA
Δ9,12,15
18:2 - CoA
Δ9,12
18:1 - CoA
Δ9
18:1 - CoA
Δ11
18:0 - CoA
FAE1
20:2 - CoA
Δ11,14
20:1 - CoA
Δ11
20:1 - CoA
Δ13
20:0 - CoA
FAE1
22:1 - CoA
Δ13
22:1 - CoA
Δ15
22:0 - CoA
KCSs
ADS2
ADS4
24:1 - CoA
26:1 - CoA
ω9
24:0 - CoA
26:0 - CoA
28:0 - CoA
30:0 - CoA
32:0 - CoA
34:0 - CoA
36:0 - CoA
38:0 - CoA
26:1 - CoA
28:1 - CoA
30:1 - CoA
ω6
30:1 - CoA
28:1 - CoA
30:1 - CoA
ω7
Wax
ADS4.2
Acyl - CoA pool
LACS
NEFA
PLA2
LPC
16:0
LPCAT
G3P
GPAT
LPA
16:0
LPAAT
PA
18:1 16:0
Δ9
PAP
Dn DAG
18:1 16:0
Δ9
CPT
PDCT
PCd DAG
18:2 16:0
Δ9,12
PDAT
DGAT
TAG
18:2 18:2 16:0
Δ9,12 Δ9,12
PC pool
PC
18:1 16:0
Δ9
FAD2
PC
18:2 16:0
Δ9,12
FAD3
PC
18:3 16:0
Δ9,12,15
PLD
Serine
SPT
18:0 - CoA
KSR
LCB
d18:0
SBH
DSD
LCB
t18:0
LCB
d18:1
Δ4t
CS
Cer
VLCFA t18:0
Cer
16:0 d18:1
Δ4t
SLD
Cer
VLCFA t18:1
Δ8c/t
Cer
16:0 d18:2
Δ4t,8c/t
FAH
Cer
hVLCFA t18:1
Δ8c/t
Cer
h16:0 d18:2
Δ4t,8c/t
GIPC
GlcCer

Figure 7

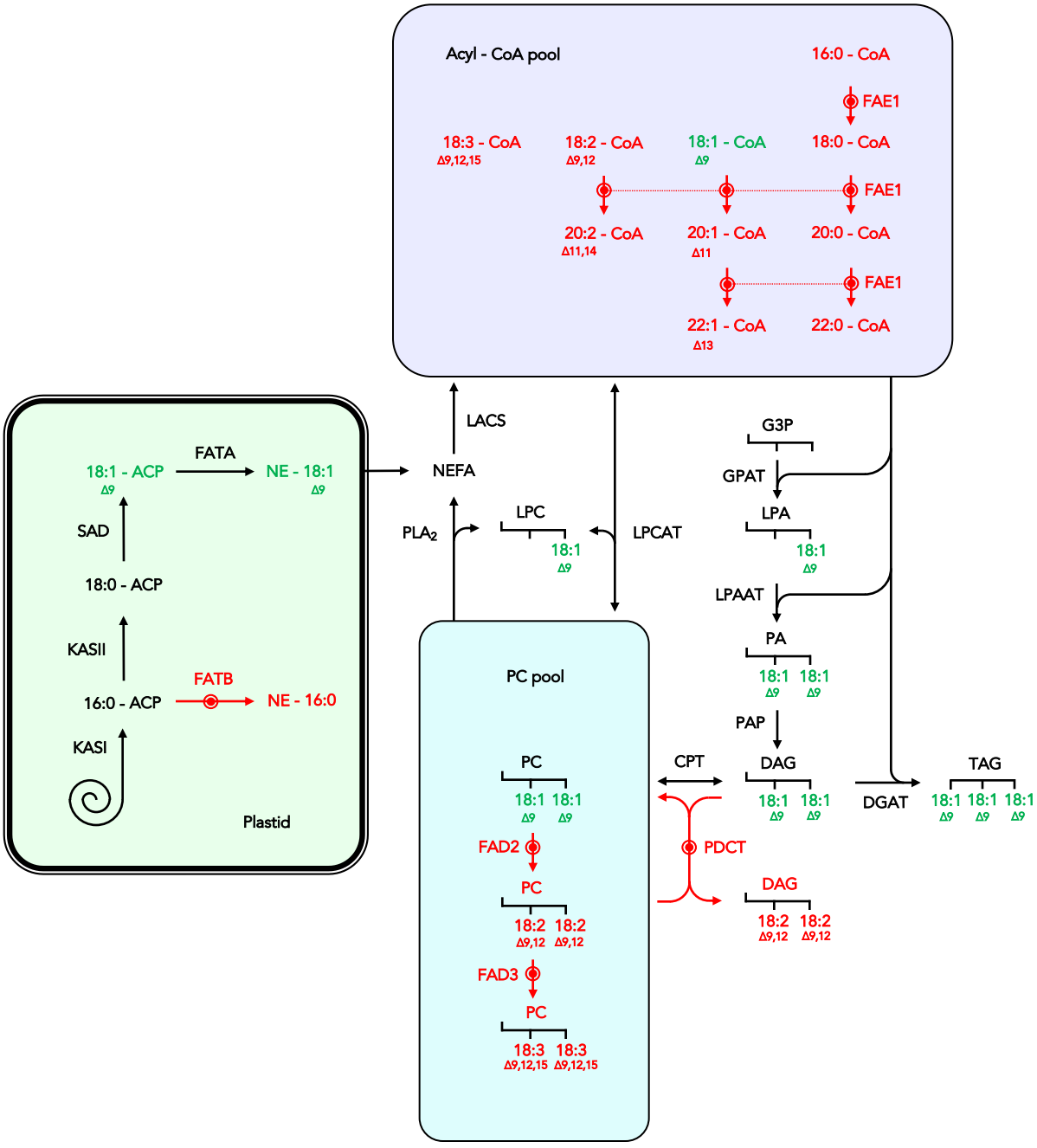
Acyl - CoA pool
16:0 - CoA
FAE1
18:3 - CoA
Δ9,12,15
18:2 - CoA
Δ9,12
18:1 - CoA
Δ9
18:0 - CoA
FAE1
20:2 - CoA
Δ11,14
20:1 - CoA
Δ11
20:0 - CoA
FAE1
22:1 - CoA
Δ13
22:0 - CoA
LACS
NEFA
FATA
18:1 - ACP
Δ9
NE - 18:1
Δ9
SAD
18:0 - ACP
KASII
FATB
16:0 - ACP
NE - 16:0
KASI
Plastid
PLA2
LPC
18:1
Δ9
LPCAT
G3P
GPAT
LPA
18:1
Δ9
LPAAT
PA
18:1 18:1
Δ9 Δ9
PAP
DAG
18:1 18:1
Δ9 Δ9
CPT
PDCT
DAG
18:2 18:2
Δ9,12 Δ9,12
DGAT
TAG
18:1 18:1 18:1
Δ9 Δ9 Δ9
PC pool
PC
18:1 18:1
Δ9 Δ9
FAD2
PC
18:2 18:2
Δ9,12 Δ9,12
FAD3
PC
18:3 18:3
Δ9,12,15 Δ9,12,15

Figure 8

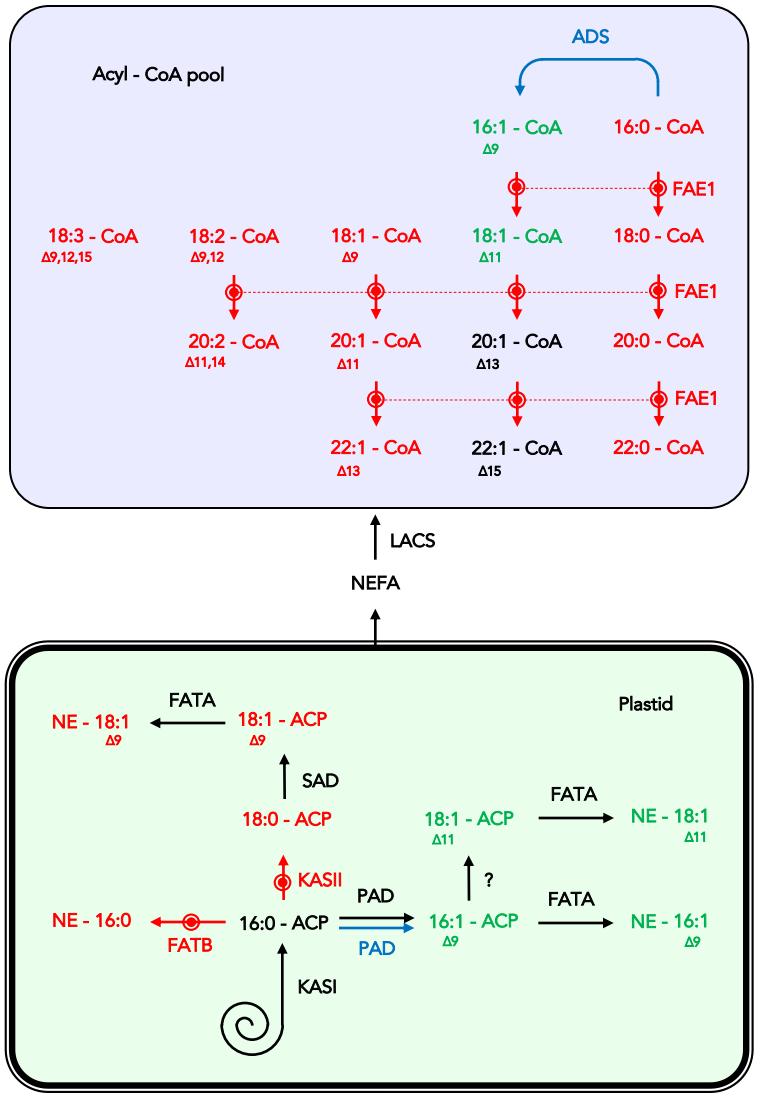
Acyl - CoA pool
ADS
16:1 - CoA
Δ9
16:0 - CoA
FAE1
18:3 - CoA
Δ9,12,15
18:2 - CoA
Δ9,12
18:1 - CoA
Δ9
18:1 - CoA
Δ11
18:0 - CoA
FAE1
20:2 - CoA
Δ11,14
20:1 - CoA
Δ11
20:1 - CoA
Δ13
20:0 - CoA
FAE1
22:1 - CoA
Δ13
22:1 - CoA
Δ15
22:0 - CoA
LACS
NEFA
Plastid
FATA
NE - 18:1
Δ9
18:1 - ACP
Δ9
SAD
18:0 - ACP
18:1 - ACP
Δ11
FATA
NE - 18:1
Δ11
KASII
PAD
?
NE - 16:0
16:0 - ACP
16:1 - ACP
Δ9
FATA
NE - 16:1
Δ9
FATB
PAD
KASI

Figure 9